Power-aware routing in multi-hop wireless networks

Akhtar, Auon Muhammad

Awarding institution:
King's College London

Title: Power-aware routing in multi-hop wireless networks

Author: Auon Akhtar

POWER-AWARE ROUTING IN MULTI-HOP WIRELESS NETWORKS

Auon Muhammad Akhtar

Institute of Telecommunications

School of Natural & Mathematical Sciences

King's College London

A thesis submitted to King's College London in partial fulfillment of the requirements for the degree of

Doctor of Philosophy

February 2013

To my loving parents, wife *Anam* and son *Mursal*.

Acknowledgements

First and foremost, I would like to thank my Lord who gave me the strength and the means to embark upon the journey to my PhD.

This thesis would not have been possible without the guidance and the support of several individuals who helped in making my time at IoT one of the most memorable experiences of my life. First of all, I would like to thank my supervisor, Prof. Hamid Aghvami, one of the most amazing personalities that I have come across in my life. He provided a stimulating environment at IoT and his motivation, knowledge and long lasting experience have been invaluable to me.

I am deeply indebted to my second supervisor, Dr. Reza Nakhai, who supported me throughout this journey. Not only did he teach me how to conduct quality research, he also taught me to maintain my integrity as a researcher. Never in my life have I seen a person as committed to his work as Dr. Nakhai. I will never forget the long hours that he spent helping me with my work. Indeed, he is an irreplaceable asset for IoT.

I wish to thank Dr. Oliver Holland for allowing me to work with him on the ACROPOLIS project. The project added an extra dimension to my work and it helped me network with professionals across Europe. I would especially like to thank Dr. Luca De Nardis, from University of Rome La Sapienza, with whom I carried out some collaborative research. I also owe my gratitude to Dr. Vasilis Frederikos who always gave me useful tips related to my work. I am particularly grateful to my colleagues at IoT, including Adnan, Tuan, Alex, Ana, Merat, Diogo, Panayiotis, Nur, Azar, Saba, Jing, Mati and many others, who gave me hours of enjoyable company. Especially, I would like to acknowledge the efforts of Adnan, Alex, Merat and Tuan who helped me in improving the quality of this work by proofreading the thesis.

Acknowledgments go to UK's Virtual Center of Excellence in Mobile and Personal Communications (Mobile VCE) and the UK Governments Engineering & Physical Sciences Research Council (EPSRC) for their financial

support. I am also grateful to the industrial members of Mobile VCE, especially Mr. John Turk and Mr. Simon Fletcher, for their continuous feedback on the work detailed in this thesis. Contributing to the Core 5 Green Radio program of Mobile VCE, the reported work has been presented and discussed to a broad audience of highly skilled individuals from a variety of telecommunications companies in the UK.

Special thanks to Ammi and Baba who always believed in me and encouraged me to take on the most difficult of challenges in life. Thanks to my wife, Anam, who holds a special place in my heart and my son, Mursal, the best gift Allah has ever given me. I dedicate this work to all my near and dear ones.

Abstract

Wireless ad hoc networks (WAHNs) are a class of wireless networks that do no rely on a pre-existing infrastructure. Due to the infrastructure-less nature of WAHNs, the nodes themselves act as routers. A wireless mesh network (WMN) is a special type of WAHN that consists of a network of access points which are connected to each other through wireless links. While a WAHN is typically formed in an ad hoc manner, when the wireless devices come within communication range of each other, a WMN often has a more planned configuration. Compared to infrastructure-based networks, some of the advantages of WAHNs and WMNs include independence from central network administration, scalability, rapid deployment, last mile connectivity and cheaper network setup.

Power consumption is an important design criteria in WAHNs and WMNs, least because it directly impacts the cost of network operation and maintenance. To add to this, the information and communication technology (ICT) industry is already being labeled as a substantial contributor to the total CO_2 emissions on the planet. For this reason, *green* ICT has become a critical issue world wide. Since routing is one of the core functions of multi-hop networks like WAHNs and WMNs, significant research effort is being made to design energy-efficient and power saving routing algorithms. This thesis focuses on power-aware and energy-efficient routing in static WAHNs and WMNs that aim to extend network connectivity through multi-hop communication. Different transmission strategies are investigated for energy efficiency. These include point to point non-cooperative transmissions, distributed beamforming and centralized beamforming. Then, several power saving routing algorithms are proposed, each tailored for a specific type of transmission strategy. The proposed algorithms aim to minimize the end to end path power consumption while satisfying the signal to noise ratio requirements of the destination and the relay nodes.

The performance of the proposed schemes is investigated thoroughly. Various figures of merit are used to highlight the efficiency of the proposed

algorithms. These include end-to-end power consumption, total hop count, end-to-end delay and throughput. While most of the simulations are carried out in MATLAB, some packet level simulations are also conducted in OMNET++. The numerical and analytical investigations highlight the achievable energy saving gains.

Contents

List of Figures

List of Tables

List of Acronyms

ANC Analog Network Coding

AoD Angle-of-Departure

APAR Adaptive Power-Aware Routing

BEP Bit Error Probability

BER Bit Error Rate

BF BeamForming

BPSK Binary Phase Shift Keying

BR Bit Region

BS Base Station

BSS Base Station Subsystem

CAN Cooperation Along Noncooperative Path

CCSPR Cooperative-Cost Shortest Path Routing

COSPNCR Cooperation Over Shortest Path Non-Cooperative Routing

CPLNC Cooperative Physical Layer Network Coding

CR Cognitive Radio

CRN Cognitive Radio Network

CSI Channel State Information

CTNCR Cooperative routing along Truncated Non-cooperative Route

DB Distributed Beamforming

DOA Direction Of Arrival

DPC Dirty Paper Coding

ECG Energy Consumption Gain

GPS Global Positioning System

GSM Global System for Mobile Communications

ICT Information Communication Technology

IFN Intermediate Forwarding Node

ISM Interference Shaping Margin

LOS Line of Sight

LTE Long Term Evolution

MAC Medium Access Control

MANET Mobile Ad hoc NETwork

MIMO Multiple-Input and Multiple-Output

MISO Multiple-Input and Single-Output

MPCR Minimum Power Cooperative Routing

MPSR Modified Power Saving Routing

MPPAR Modified Progressive Power Aware Routing

MS Mobile Station

NCSP Non-cooperative Shortest Path

OTBF Orthogonal Transmit BeamForming

PACR Power Aware Cooperative Routing

PHY Physical

PLNC Physical Layer Network Coding

PPAR Progressive Power Aware Routing

PSR Power Saving Routing

QoS Quality of Service

QPSK Quadrature Phase Shift Keying

RF Radio Frequency

SDP SemiDefinite Programming

SINR Signal to Interference plus Noise Ratio

SNER Source Node Expansion Routing

SNR Signal to Noise Ratio

ULA Uniform Linear Array

UMTS Universal Mobile Telecommunications System

UWB Ultra Wide Band

WAHN Wireless Ad hoc Network

WiFi Wireless-Fidelity

WiMax Worldwide interoperability for Microwave access

WMN Wireless Mesh Network

WLAN Wireless Local Area Network

WSN Wireless Sensor Network

Chapter 1

Introduction

Over the last two decades, telecommunication networks have seen an explosive growth, mainly due to the rapid advancements in wireless communications. A plethora of wireless technologies have emerged, including Wireless-Fidelity (WiFi), Bluetooth, ZigBee, Ultra Wide Band (UWB), Worldwide Interoperability for Microwave Access (WiMax), etc. These technologies are being supported by an ever increasing number of devices such as laptops, tablets, smartphones, etc., allowing them to connect to a variety of networks.

In general, wireless networks can be broadly categorized into infrastructure-based networks and infrastructure-less networks. Examples of infrastructure-based networks include Global System for Mobile Communications (GSM), Universal Mobile Telecommunications System (UMTS), Long Term Evolution (LTE) and Wireless Local Area Networks (WLANs). All these standards are based on a fixed, wired, backbone infrastructure. Through this backbone network, the data traffic is routed over the internet. Contrary to this, infrastructure-less networks do not rely on such a wired backbone and are created when wireless devices communicate directly with one another, through point-to-point connections. For example, wireless ad hoc networks (WAHNs) are decentralized wireless networks that do not rely on a pre-existing infrastructure. The independence from a pre-established infrastructure is achieved by increasing the node functionality. For example, a node in a WAHN directly forwards the data to the other nodes, thus eradicating the need for routers or access points. Compared to infrastructure-based networks, some of the advantages of WAHNs include independence from central network administration, scalability, rapid deployment, last mile connectivity and cheaper network setup. Some of the major utilization envisioned for WAHNs include disaster management, military applications, and extended network connectivity.

Different types of WAHNs include mobile ad hoc networks (MANETs), wireless mesh networks (WMNs) and wireless sensor networks (WSNs). An example of a MANET is shown in Figure 1.1(a), where the mobile terminals communicate with each other over the wireless channel. Such a network can be used in battlefields or in a disaster-hit area. Figure 1.1(b) illustrates an example of a WMN where the static access points act as wireless routers while the mobile nodes are the mesh clients. Such networks can be used to implement a rooftop network which provides last mile connectivity to the residents in a neighborhood. As the data rate requirements increase, the range of wireless network coverage is reduced, raising investment costs for building infrastructure with access points to cover service areas. WMNs are unique enablers that can reduce this cost due to their flexible architecture. Finally, Figure 1.1(c) depicts an example of a WSN that collects the environment data and sends it to a central server.

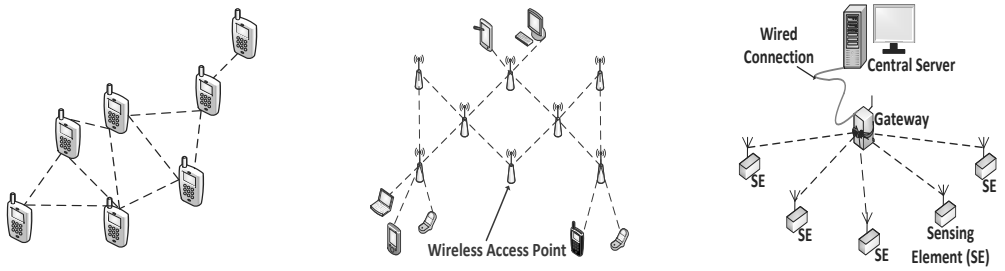

(a) (b) (c)

Figure 1.1: Types of wireless ad hoc networks. The dashed lines represent the wireless link between the terminals. (a) A mobile ad hoc network formed of seven mobile terminals, (b) a wireless mesh network of access points and (c) a wireless sensor network.

WAHNs are purely distributed systems and routing is an important function of such multi-hop networks. Due to the lack of dedicated routers and routing databases, the often limited capabilities of the participating nodes and the frequent topology changes, routing in WAHNs is a challenging task and a number of routing protocols for WAHNs have been proposed in the past [1–5]. The works reported in [1–5] cover different aspects of routing in WAHNs, ranging from capacity and throughput maximizing routing protocols to power-aware routing protocols.

1.1 Scope of the Work

The thesis focuses on power-aware and energy-efficient routing in static WAHNs that aim to extend network connectivity through multi-hop communication. Specifically, WMNs of wireless access points and WAHNs of randomly distributed nodes are taken

into consideration. In such networks, power consumption is one of the key factors in maintaining the cost of network operation. With the growing energy prices worldwide, operators are increasingly concerned regarding the maintenance of these networks. Furthermore, the information and communication technologies (ICT) industry is already being labeled as a substantial contributor to the total CO_2 emissions on the planet and a significant portion of this is contributed by the wireless and mobile communications industry. It has been shown in [6] that the CO_2 footprint of ICT is 25% of the 2007 carbon footprint for cars worldwide. As another figure of merit, it is expected that in near future, ICT related activities will account for 14% of the overall electrical energy consumption worldwide [7]. In such circumstances, it comes as no surprise that green ICT is attracting significant attention worldwide. For example, in Europe, EARTH (energy aware radio and network technologies) [8] and the Green Radio program within UK's MOBILE VCE [9] are leading from the front in designing *green* radio architectures and technologies. In Asia, Green-IT [10] from Japan is focused on developing energy consumption metrics and energy efficiency standards for networking technologies. On a more global scale, Green Touch [11] aims to deliver the architecture, specifications and road map to increase network energy efficiency by a factor of 1000 as compared to the levels in 2010.

Since routing is one of the basic functions of multi-hop networks like WAHNs and WMNs, a lot of research effort is being made to design energy-efficient and power saving routing algorithms for such networks [5, 12]. In this thesis, a cross-layer design approach is adopted to design power-efficient routing algorithms. At the physical layer, different energy-efficient transmission techniques are proposed and investigated. Based on these techniques, several power saving routing algorithms are proposed at the network layer. Each of these algorithms is tailored for a specific type of transmission strategy. The algorithms are designed based on the transmission power consumption and the fixed circuit power consumption.

The performance of the proposed schemes is investigated thoroughly. Various figures of merit such as end-to-end power consumption, total hop count, end-to-end delay and throughput are used to evaluate the efficiency of the proposed algorithms. While most of the simulations are carried out in MATLAB, some packet level simulations are also conducted in OMNET++. The results show significant overall improvement in the performance of routing algorithms, in terms of power consumption, as compared to several well-known baseline power saving routing algorithms.

1.2 Thesis Contributions

1.2.1 Contributions

The contributions of this thesis lead to the design of several power saving routing algorithms for WMNs and WAHNs. Some key outcomes and findings of this work are summarized below:

1. The first proposed algorithm is presented in chapter 3. Initially, the chapter highlights the impact of fading on existing power saving routing algorithms. Through analysis, it is shown that the fading coefficients, due to their randomness, cannot be incorporated directly into the existing power aware routing algorithms, hence, the performance of these algorithms is susceptible to the impact of multipath reflections. Two decision metrics are introduced, which can be used to select the next hop destination. Using these metrics, a power-aware routing algorithm is proposed. The algorithm is adaptive with realistic channel variations in terms of multipath fading, and hence, is suitable for interconnecting the base station subsystems (BSS) in a cellular mesh network or interconnecting the randomly placed nodes in an ad hoc network. Results show that the proposed routing algorithm significantly reduces the power consumption as compared to the baseline routing algorithm. Furthermore, this power saving is achieved while consuming almost the same number of hops as the baseline routing scheme.

2. A distributed-beamforming based cooperative routing algorithm is presented in chapter 4. The proposed power-aware cooperative routing (PACR) algorithm finds an optimal route from the source to the destination by taking into consideration the circuit power consumption of the cooperative communication. Unlike the previous works, in PACR, the transmitting nodes cooperatively select the next hop destination and the algorithm is distributed, i.e., it does not require a pre-determined route from source to destination. The concept of supernode with improved power efficiency is introduced to model a group of cooperating base stations as a single node and this enables us to find the optimal distance for cooperative transmission. Simulation results confirm PACR's improved energy saving potential over the baseline cooperative and non-cooperative routing algorithms. This improved power saving is achieved by incorporating fewer number of hops as compared to the baseline algorithms. PACR is suitable for macro and micro cellular networks with cell radii ranging from 50m to 1500km.

3. Power and interference aware routing is investigated in an underlay multi-hop secondary network. Transmit beamforming is utilized in order to guarantee coexistence of the secondary users with the primary nodes. Although beamforming has been proposed in the past as a way to improve the capability of secondary network nodes, the work presented in this thesis goes beyond previous attempts by taking into account beamforming in the selection of relays in multi-hop connections. A new cost metric is proposed which is used to design an optimized, beamforming based routing algorithm with three-fold objective: to minimize the end to end path power consumption; to minimize the co-channel interference imposed within the secondary network and to minimize the number of primary interference constraint violations. The proposed strategy is compared with previous work that adopted beamforming in the secondary network without changing the path. The computer simulations are performed by combining a signal processing tool, i.e., MATLAB, and a network simulator, i.e., OMNet++. Simulation results from MATLAB confirm that the optimized routing algorithm outperforms the original routing algorithm in terms of both, the interference generated within the secondary network and the number of primary interference constraint violations. Furthermore, it is shown that for networks with a large number of primary nodes, the optimized algorithm outperforms the baseline algorithm in terms of power consumption. Finally, the simulations carried out in OMNet++ confirm the improved throughput of the secondary network when no constraints from primary nodes are imposed, while they highlight a trade off between coexistence capability and secondary network performance when the presence of primary nodes has to be taken into account.

1.2.2 List of Publications

The publications that are related to the contributions of the thesis are as follows.

Journals

1. **A. M. Akhtar**, M. R. Nakhai, and A. H. Aghvami, "On the use of cooperative physical layer network coding for energy efficient routing," IEEE Transactions on Communications, pp. 1-12. (To Appear, Accepted November 2012).

2. **A. M. Akhtar**, M. R. Nakhai, and A. H. Aghvami, "Power aware cooperative routing in wireless mesh networks," Communications Letters, IEEE, vol. 16, no. 5, pp. 670-673, May, 2012.

3. **A. M. Akhtar**, M. R. Nakhai, and A. H. Aghvami, "Energy efficient adaptive routing in wireless ad hoc and mesh networks," IET Networks, vol. 1, no. 4, pp. 249-256, Dec. 2012.

4. **A. M. Akhtar** and M. R. Nakhai, "Transmit beamforming and interference shaping in cellular cognitive radio networks," IET Communications, vol. 5, no. 14, pp. 2052-2058, Sept., 2011.

Conference Proceedings

5. **A. M. Akhtar**, L. D. Nardis, M. R. Nakhai, O. D. Holland, M.-G. Di Benedetto, and A. H. Aghvami, "Multi-hop cognitive radio networking through beamformed underlay secondary access," IEEE ICC 2013 (To Appear).

6. **A. M. Akhtar**, M. R. Nakhai, and A. H. Aghvami, "CPLNC Based Energy Efficient Routing in Rayleigh Fading Networks," IEEE ICC 2013 (To Appear).

7. **A. M. Akhtar**, M. R. Nakhai, and A. H. Aghvami, "On energy efficient routing using cooperative physical layer network coding," IEEE GLOBECOM 2012, pp. 2815-2820, Dec. 2012.

8. **A. M. Akhtar**, M. R. Nakhai, and A. H. Aghvami,"Power saving cooperative path routing in static wireless networks", in Proc. IEEE ICC'12 Workshops, pp. 5906-5910, June, 2012.

9. **A. M. Akhtar**, M. R. Nakhai, and A. H. Aghvami, "Adaptive power aware routing in wireless mesh networks," in Proc. IEEE VTC-Spring 2011, Budapest, Hungary, 15-18 May, 2011. (Best Paper Award).

10. **A. M. Akhtar**, O. D. Holland, T. A. Le, M. R. Nakhai, and A. H. Aghvami, "Cooperative cognitive radio beamforming in the presence of location errors," in Proc. IEEE VTC-Spring 2011, Budapest, Hungary, 15-18 May, 2011.

11. L. D. Nardis, M.-G. Di Benedetto, **A. M. Akhtar**, and O. D. Holland,"Combination of DOA and beamforming in position-based routing for underlay cognitive wireless networks", in proc. CrownCom 2012.

Book Chapters

12. M. R. Nakhai, T. A. Le, **A. M. Akhtar**, and O. D. Holland,"Cognitive and cooperative techniques for energy-efficient cellular wireless communications," book

chapter in Green Radio Communication Networks, Cambridge University Press.

1.3 Thesis Outline

The rest of this thesis is organized as follows. Chapter 2 provides a literature review of the works related to the proposed research topic. The aim is to provide a technical background that is required to understand the problem area that is addressed in this thesis. Based on various types of routing strategies and objectives, the chapter divides power-aware routing protocols into different categories. While all these categories are discussed in general, the chapter focuses specifically on the class of power-aware routing protocols that are related to the work presented in this thesis.

After reviewing the related literature in Chapter 2, the main contributions of the thesis are discussed in chapters 3, 4 and 5. Chapter 3 focuses on single antenna systems. After analyzing the impact of fading on power saving routing algorithms, a new power aware non-cooperative routing algorithm is proposed. Chapter 4 proposes a cooperative routing algorithm which is based on distributed beamforming. Chapter 5 dwells upon power and interference aware routing in a multi-hop, ad hoc cognitive radio network. The concluding remarks together with some avenues of future research are detailed in Chapter 6.

Chapter 2

Background Study

This chapter provides a detailed overview of the existing research works on power-aware routing in WAHNs. Due to the absence of a fixed infrastructure, the nodes in a WAHN communicate with each other through radio transmissions, either directly or indirectly through relaying. Typically these nodes are battery powered and have limited energy supplies. When a node runs out of battery, it ceases to function. Consequently, the network is partitioned and communication is disrupted. Thus, power consumption is one of the key factors that affect the overall performance of a WAHN. Even for scenarios where power supply is not an issue, for example, rooftop networks that provide last mile connectivity, the power consumption still maintains its importance as a key performance metric for two reasons: firstly, it directly impacts the cost of operating the network and secondly, it effects the environment due to the greenhouse gas emissions that result from generating electricity [13]. Since routing is one of the core functions of WAHNs, a lot of research effort has been made in the past to design power-aware and energy efficient routing algorithms for such networks [5, 12, 14–20]. The remainder of this chapter discusses these research contributions.

2.1 Introduction

As mentioned previously, developing power-aware routing protocols for ad hoc wireless networks has been an extensive research area in recent years, and many protocols have been proposed from a variety of perspectives. In [5], Li et al. survey a number of contemporary research papers on energy aware routing in wireless ad hoc networks. The authors broadly divide the power-aware routing protocols into two categories: activity-based and connectivity-based protocols. Activity-based protocols address the issue of power consumption as it relates to network activity, i.e., the actual transmission of data

between nodes in the network. On the other hand, connectivity-based routing protocols reduce power consumption while ensuring effective connectivity for the overall network. In [12], the authors discuss the core requirements for routing in WMNs and present complete descriptions of several routing schemes available in literature. Reference [14] proposes five different matrices that can be used to classify power-aware routing algorithms for mobile ad hoc networks. Important research papers related to different layers of the protocol stack have been reviewed in [15], which also proposes several metrics to study the performance of energy-efficient routing algorithms. These metrics include: *Energy consumed per packet; Time to network partition; Variance in power levels across mobiles; Cost per packet and maximum mobile cost.* In [16], Goldsmith and Wicker discuss the design challenges of energy-efficient protocols in various layers of the protocol stack. The authors show that cross layer design of these protocols is imperative to meeting emerging application requirements, particularly when energy is a limited resource. The study on WSNs in [17] classifies the routing techniques based on the network structure into three categories: flat, hierarchical, and location-based routing protocols. In flat routing, each node typically plays the same role and sensor nodes collaborate to perform the sensing tasks. In hierarchical routing, higher energy nodes are used to process and send the information, while low-energy nodes are used to perform the sensing in the proximity of the target. Finally, in location based routing, sensor nodes are addressed by means of their locations. Additionally, [17] also studies the design trade-offs between energy and communication overhead savings in each routing paradigm.

In [18], the authors study energy efficient multicasting in WAHNs with both, omni-directional and directional antennas. The study divides energy-aware broadcast/multicast problem into two categories: the MEB/MEM (minimum energy broadcast/multicast) problem and the MLB/MLM (maximum lifetime broadcast/multicast) problem. MEB/MEM minimizes the total transmission power consumption of all nodes involved in the multicast session while MLB/MLM maximizes the operation time until the battery depletion of the first node involved in the multicast session. Reference [19] presents a few energy-efficient routing techniques for wireless multimedia sensor networks. Further, a classification of the routing protocols for such networks is presented. The study is based on the energy efficient techniques combined with quality of service (QoS) assurance for wireless multimedia sensor networks. In [20], Pantazis et al. classify energy efficient routing protocols into four main schemes: *Network structure based; Communication model based; Topology based and reliability based routing.* The authors discuss the performance of different routing schemes in terms of advantages,

drawbacks, scalability, mobility and robustness.

The current chapter builds on the above described works by extensively reviewing a number of recent papers and categorizing known power-aware routing algorithms into different classes as explained in the next section.

2.2 Classification of Power-aware Routing Algorithms

Generally, the power-aware routing algorithms can be classified into two main categories:

1. Non-cooperative routing algorithms.
2. Cooperative routing algorithms.

Non-cooperative Routing Algorithms

Non-cooperative routing algorithms are those algorithms in which the source and the relay nodes individually select, and forward the data to, the next hop destination [1] (NHD). In such algorithms, all the radio transmissions are either point to point or point to multipoint. The term *non-cooperative* here means that the network nodes which are located in close vicinity to a transmitting node do not help the transmitter in sending data towards the next hop destination.

Cooperative Routing Algorithms

Cooperative routing algorithms are those algorithms in which the source and the relay nodes are helped by their neighboring nodes in transmitting the data towards the next hop destination. These algorithms combine energy-efficient route selection at the network layer with efficient transmission schemes at the physical layer.

Figure 2.1 illustrates a classification structure for different types of power-aware routing algorithms for multi-hop wireless networks. As shown in the figure, the non-cooperative energy efficient routing algorithms can be divided into three main categories: Broadcast/Multicast; Unicast and network structure and connectivity based algorithms. In broadcast/multicast routing, data packets are efficiently distributed among a set of listeners in multipoint networks. Such routing uses point to multipoint transmissions at the physical layer. In unicast routing, at each hop along the route towards the destination, the data is transmitted from a single transmitting node to a

[1] Next hop destination is the destination of each hop along the route towards the final destination

Figure 2.1: Classification of power-aware routing algorithms for wireless ad hoc networks.

single receiving node. Unicast routing is further divided into progressive energy saving, network lifetime maximizing and hybrid routing protocols. Progressive energy saving routing algorithms minimize the energy consumption per packet as it progresses from the source towards the destination. The goal of these algorithms is to find a routing path with minimum energy consumption. One drawback of the progressive energy saving routing algorithms is the overuse of a small subset of nodes. Given their goal of minimizing energy consumption, progressive energy saving routing algorithms do not account for the fact that some nodes might be over utilized, resulting in rapid battery drainage and ultimately, the partitioning of the network. Maximizing the network life algorithms remove this drawback by consuming the node energy in a more balanced manner, i.e., these algorithms distribute the traffic within the network such that no specific group of nodes is over-utilized. Finally, the network structure and connectivity based routing algorithms organize the network topology and structure such that the energy consumption is minimized while maintaining effective network connectivity.

As shown in Figure 2.1, cooperative routing algorithms can be divided into two main categories. Each of these two categories has already been defined above. As mentioned previously, the main difference between the cooperative and non-cooperative routing algorithms is the transmission strategy used at the physical layer. The next two sections discuss the relevant research contributions for the non-cooperative and the cooperative routing algorithms.

2.3 Non-cooperative Routing Algorithms

In this section, we survey a number of research works on non-cooperative power-aware routing algorithms. Before we begin, it is imperative to explain the commonly used power consumption model. The power consumption between two nodes, at a distance d from one another, is given as $P = \beta d^{\alpha} + C$, where β is a constant which depends on the receiver noise power, the receiver signal-to-noise-ratio (SNR) requirements and the transmitter power amplifier efficiency. Moreover, α is the pathloss exponent and C is power consumed by the radio electronics which depends on factors such as processing, encoding, and decoding at each node [21–23].

2.3.1 Unicast

Unicast based energy efficient routing is a well investigated form of power-aware routing. As mentioned previously, it can be further divided into progressive energy saving and network lifetime maximizing routing algorithms. There are also hybrid routing

algorithms which try to minimize power consumption while maximizing the network lifetime. Such hybrid algorithms will be discussed at the end of this subsection.

Progressive Energy Saving Routing Algorithms

As mentioned previously, these algorithms aim to minimize the energy consumption per packet as it propagates from the source towards the destination. If nodes have information about position and activity of all other nodes in the network, then the optimal power saving algorithm, that minimizes the total energy per packet, can be obtained by applying Dijkstra's single source shortest weighted path algorithm. Each edge weight is then set as $u(d) = \beta d^{\alpha} + C$, where d is the length of the edge.

In [21], Stojmenovic and Lin propose a location-aided power saving routing algorithm for static wireless ad hoc networks. The authors assume that each node within the network is aware of its own location, the location of each of its neighbors and the location of the destination. This information can be obtained through global positioning system (GPS) services or using other so called location services [24]. Through analysis, it is shown that for a source-destination pair denoted by S and D, respectively, and separated by a distance d, direct transmission between S and D is optimal if $d \leq \sqrt[\alpha]{\frac{C}{\beta(1-2^{1-\alpha})}}$, otherwise, the data should be routed with the help of intermediate relay nodes. When transmitting a message, each originating node S (either the source node or one of the intermediate nodes) will always select the NHD that minimizes the total power needed for the transmission from S to D, which is approximated by

$$P(S, D) = \beta r^{\alpha} + C + sC(\beta(\alpha - 1)/C)^{1/\alpha} + s\beta(\beta(\beta(\alpha - 1)/C)^{(1-\alpha)/\alpha}, \qquad (2.1)$$

where r is the distance between S and the selected NHD while s is the distance between the NHD and D. Numerical investigations carried out in [21] show that the proposed distributed power efficient routing algorithm outperforms all known GPS-based algorithms for different network sizes.

The work in [21] is extended in [22], where the authors study the fundamental impact of localization errors in the design of energy-efficient geographic routing algorithms. An in-depth analysis of the impact of location errors on geographic routing in terms of energy efficiency is carried out. By incorporating location error statistics into an objective function, the authors propose a new energy-efficient geographic routing algorithm. First, the authors minimize (2.1) over the set $v = \{(r, s) : r > 0, s > 0, r + s \geq d\}$. By modeling this problem as a multi-variable constrained optimization problem, the authors show that the power is minimized when S, NHD and D are all collinear and

that the optimal distance between S and NHD is given as $d_{opt} = \sqrt[\alpha]{\frac{C}{\beta(\alpha-1)}}$. Denoting this optimal location as L_O, the proposed algorithm forwards data to a neighboring node which has the minimum expected distance from L_O. Extensive performance evaluations show that the proposal is robust to location errors, thus statistically minimizing consumed transmit power as a packet is relayed from source to destination.

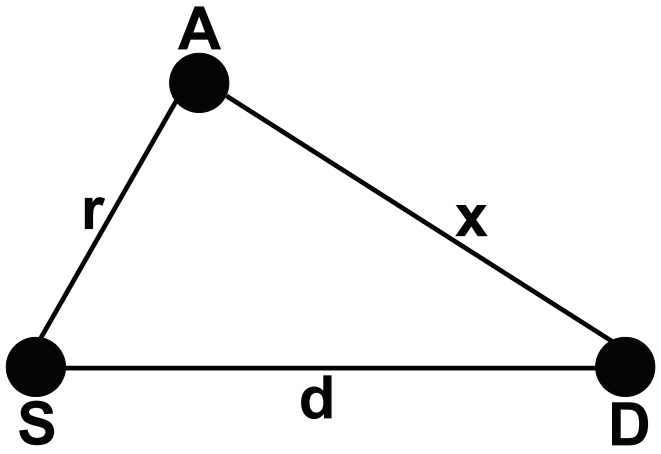

Figure 2.2: Selecting the best neighbor in localized routing protocols.

In [25], Kuruvila et al. propose two progress and location based power-aware routing algorithms. The algorithms can be explained with the help of Figure 2.2. Let $|SA| = r$, $|SD| = d$ and $|AD| = x$, with $x < d$. The first algorithm, *Power Progress Algorithm*, is based on the notion of proportional progress, i.e., the power used to make a portion of the progress towards the destination. The source node S forwards its information to a neighboring node A that minimizes the function $(r^\alpha + C)/(d - x)$, where the numerator represents the power consumed in transmitting from S to A while the denominator represents the portion of the progress made towards the destination. With similar advance continuing, there would be $d/(d - x)$ such steps, and the total cost for the whole route would be $(r^\alpha + C)d/(d - x)$. The second algorithm, called *Iterative Power Progress Algorithm*, is an extension of the Power Progress algorithm. The algorithm is explained as follows: At each hop, after selecting the node A as explained previously, the algorithm finds a neighboring node B which satisfies $(power(|SB|)+power(|BA|)) < power(|SA|)$ and has the minimum $(power(|SB|) + power(|BA|))$ measure. If such a node B exists, then it replaces SA as the NHD. This process is iteratively repeated until no further improvement is possible and node S forwards the message to the selected NHD. The process is repeated at every hop until the final destination is reached.

Xue and Li [26] propose a distributed location-aided power-aware routing (LAPAR)

algorithm. The algorithm is based on the notion of *relay regions*. The relay region of a source node S and a relay node R is the set of destination nodes for which relaying through R is more power efficient than transmitting directly from S [23]. In LAPAR, the routing decisions are based on the information regarding a node's neighbors and the location of the destination node. If the destination node lies in a single neighbor's relay region, that neighbor is chosen as the NHD. If the destination node lies in the intersection of relay regions for multiple neighbors, a greedy strategy is used to select the NHD. Simulation results show that LAPAR adapts well to node mobility.

The Power-Aware Routing Optimization protocol (PARO) [27] reduces transmission power by taking advantage of intermediate forwarding. Using PARO, one or more intermediate nodes called *redirectors* elects to forward packets on behalf of source-destination pairs, thus reducing the aggregate transmission power consumed by wireless devices. PARO is applicable to a number of networking environments including sensor networks, home networks and mobile ad hoc networks.

In [28], Ko and Vaidya propose location aided routing (LAR) protocol for mobile ad hoc networks. In LAR, when node S wants to establish a route to node D, it computes an expected zone for D based on available position information. If no such information is available, LAR is reduced to simple flooding. If location information is available (e.g., from a route that was established earlier), a request zone is defined as the set of nodes that should forward the route discovery packet. The request zone typically includes the expected zone. Two request zone types have been proposed in [28]. The first is a rectangular geographic region. In this case, nodes will forward the route discovery packet only if they are within that specific region. This type of request zone is shown in Figure 2.3 (Redrawn from [28]). The second is defined by specifying (estimated) destination coordinates plus the distance to the destination. In this case, each forwarding node overwrites the distance field with its own current distance to the destination. A node is allowed to forward the packet again only if it is at most some δ (system parameter) farther away than the previous node.

In [29], Subbarao proposes the minimum power routing (MPR) algorithm, which addresses both, reliability and power consumption issues. The algorithm is based on channel inversion based power control. Each node transmits with just enough power to ensure reliable communication. The transmit power for a link $i - j$, where i is the transmitter and j is the receiver, is given as $P_{ij} = \frac{\mathcal{E}_b}{h_{ij} d_{ij}^{-\alpha}}$, where $\mathcal{E}_b$ is the desired bit-energy-to-noise-density ratio at node j, h_{ij} is the channel coefficient which also includes the interference for the link $i - j$ and d_{ij} is the distance between i and j. When calculating potential transmission costs for reliable message delivery, link error

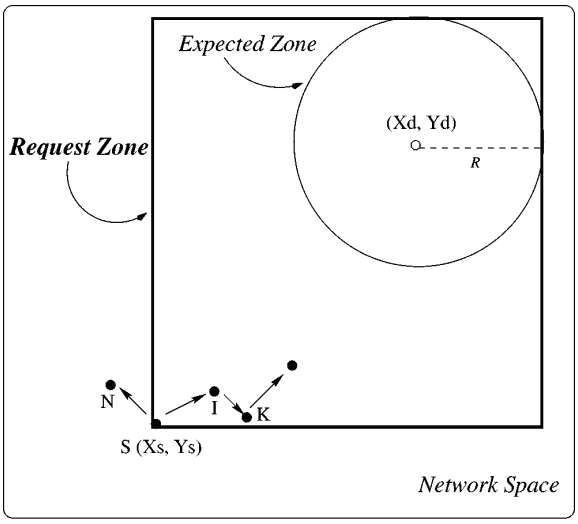

Figure 2.3: Example of request and expected zones in LAR.

rates are also taken into consideration.

In [30], Zimmerling et al. propose the minimum energy relay routing (MERR) algorithm for linear wireless sensor networks. The MERR is based on the idea that the distance between two nodes that transmit data is very closely related to the energy consumed on the entire path. Each sensor seeks independently for that node within its maximum transmission range whose distance is closest to the optimal distance d_{opt}, explained earlier in this section. Once all sensors have decided on their respective next hop node, they adjust their transmission power to the lowest possible level such that the radio signal can still be received by this node without any errors. In operation, a sensor transmits always to its preassigned next-hop node, regardless of whether it is data received from other upstream nodes or data obtained by its own sensor readings.

Maximizing Network Lifetime Routing Algorithms

One of the drawbacks associated with progressive energy saving routing algorithms is the lack of consideration for the remaining battery power of the nodes participating in the routing process. This results in the over-use of a subset of nodes which rapidly drain out their batteries, resulting in possible partitioning of the network. This disables further information delivery even though there are many remaining nodes with plenty of energy. To make up for this drawback, maximizing network lifetime protocols consume the node energy in a more balanced manner. In [31], the authors consider the problem of energy-aware routing with distributed energy replenishment. They provide an algorithm that achieves a logarithmic competitive ratio and is asymptotically

optimal with respect to the number of nodes in the network.

The energy-aware temporarily ordered routing algorithm (E-TORA), proposed in [32], selects routes according to the hop-count and the remaining energy of the network nodes. The E-TORA mechanism is based on selecting the route that maximizes the function $f = \zeta\frac{\mathcal{E}_{\min}}{\mathcal{E}} + (1-\zeta)\frac{h}{h_{\min}}$, where ζ is a constant between 0 and 1, $\mathcal{E}_{\mathbf{min}}$ is the minimal energy of the nodes on the route, $\mathcal{E}$ is the average energy of the nodes on the route, h is the hop count of the route and $h_{\min}$ is the hop count of the shortest path. Results show that E-TORA effectively balances the energy consumption of each node and evidently, increases the lifetime of the network.

In [33, 34], Chang and Tassiulas propose distributed energy-efficient algorithms by formulating the routing problem with the objective of maximizing the system lifetime given the sets of origin and destination nodes and the information generation rates at the origin nodes. A class of flow augmentation algorithms and a flow redirection algorithm is proposed, which balance the energy consumption rates among the nodes in proportion to their energy reserves. Through linear programming, the authors compute the optimal achievable lifetime of the network and show that when there are multiple power levels then the achievable lifetime is close to the optimal one most of the time. Simulation results confirm that the proposed schemes maximize the network lifetime by as much as 60% when compared with conventional minimum transmitted energy routing.

The minimum battery cost routing (MBCR) algorithm, proposed in [35], utilizes the technique of cost function to maximize the lifetime of the network. In MBCR, the battery cost R_j, for the route j with D_j nodes is given as $R_j = \sum_{i=0}^{D_j-1} f_i(c_i^t)$, where $f_i(c_i^t) = \frac{1}{c_i^t}$ and c_i^t is the remaining battery capacity of the node i at time t. The algorithm attempts to find the path which has the minimum battery cost, i.e., it selects $R_i = \min\{R_j | j \in A\}$, where A is the set containing all possible routes. In addition to MBCR, [35] also proposed the min-max battery cost routing (MMBCR) algorithm. The algorithm is an extension to MBCR and it is based on the observation that with the summation based cost function used in MBCR, the algorithm can still select a route containing nodes with little remaining battery capacity. For example. if the other nodes along the route have large remaining capacity. This issue is addressed in MMBCR where the battery cost R_j is defined as $R_j = \max_{j \in route\_j} f_i(c_i^t)$.

In [36], Yu et al. propose the geographic energy-aware routing (GEAR) algorithm which utilizes energy-aware and geographically informed neighbor selection heuristics to route a packet towards the target region. Two main characteristics of this protocol are: 1) When a closer neighbor to the destination exists, GEAR picks a NHD among all the

neighbors that are closer to the destination. 2) If no such neighbor is available, GEAR picks a NHD that minimizes some cost value of this neighbor. The main advantage of the GEAR is that each node knows its own remaining energy level and its neighbors' remaining energy levels through a simple neighbor hello protocol. Simulation results carried out in [36] suggest that GEAR performs significantly better than the baseline, non-energy-aware routing algorithm.

Singh et al. [14] propose to use a function $f(A) = 1/g(A)$, where g(A) denotes the remaining lifetime of node A ($g(A)$ is normalized to be in the interval [0,1]) while $f(A)$ denotes node A's reluctance to forward packets. Thus reluctance grows significantly when lifetime approaches 0. The reluctance $f(A)$ is used as a weight in a shortest weighted path algorithm. The algorithm attempts to choose a path that minimizes the sum of $f(A)$ for nodes on the path. In [37], Mabrukh and Subbarao propose the maximum survivability routing (MSR) algorithm which aims at preserving network connectivity by choosing routing paths according to the remaining battery life of nodes along the route towards the destination. In MSR, the cost function for a route R is given as $C_R \equiv f(T_i, i \in R) = (\sum_{i \in R}(1/T_i)^\eta)^{1/\eta}$, where $\eta \geq 1$ is a parameter while T_i is an estimate of the remaining battery life. T_i is defined as the ratio of the node's remaining power and power draining rate.

In [21], Stojmenovic and Lin propose a cost aware localized algorithm which is based on constant power for each transmission. The cost $c(A)$ of a route from S to D via a neighboring node A is given as $c(A) = \frac{1}{g(A)} + N$, where $g(A)$ denotes the remaining lifetime of A while N is the cost of remaining path. N is assumed to be proportional to the number of hops between A and D. The number of hops, in turn, is proportional to the distance $d = |AD|$, and inversely proportional to the transmission radius R. Thus $N = td/R$, where factor t is a constant which depends on the network conditions. The cost $c(A)$ of a route from S to D via A is thus estimated to be $c(A) = f(A) + td/R$. If the destination is one of the neighbors of node S currently holding the packet then the packet will be delivered to D. Otherwise, S will select one of its neighbors A which will minimize $c(A)$. The algorithm proceeds until the destination is reached, if possible, or a node has no closer node to destination than itself.

Kim et al. [38] focus on MANETs. The authors are of the view that the battery's drain rate is a more useful metric than the remain capacity. Accordingly, the cost function used in [38] for a node n_i is given as $C_i = \frac{RBP_i}{DR_i}$, where RBP_i is the residual battery power and DR_i is the battery's drain rate. Each node computes its drain rate based on changes in its energy level and adjusts its cost accordingly. The lifetime L_p of a routing path P equals the minimum value of C_i over the entire path. The authors

propose a minimum drain rate (MDR) mechanism which selects the path with the highest lifetime value. Performance evaluation, carried out in ns-2, shows that MDR can prolong the lifetime of both, network nodes and connections.

The distributed energy-aware routing algorithms proposed in [39] focus on maximizing the amount of information transmitted per energy unit while also balancing energy usage among all network nodes. Notably, the authors propose two decision matrices. The first matric, denoted as D_{ij}, for a link (i, j), is defined as $D_{ij} = \frac{P_{ij}}{\min(R_i, R_j)}$, where P_{ij} is the power required to transmit data from node i to node j while R_i and R_j represent the residual energies of nodes i and j, respectively. The path which minimizes D_{ij} is then selected to route the information. The second metric attempts to find paths with more residual energy even though it may consume additional energy. It is defined as $D_{ij} = W_p \frac{P_{ij}}{P_{\max}} + W_e \frac{E_j^o}{E_j^r}$, where W_p and W_e are weights that can be used to favor either of the two terms, $P_{\max}$ is the maximum transmission power level while E_j^o and E_j^r, respectively, represent the initial energy level and residual energy level of node j.

Hybrid Routing Algorithms

Hybrid routing algorithms attempt to find the minimum energy paths while maximizing the network lifetime. Stojmenovic and Lin [21] propose two different ways to combine power and cost metrics into a single power-cost metric, based on the product and sum of two metrics, respectively. If the product is used, then the power-cost of sending message from S to a neighbor A is equal to $powercost(S, A) = f(A)u(r)$, where $|AS| = r$, $f(A)$ is a function of the remaining battery lifetime for node A and $u(r) = \beta r^{\alpha} + C$. The sum, on the other hand, leads to $powercost(S, A) = au(r) + bf(A)$, for suitably selected values of a and b. In the proposed power-cost efficient routing algorithm, the node S currently holding the message forwards it to a neighbor A that minimizes $powercost(S, A)$. More works based on hybrid routing algorithms can be found in [35, 40, 41].

2.3.2 Multicast/Broadcast Algorithms

Wireless ad hoc networks make extensive use of multicasting and broadcasting during communication. Given the energy constraints placed on the networks nodes, designing energy-efficient multicasting and broadcasting protocols in WAHNs has readily become an active research area. In [42], Wan et al. propose the shortest path first (SPF) multicast algorithm which is based on the Takahashi-Matsuyama Steiner tree heuristic [43]. SPF maintains a directed tree rooted at the source node. The tree starts with the

source node. At each iteration, a path to one of the desired destinations, which is not already included into the tree, is added to the tree. The added path is the one which consumes minimum power from one of the nodes already included in the tree. This path is be found by collapsing the entire tree into one artificial node and then applying the single-source shortest-path algorithm. The algorithm continues until all the desired destinations are included in the tree. The authors in [42] also propose the minimum incremental path first (MIPF) algorithm, which is similar to SPF except that the new path included in the tree is the one with the least incremental power [1].

The broadcast incremental power (BIP) algorithm, presented in [44], is similar to the Prims minimum spanning tree (MST) algorithm. BIP maintains a minimum-energy broadcast tree rooted at the source node. The algorithm begins by searching for the node which can be reached with minimum power by the source node. Once found, this new node is added to the tree. The algorithm then repeatedly determines which new node can be reached with minimum additional cost from the nodes already in the tree and adds the new node into the tree. The algorithm continues until all the nodes are included into the tree. The BIP algorithm can used be used for multicast transmission as well, by eliminating the transmissions that are not required by the multicast group. Another extension to BIP is presented in [45], where the authors also take the residual battery level of a node into consideration. Similarly, in [46], the authors propose the multicast incremental-decremental power (MIDP) algorithm which is based on a broadcast tree instead of a multicast tree. The algorithm iteratively reconstructs the broadcast tree by switching a tree arc with a non-tree arc to obtain the maximal decremental power of the corresponding multicast tree. Finally, it prunes the broadcast tree to be a multicast tree.

Leung et al. [47] propose the distributed minimum-energy multicast (DMEM) algorithm which is a distributed minimum energy multicast algorithm with a set of localized operations for wireless ad hoc networks. In these operations, each node requires only the knowledge of and distances to all its neighboring nodes. In each iteration of DMEM, all the network nodes, including the tree nodes and the non-tree nodes, perform a localized operation to find a new transmission power such that the tree topology still holds while the tree power is reduced. Simulation results show that DMEM performs better than MIDP for medium and large sized groups while MIDP is better for the smaller sized groups.

In [48], Jiang et al. propose the energy-efficient multicasting routing protocol

[1]The incremental power of a path is defined as its total power minus the transmission power of the first node in the tree.

(E^2MRP). Instead of one, E^2MRP iteratively uses two route selection metrics. The first metric minimizes the energy consumed per packet while the second one minimizes the maximum node cost. The first cost function, i.e., the one that minimizes the energy consumed per packet, is given as

$$C_{R_k} = \sum_{i=1}^{p-1} P_{i,i+1} = \sum_{i=1}^{p-1} d^{\alpha}(n_i, n_{i+1}), \tag{2.2}$$

where R_k is the route consisting of the nodes $n_1, n_2, ..., n_p$, $P_{i,i+1}$ is the transmission power from n_i to n_{i+1} and $d(n_i, n_{i+1})$ is the inter-node distance. The cost for the second metric, i.e., the one that minimizes the maximum node cost, is given as

$$C_i(V_i(t)) = \psi / V_i(t), \tag{2.3}$$

where ψ is a constant and $V_i(t)$ denotes the energy of n_i at time t. $C_i(V_i(t))$ represents the reluctance of n_i to relay a packet. When a source node has multicasting data to send, it floods a multicast request message. The destination nodes calculate the costs of multiple routes, and select the route with the minimum cost as the multicasting route. The relaying group is established after the destinations send back the reply message.

Thus far, all the broadcast/multicast algorithms discussed in this survey were based on nodes with omni-directional antennas. In [49] however, Hou et al. propose the maximum life-time routing for multicast with directional antennas (MLR-MD) algorithm. Initially, MLR-MD algorithm starts with a single beam from the source covering all multicast destination nodes. Then, it iteratively improves the lifetime performance of the current solution by identifying the nodes with the smallest lifetime and revising routing topology as well as corresponding beam-forming behavior for an increased network lifetime. The authors claim that the algorithm has strictly polynomial time complexity. More detailed surveys on energy-efficient multicasting and broadcasting can be found in [5, 18, 50].

2.3.3 Network Structure & Connectivity Based Routing Algorithms

In WAHNs, the nodes are connected to each other through wireless links. As a nodes transmission power is adjusted, the network topology changes accordingly. Moreover, the radios utilized for communication consume power not only when operating (trans-

mitting/receiving), but also when idle or listening. This idle energy consumption is, over time, significant and cannot be ignored. Thus, these radios can be turned off to save power. Yet another method to minimize power consumption is to assign a hierarchal structure to the network where nodes with high energy levels are selected as the control nodes to maintain communication within a cluster of nodes. Thus, the network structure and connectivity based routing algorithms alter network topology such that energy consumption is minimized while maintaining effective network connectivity.

The low energy adaptive cluster hierarchy (LEACH) protocol proposed in [51] is a clustering based hierarchal routing protocol. LEACH is divided into two phases. In the first phase, the nodes arranged into clusters and the cluster heads are selected. The cluster heads aggregate, compress and forward the data to the base station. During each round, a stochastic algorithm is used by each node to determine whether or not it should become a cluster head. Once a node becomes a cluster head in a given round, it cannot become cluster head again for P subsequent rounds, where P is the desired percentage of cluster heads. After P subsequent rounds, the probability of a node becoming a cluster head in each round is 1/P. This rotation of cluster heads leads to a balanced energy consumption to all the nodes and hence to a longer lifetime of the network. In the second phase, the data is sent to the base stations. In order to minimize the overhead, the duration of this second phase is kept longer than the the first phase. Moreover, each node that is not a cluster head selects the closest cluster head and joins that cluster. The cluster head creates a schedule for each node in its cluster to transmit its data. Results show that LEACH provides the high performance needed under the tight constraints of the wireless channel. Authors in [51] also propose the LEACH-C which is a centralized LEACH protocol in that the base station forms the node clusters.

In [52], Xu et al. propose the basic energy-conserving algorithm (BECA). BECA attempts to turn off the radios of the nodes which are not sending, forwarding or receiving any data. The algorithm is based on the flow diagram shown in Figure 2.4. Initially, a node is assumed to be in the *sleeping* state. If there is any local information that needs to be transmitted, the node goes into the *active* state. Otherwise, it waits for T_s seconds before going into the *listening* state. Once in the listening state, the node listens if there is any data to send or receive. After listening to T_l seconds, if there is no data to send/receive, the node goes back to sleep state, otherwise, i.e., if there is data to send/receive, the node goes into the active state. Once a node enters the active state, it sends/receives the data and then waits in this state for T_a seconds. If there is no further data to process, the node goes back into the sleeping state. If

a receiver node is in the sleep state when a transmitter sends its data, the sender repeatedly retransmits its message until the data is successfully delivered. Simulation results confirm that BECA can achieve an energy saving of up to 40% as compared to the traditional routing protocols for wireless ad hoc networks.

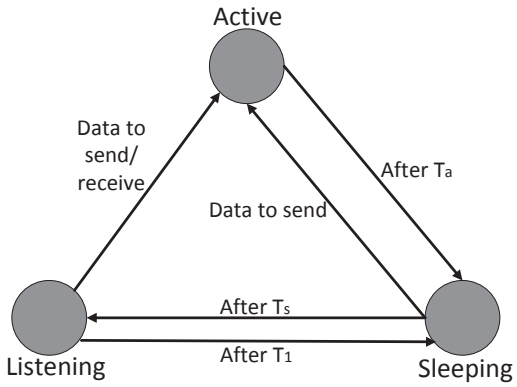

Figure 2.4: Radio states and state transitions in BECA.

Manjeshwar and Agrawal [53] propose the adaptive threshold sensitive energy efficient sensor network (APTEEN) algorithm for WSNs. APTEEN aims at capturing periodic data collections and reacting to time critical events in an energy efficient manner. A central base station organizes the nodes into clusters. Thereafter, the cluster heads broadcast the required parameters such as 1) Attributes which consist of physical parameters which the user is interested in obtaining data about; 2) Hard and soft thresholds which are the values of the attributes which can trigger a node to transmit data; 3) TDMA schedule which assigns a slot to a node and 4) Count time which is the maximum time period between two successive reports sent by a node. Following this broadcast, the cluster heads perform data aggregation. APTEEN offers the added flexibility of allowing the user to set the count time and threshold values for the attributes. Energy consumption is controlled by the count time and the threshold values.

In [54], Lotf et al. propose the extending lifetime of cluster head (ELCH) protocol which aims to extend the life of the network utilizing a hybrid protocol, which combines the cluster architecture with multi-hop routing. In ELCH, the sensor nodes vote for their neighbors in order to elect the most suitable cluster head. Initially, the nodes elect the best cluster head and form the clusters accordingly. The clusters are formed in a way that they consist of one cluster-head and some sensors. The sensors are chosen based on their location. TDMA is used for each cluster member in each round. At each selection round, each cluster-head maintains a table with maximum power for each node within the cluster. After the above process is completed, the cluster heads

form a multi-hop routing backbone. All the nodes pass their information to their local cluster heads while the cluster heads forward the data to the sink through multi-hop routing.

Reference [55] describes the development of an efficient routing protocol, named scaling hierarchical power efficient routing (SHPER). The algorithm assumes the co-existence of a static base station and a set of static homogeneous sensor nodes which are randomly distributed within a delimited area of interest. The base station is located far away from the sensor nodes. It is further assumed that the base station has unlimited power supply while the network nodes are energy constrained. Thus, the base station is able to transmit with high enough power to reach all nodes within the sensor network. SPHER starts with a broadcast transmission in which the base station transmits a TDMA schedule. In response to this, the sensor nodes advertise themselves and the base station estimates the distance to each of the sensor nodes through this advertisement. Following this, the base station selects the high energy nodes as cluster heads informs all the nodes about cluster head IDs and their relateed threshold values. Each cluster head finds the most energy efficient route towards the base station.

More works related to network structure and connectivity based algorithms can be found in [5, 19, 20]

2.4 Cooperative Routing Algorithms

Cooperative routing is a relatively new paradigm in energy efficient routing with most of the works starting in 2003/4. Energy efficient cooperative routing algorithms are truly cross-layered algorithms as they attempt to simultaneously optimize the performance of the physical and the network layer in terms of energy efficiency. The algorithms can be classified into progressive energy saving and maximizing network lifetime routing algorithms. We begin with a survey of progressive energy saving cooperative routing algorithms.

2.4.1 Progressive Energy Saving Cooperative Routing Algorithms

One of the pioneer works in progressive energy saving cooperative routing algorithms was presented in [56]. A more detailed version of the same work was presented in [57]. In [56, 57], the authors utilize cooperative diversity at the PHY layer to design power saving routing algorithms. Initially, the authors formulate the problem of minimizing

the transmission power when a group of nodes transmits the same information simultaneously towards the destination. The sum power is minimized under the constraint that the received SNR at the destination is larger than a minimum required threshold. Then, the authors design a Dynamic Programming based optimal cooperative routing algorithm. Through analytic derivations, it is shown that the optimal algorithm can achieve energy saving gains of 39% and 56% in regular line and grid networks with a large number of nodes, respectively. Following this, two sub-optimal algorithms are proposed with polynomial complexity. The first sub-optimal algorithm, known as cooperation along the minimum energy non-cooperative path (CAN-L), is a centralized routing algorithm. CAN-L initially calculates the optimal non-cooperative route towards the destination. Then, the last L nodes along the optimal non-cooperative route cooperate to transmit data towards the next hop destination. The second algorithm, called progressive cooperation (PC-L), finds the optimal non-cooperative route by combining all or a subset of nodes in a *reliable* set into a single node, denoted by super node, and finding the shortest non-cooperative route between the super node and the destination. Through simulations, it is shown that these algorithms can achieve average energy savings of about 50% in random networks, as compared to the non-cooperative schemes. Building on the above described works, in [58], Li et al. present an integer programming formulation of the minimum energy cooperative path problem towards an optimal solution for static wireless networks where the locations of the nodes are known a priori.

The minimum energy cooperative path problem is shown to be NP-complete in [59, 60]. Further, the authors propose the cooperative shortest path (CSP) routing algorithm to approximate the minimum energy path between the source and the destination nodes. CSP uses the Dijkstra's shortest path algorithm as the basic building block and reflects the cooperative transmission properties in the relaxation procedure. Assuming $d[u]$ represents the estimated total cost of the cooperative shortest path from the source node S to node u, at each hop, if $d[v] > d[u] + Coop(uv)$, then $d[v] = d[u] + Coop(uv)$ and node u is selected as the predecessor to node v. The rest of the algorithm follows a similar structure as Dijkstra's algorithm. Through simulations, it is shown that the proposed CSP algorithm consistently outperforms the non-cooperative shortest path algorithms under different network conditions. Finally, the authors also discuss the distributed implementation of their proposed algorithm. In [61], Sikora and Laneman analyze cooperative routing in linear wireless network for both, power-limited and bandwidth-limited regimes.

In [62], Yang et al. investigate the cooperation efficiency of the multiple-relay

channel when carrier-level synchronization is not available and all nodes use a decode-forward scheme. The authors show that an optimal sequential path and a corresponding power allocation policy always exists for every channel realization. Since the optimal path, due to its complexity, cannot be implemented in practice, the authors propose two heuristic algorithms, namely, cooperative routing along truncated non-cooperative route (CTNCR) and source node expansion routing (SNER). CTNCR initially finds the optimal non-cooperative path between the source and the destination. Then, the algorithm sets the source node as the *active* node. Among the active node's downstream nodes, the one which requires the least power to decode the message successfully is selected as the next hop destination while all other nodes are removed or truncated from the path. The procedure continues until the destination is reached. The second algorithm, i.e., SNER, divides the network into undecoded and decoded sets: the undecoded set only has the source initially while the decoded set has the rest of the nodes. In each iteration, one node that requires the least transmission power is added to the first set until the destination is reached.

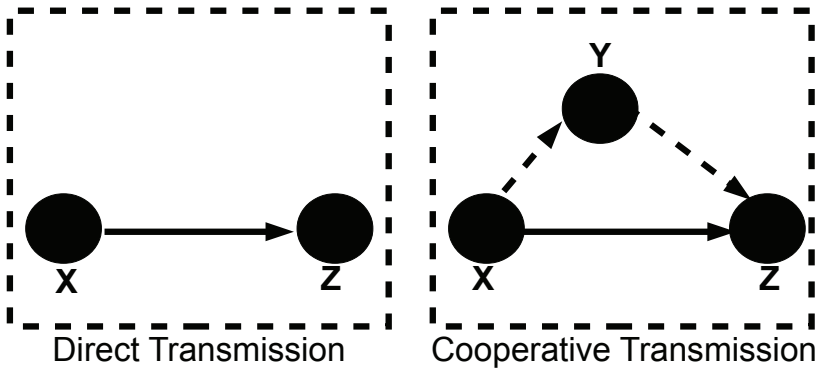

Figure 2.5: Cooperative Transmission and Direct Transmission modes.

In [63], the authors investigate power-aware cooperative routing in networks with flat quasi-static fading channels. The channel coefficients are assumed to be constant during a complete frame, and may vary from a frame to another. Further, all the channel terms are assumed to be independent of one another. The authors define two modes of transmission, namely, direct transmission and cooperative transmission. The two modes can be explained with the aid of Figure 2.5. In direct transmission, a node x transmits non-cooperatively towards node z. In cooperative transmission, node x transmits directly towards node z while node y overhears this transmission, i.e., due to the broadcast nature of the wireless medium. If z does not decode the transmitted

symbol successfully and y overhears it successfully, then y re-transmits the symbol instead of x. If both y and z do not successfully receive the transmitted symbol, then x re-transmits. The authors derive the transmission power required to minimize the overall power consumption of the cooperative transmission. Based on these transmission modes, the authors design a distributed power efficient routing algorithm, namely, Minimum Power Cooperative Routing (MPCR). MPCR utilizes cooperative transmission as a basic building block and uses Distributed Bellman-Ford shortest path algorithm to calculate the optimal power-saving route. Theoretical analysis shows that in regular line and grid networks, MPCR can achieve power saving of 65.61% and 29.8%, respectively. From simulation results, MPCR algorithm can have 37.64% power saving in random networks compared to other cooperation-based routing algorithms.

Dehghan et al. [64] study the energy efficiency and throughput performance of cooperative routing for wireless networks. The authors argue that while the energy efficiency of cooperative beamforming has been extensively explored in literature, its impact on network throughput has been overlooked. It is shown that although cooperative routing is more efficient in terms of energy savings, however, it results in a sharp reduction in network throughput as compared to non-cooperative routing. Various reasons for this performance degradation are identified and solutions are proposed that increase network throughput by exploring multi-beam cooperative beamforming in which multiple nodes cooperatively beamform towards multiple destinations simultaneously [65].

2.4.2 Maximizing Network Lifetime Routing Algorithms

In [66], Zhou et al. adopt cooperative mutiple-input-single-output (MISO) based routing strategy for energy-constrained wireless sensor networks. Initially, the paper analyzes the physical layer energy consumption model of cooperative transmission in the scenarios of one hop and hop-to-hop for energy-efficient routing in order to prolong the network lifetime. Then, the authors propose a cluster based cooperative routing algorithm. The proposed algorithm divides the network into clusters with the cluster heads selected in a similar way as the LEACH algorithm described earlier in Section 2.3.3. Following this arrangement of the network, the algorithm consists of two phases. In the first phase, the cluster heads of each cluster select the most suitable set of cooperating nodes to participate in transmission from node i towards the cluster head j.

The cooperating nodes are selected based on a cost function which is defined as

$$p_{ij}^{c} = \frac{\sum_{l \in c_{ij}} E_{bt\_t\_lj}^{miso}}{\max_{l \in c_{ij}} E_l} . \frac{\sum_{l \in c_{ij}} E_{bt\_r\_lj}^{miso}}{E_j}, \tag{2.4}$$

where c_{ij} is the set of cooperating nodes used to transmit data from node i to cluster head j while $E_{bt\_t\_lj}^{miso}$ and $E_{bt\_r\_lj}^{miso}$ respectively represent the transmission and circuit energy consumption of a single cooperative MISO link from cooperating nodes l to cluster head j. The set of cooperating nodes which minimizes (2.4) is selected. In the second phase, a source node S calculates the shortest cost path towards its destination D. While calculating the shortest path, the cost for a link $i - j$ is calculated on the basis of cooperative transmission from i to j. Simulation results show that the proposed algorithm significantly prolongs the network lifetime as compared to the non-cooperative routing algorithms for WSNs.

Space-time block-code encoded (STBC) cooperative transmission is investigated in [67], where Li et al. study the cooperation overhead, synchronization and energy efficiency of cooperative transmission. An analysis of the trade-off between transmission power consumption and the overhead and electronic circuit energy consumption is presented. Further, the authors in [67] incorporate cooperative transmission into the LEACH protocol proposed in [51] to improve its energy saving potential. Simulation results suggest that LEACH with cooperative transmission can prolong the network lifetime by 30%.

In [68], Pandana et al. propose a joint cooperative transmission and energy aware routing algorithm to prolong the network lifetime. Initially, the authors propose a maximum lifetime power allocation scheme by re-deriving the minimum power allocation problem proposed in [57]. The authors are of the view that the route with extremely low residual energy node can be avoided by weighting the energy metric with the normalized residual energy of each node. With this idea as a corner stone to their work, the authors propose two centralized algorithms, namely, Centralized cooperative MTE-n and Centralized cooperative FA(x_1, x_2, x_3)-n. The MTE-n algorithm initially finds the minimum energy cooperative path between the source and the destination nodes by using the link cost for cooperative transmission as the weight for each edge. The last n nodes along this minimum energy route are selected for cooperative transmission. At each hop, each cooperating node is allocated the optimal transmission power required to maximize network lifetime. The FA-n algorithm is similar to MTE apart from the first step, i.e., the algorithm begins by selecting the optimal route using the flow augmentation (FA) algorithm presented in [34]. While the above two algorithms

are centralized, their distributed counterparts are also presented in [68]. Simulation results confirm that the proposed distributed algorithm significantly prolongs the network lifetime as compared to the baseline non-cooperative routing algorithms.

2.5 Concluding Remarks

The chapter reviewed a plethora of energy-efficient and power-aware routing protocols designed for wireless ad hoc networks. Based on the transmission techniques used at the physical layer, this study broadly classified the power saving routing algorithms into two main categories, i.e., non-cooperative and cooperative routing algorithms. The algorithms belonging to each of these two categories were further divided into various groups, based mainly on the routing techniques used at the network layer.

The remainder of this thesis focuses on progressive energy saving routing algorithms for static wireless ad hoc and mesh networks that aim to extend network connectivity. Example scenarios include wireless roof-top networks, setup to provide last mile connectivity to residents of a neighborhood. Mostly, such networks have continuous energy supply, so the network lifetime is not a critical issue. However, the cost of maintaining and operating the network is directly related to the network power consumption. Consequently, it is important to focus on progressive energy saving routing algorithms, since they minimize the end-to-end power consumption.

Chapter 3

Adaptive Power-Aware Routing

Since the existing energy efficient routing algorithms are fixed and unaware of the channel fading dynamics, they may be suitable if the antennas at network nodes are situated in very high altitudes and have highly directive links. Although, some physical experimental results suggest that even in such scenarios the effect of fading may not be negligible. Particularly in urban areas, the impact of fading cannot be ignored. Thus, when deployed in real world scenarios, current energy efficient routing algorithms suffer from severe performance degradation in terms of power consumption. This chapter investigates the impact of fading on power saving routing algorithms and introduces fading aware decision metrics that help the current node select the optimal next hop destination. Then, using these metrics, a new power saving routing algorithm is proposed that takes into account the fading effect. The algorithm is optimized based on the location knowledge of the nodes and the localized channel condition of each node. Simulation results confirm that the proposed algorithm outperforms the existing well-known power saving routing algorithm.

3.1 Introduction

As mentioned previously, this research focuses mainly on the active energy saving routing algorithms, i.e., the algorithms that minimize the power consumed per packet, [21, 26, 27, 69]. All these active energy saving routing algorithms only use the distance between the network nodes as the metric to select the optimal route towards the destination. Since these algorithms are unaware of the channel fading dynamics, they may be suitable for cellular networks that have high base station (BS) towers with highly directional transmissions. Although, some physical experiments suggest that even in such scenarios, the effect of fading is not be negligible [70–72]. Particu-

larly in urban environments, the impact of fading cannot be ignored. Thus, the above mentioned routing algorithms suffer from severe performance degradation in terms of power consumption, when implemented in a real environment.

In view of the above argument, this chapter focuses implicitly on the impact of the characteristics of the physical (PHY) layer on the performance of the network layer. The power-saving routing (PSR) algorithm, introduced in [21], is used as the baseline routing scheme. PSR takes into account only the path loss component of the channel. As shown later in the chapter, the fading coefficients cannot be incorporated directly into PSR, due to their randomness, hence, the performance of the PSR algorithm is susceptible to the impact of multipath reflections. Keeping this drawback in view, the current chapter introduces two decision metrics which can be used to select the next hop destination. Using these metrics, a new power-aware routing algorithm is proposed that is adaptive with realistic channel variations in terms of multipath fading, and hence, is suitable for interconnecting the base station subsystems (BSS) in a cellular mesh networks or interconnecting the randomly placed nodes in an ad hoc network. Results show that the proposed routing algorithm significantly reduces energy consumption as compared to PSR. Furthermore, this power saving is achieved while consuming almost the same number of hops as the baseline routing scheme.

The rest of the chapter is organized as follows. Section 3.2 describes the system model in detail. Section 3.3 discusses PSR and analyzes the impact of fading on it. A new power saving routing algorithm is proposed in Section 3.4 while the simulation results are shown Section 3.5. Finally, the conclusions are drawn in Section 3.6.

3.2 System Model

This section derives the system model that is used throughout this chapter.

3.2.1 Network Architecture

Two different types of network are considered in this study. The first is a cellular wireless mesh network, consisting of a large number of regularly distributed cellular base stations. This scenario is shown in Figure 3.1, where the base station (BS) is located at the center of each cell. The second network is a wireless ad hoc network consisting of a set of randomly distributed nodes within a specified region, as shown in Figure 3.2. It is assumed that each node or BS has an omnidirectional antenna. Notice that in the following, the term node can refer to the nodes in the ad hoc network of Figure 3.2 or the base stations in the wireless mesh network of Figure 3.1.

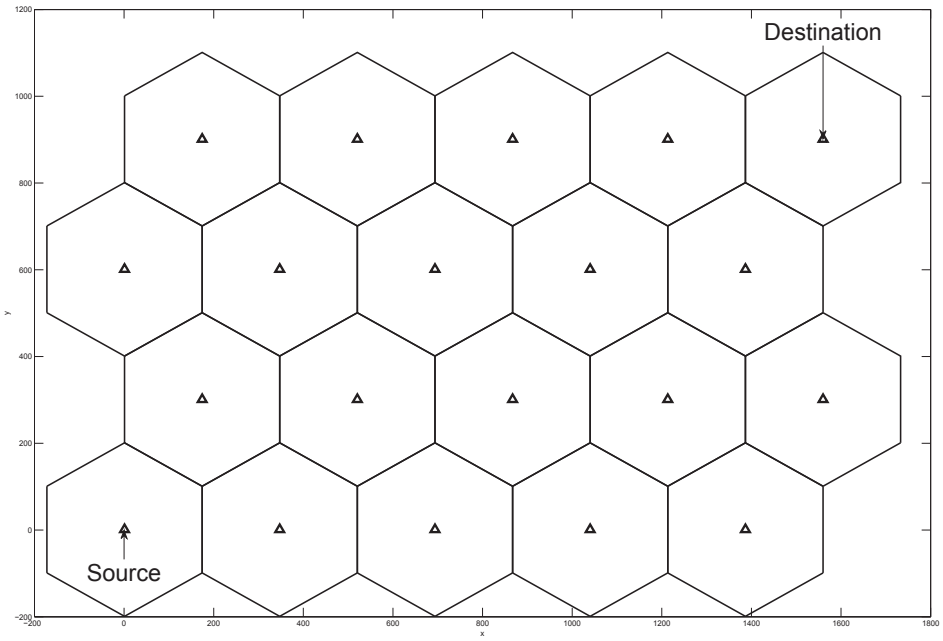

Figure 3.1: A wireless mesh network of cellular base stations.

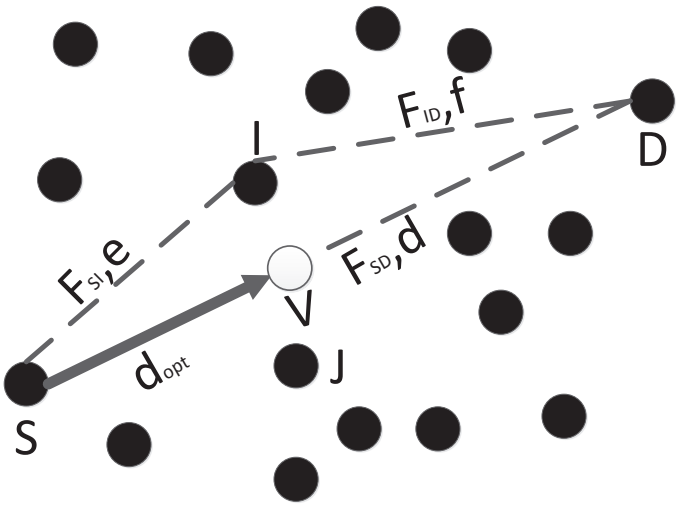

Figure 3.2: An ad hoc wireless network.

3.2.2 Channel Model

The channel model between the transmitter a_m and receiver z_n is given as

$$h_{mn}(t) = F_{mn}(t)\sqrt{1/L_{mn}}, \tag{3.1}$$

where $h_{mn}(t)$ represents the channel gain, $F_{mn}(t)$ represents the Rician fading coefficient while L_{mn} is the distance dependent pathloss. The fading parameter $F_{mn}(t)$ is modeled as [73], [74]

$$F_{mn}(t) = \sqrt{\frac{K}{K+1}} + \sqrt{\frac{1}{K+1}} M_p(t), \tag{3.2}$$

where K denotes the ratio of deterministic-to-scattered power while $M_p(t)$ represents the statistically independent, unit variance, complex Gaussian random variable. Furthermore, the pathloss is modeled as

$$L_{mn} = (4\pi/\lambda)^2 d_o^{2-\alpha} d_{mn}^{\alpha}, \tag{3.3}$$

where α is the pathloss exponent, λ is the wavelength, d_o is the reference distance for the antenna far field while d_{mn} is the distance between the transmitter a_m and the receiver z_n.

3.2.3 Link Cost Model

This section formulates the link costs associated with the transmission of information over a single hop. It is assumed that the power transmitted by node a_m is given by P_m. The signal received by node z_n, due to transmission from node a_m is given by

$$y_n(t) = h_{mn}(t)\sqrt{P_m} s_n(t) + \eta_n(t), \tag{3.4}$$

where $h_{mn}(t)$ represents the channel between nodes a_m and z_n, $s_n(t)$ is the data symbol intended for node z_n and $\eta_n(t)$ is the receiver noise with power P_η. To simplify notation, the time arguments t are dropped. For successful decoding, it is assumed that the receiver z_n requires a minimum SNR of γ_n. With these assumptions, the point to point transmission link cost is given as

$$LC(a_m, z_n) \equiv P_t = \frac{\gamma_n P_\eta}{|h_{mn}|^2}, \tag{3.5}$$

3.2.4 System Power Consumption Model

The power consumption model plays an important role in the performance evaluation of any power saving routing algorithm. This work utilizes the power consumption model presented in [69] and [75]. The power consumed per hop is given by

$$P_c = \frac{P_t}{\mu} + C, \tag{3.6}$$

where P_t is the link cost explained in Section 3.2.3, μ is the power amplifier efficiency and C is the incremental power consumed by the transmitter and receiver radio electronics. C includes the energy consumed in computer processing and encoding/decoding at each node. Using (3.1), (3.3) and (3.5) in (3.6), one can write

$$P_c = \frac{\beta}{|F_{mn}|^2} d_{mn}^{\alpha} + C, \tag{3.7}$$

where

$$\beta = \frac{\gamma_n P_\eta (4\pi/\lambda)^2 d_o^{2-\alpha}}{\mu}. \tag{3.8}$$

The overall power, consumed by the whole system is equal to the summation of the power consumed per hop.

3.3 The Baseline Routing Scheme

3.3.1 Power Saving Routing Algorithm

In this section, the baseline PSR algorithm [21] is described briefly. In PSR, it is assumed that the source or the current node has knowledge about its own location, the location of the destination and the location of each of its neighbors. A neighbor is defined as a node that lies within the transmission range of the current node. Due to the static nature of the network under consideration, the locations of the neighbors are calculated only once, i.e., when the network is being setup. As far as the location of the destination is concerned, it can be obtained by using the so called location service [24]. The PSR algorithm attempts to find the existing network nodes which are closest to the shortest path, in terms of Euclidean distance, from the current node to the destination. Let us consider the scenario shown in Figure 3.2 where S is the source node and D is the destination node. From the figure, let $e = |SI|$, $f = |ID|$ and $d = |SD|$. S transmits directly to node D if [21]

$$d < \sqrt[\alpha]{\frac{C}{\beta(1-2^{1-\alpha})}}, \tag{3.9}$$

where C, α and β have already been defined in Section 3.2. If $d \geq \sqrt[\alpha]{\frac{C}{\beta(1-2^{1-\alpha})}}$, an intermediate forwarding node (IFN), labeled as I in Figure 3.2, is selected to minimize

the function

$$u(e,f) = \beta e^{\alpha} + C + f(C(\beta(\alpha-1)/C)^{1/\alpha} + \beta(\beta(\alpha-1)/C)^{(1-\alpha)/\alpha}), \tag{3.10}$$

over the set

$$v = \{(e,f) : e > 0, f > 0, e + f \geq d\}. \tag{3.11}$$

This problem is modeled as a multi-variable constrained optimization problem to find the minimal value of function u over the constrained set v of two variables, e and f, and solved using the method of Lagrange multipliers [22]. The solution to the above problem is

$$d_{opt} = \sqrt[\alpha]{\frac{C}{\beta(\alpha-1)}}. \tag{3.12}$$

The minimum occurs when $e + f = d$, i.e., S, I and D are all collinear. Thus, a virtual node V is placed between S and D, at a distance d_{opt} from S and the network node which is located closest to this virtual node is selected as the next hop destination. Once the location of the virtual node is calculated, node S selects the network node which is located closest to this virtual node as the IFN and forwards the data to this intermediate node. This process is shown in Figure 3.2, where it is assumed that, without loss of generality, node I is the closest node to node V. Thus, S sends the data to I and I forwards it to D. This process is repeated at the source and every intermediate node until the final destination is reached.

3.3.2 Impact of Fading on Power Saving Routing Algorithm

As mentioned previously, the PSR algorithm is unaware of channel fading dynamics. This means that $|F_{mn}|^2$ in (3.7) is considered to be 1, i.e., PSR assumes that there is no fading. PSR is suitable for networks where the BS towers are at high altitude and the communication is line of sight (LOS). For nodes with smaller antenna towers, the impact of fading cannot be ignored. Thus, the route calculated by PSR is not optimal in terms of power consumption. Due to the randomness of the fading process, the fading coefficients cannot be predicted ahead of time. Additionally, the fading conditions between the source node and each of its neighbors are also not the same. Due to this randomness and unpredictability, the fading coefficients cannot be incorporated directly in the route selection process of PSR. If an attempt is made to directly incorporate the fading process parameters into PSR, the optimal distance equation of (3.12) becomes

equal to (See Appendix A)

$$d_{opt} = \sqrt[\alpha]{\frac{C|F_{ID}|^2}{\beta(\alpha-1)}} \sqrt[\alpha-1]{\frac{|F_{SI}|^2((\alpha-1)/|F_{ID}|^2+1)}{\alpha}}. \tag{3.13}$$

From (3.13), it can be seen that the source base station will need to know the fading process parameters for the next hop destination, before it actually selects the next hop destination, which is not possible, since the fading coefficients are random and vary from link to link. Hence, it is not possible to directly incorporate fading in the power saving routing algorithm. To account for this fading loss, we propose a hybrid, decentralized routing algorithm, as explained in the next section.

3.4 Adaptive Power-Aware Routing Algorithm

Based on the arguments provided in Section 3.3.2, the power-saving routing algorithm is extended so that a base station can make a decision on the basis of locally available information and the channel fading coefficients. The proposed algorithm attempts to find the next hop destination that minimizes power consumption in the presence of multipath fading, and then decides whether to use this next hop destination or transmit directly to the final destination.

Referring to Figure 3.2, where S and D are the source and the destination nodes, respectively, the proposed adaptive power-aware routing (APAR) algorithm is described in three steps, as follows:

3.4.1 Step 1: Calculation of the optimal position for the virtual node

Using the baseline power-saving routing algorithm [21], calculate the optimal position for the next hop destination, i.e., the virtual node V at distance d_{opt} from S.

3.4.2 Step 2: Finding the intermediate forwarding node

Select the optimal forwarding node IFN. The algorithm initially looks for two neighboring nodes which are located nearest to the virtual node V. For example, in Figure 3.2, let the two nearest nodes be denoted by I and J. Furthermore, let us assume that the channel gain between S and I is given by h_{SI} while the gain between S and J is given

by h_{SJ}. Now, there are two metrics that can be used to choose between nodes I and J. The first metric simply compares the channel gains, i.e.,

if $h_{SI} > h_{SJ}$ **then**
  IFN = I
else
  IFN = J
end if

The above method selects the next hop destination as the node with better channel condition. However, one also needs to ensure that the route calculated by APAR remains close to the shortest path between the source and the destination. Since the current node knows the location of the destination and the two candidates for the next hop destination, it can easily calculate d_{ID} and d_{JD}, the distances between I and D and J and D, respectively. Then the algorithm decides between I and J based on the channel condition and the remaining distance to destination, i.e.,

if $h_{SI}/d_{ID} > h_{SJ}/d_{JD}$ **then**
  IFN = I
else
  IFN = J
end if

Thus, with the second metric, the algorithm compares the channel gain to remaining distance ratios for the two nodes and selects the node with a higher value of this ratio as the next hop destination.

3.4.3 Step 3: Decide whether to transmit directly or through the intermediate node

In this step, the current node decides whether it should transmit its data directly to the destination or forward it to an intermediate forwarding node. For example, suppose that the node I is selected as the IFN, in Step 2. Let F_{SI}, F_{ID} and F_{SD} represent the fading coefficients between SI, ID and SD, respectively. If the destination D is not a neighbor of the node S, then S forwards the message to I. If D is a neighbor of S, then the algorithm decides between direct and intermediate node forwarding as follows:
Assuming that the distance between S and D is d, S transmits to I if the following

two conditions hold:

$$d > \sqrt[\alpha]{\frac{C}{\beta\left(\frac{1}{|F_{SD}|^2} - \frac{\left(\frac{1}{1+\sqrt[\alpha-1]{\frac{|F_{SI}|^2}{|F_{ID}|^2}}}\right)^\alpha}{|F_{ID}|^2} - \frac{\left(\frac{\sqrt[\alpha-1]{\frac{|F_{SI}|^2}{|F_{ID}|^2}}}{1+\sqrt[\alpha-1]{\frac{|F_{SI}|^2}{|F_{ID}|^2}}}\right)^\alpha}{|F_{SI}|^2}\right)}} \tag{3.14}$$

and

$$\frac{1}{|F_{SD}|^2} - \frac{\left(\frac{1}{1+\sqrt[\alpha-1]{\frac{|F_{SI}|^2}{|F_{ID}|^2}}}\right)^\alpha}{|F_{ID}|^2} - \frac{\left(\frac{\sqrt[\alpha-1]{\frac{|F_{SI}|^2}{|F_{ID}|^2}}}{1+\sqrt[\alpha-1]{\frac{|F_{SI}|^2}{|F_{ID}|^2}}}\right)^\alpha}{|F_{SI}|^2} > 0. \tag{3.15}$$

See Appendix B for a detailed derivation of (3.14) and (3.15). Otherwise, S transmits directly to D if either of the following conditions holds:

$$d \leq \sqrt[\alpha]{\frac{C}{\beta\left(\frac{1}{|F_{SD}|^2} - \frac{\left(\frac{1}{1+\sqrt[\alpha-1]{\frac{|F_{SI}|^2}{|F_{ID}|^2}}}\right)^\alpha}{|F_{ID}|^2} - \frac{\left(\frac{\sqrt[\alpha-1]{\frac{|F_{SI}|^2}{|F_{ID}|^2}}}{1+\sqrt[\alpha-1]{\frac{|F_{SI}|^2}{|F_{ID}|^2}}}\right)^\alpha}{|F_{SI}|^2}\right)}} \tag{3.16}$$

or

$$\frac{1}{|F_{SD}|^2} - \frac{\left(\frac{1}{1+\sqrt[\alpha-1]{\frac{|F_{SI}|^2}{|F_{ID}|^2}}}\right)^\alpha}{|F_{ID}|^2} - \frac{\left(\frac{\sqrt[\alpha-1]{\frac{|F_{SI}|^2}{|F_{ID}|^2}}}{1+\sqrt[\alpha-1]{\frac{|F_{SI}|^2}{|F_{ID}|^2}}}\right)^\alpha}{|F_{SI}|^2} \leq 0. \tag{3.17}$$

Unlike PSR, the above equations allow the current node to select between direct and multi-hop relaying based on the fading conditions of the channel. Equations (3.14)-(3.17) are derived based on a comparison between consumed powers by the direct path and the forwarding intermediate node (See Appendix B). Although (3.14) is derived for an idealistic scenario where it is assumed that S, I and D are all collinear, results in Section 3.5 confirm that it can be used as a valid approximation for the threshold point in deciding between transmitting directly to D and forwarding the data to I.

Due to the static nature of the network, the optimal route is calculated only once. After the initial setup, each sending node only monitors the fading parameters for each of the two nodes selected in Step 2 of the algorithm, i.e., nodes I and J. The proposed adaptive power-aware routing algorithm is summarized in Algorithm 3.1 where the n^{th}

hop destination found during the routing process is denoted by $BS(n)$.

Algorithm 3.1 Adaptive power-aware Routing Algorithm

Require: Wireless network, with source S, destination D and location of nodes.

1: Initialize $n = 0$.
2: $BS(n) \leftarrow S$.
3: **while** $BS(n) \neq D$ **do**
4: Find the virtual node position.
5: Find the optimal intermediate forwarding node IFN.
6: Decide whether $BS(n+1) =$ D or $BS(n+1) =$ IFN.
7: Send message to $BS(n+1)$.
8: Update route table.
9: $n = n + 1$.
10: **end while**

Note that the above algorithm is run only once for the whole route. In Step 8, the algorithm saves the location of both, nodes I and J in the route table of each node.

3.5 Performance Evaluation

In this section, the proposed APAR algorithm is implemented in a wireless mesh network of cellular base stations and an ad hoc network of randomly distributed wireless nodes. The performance of APAR is compared against the PSR algorithm.

3.5.1 Simulation Setup

For experimental setup, a wireless mesh network with 110 base stations is considered, as shown in Figure 3.1. It is assumed that each base station consumes 50nJ/bit of energy [51],which includes their energy consumption due to signal processing, the noise power is -101dBm. The traffic flow generated at the source is 100Kbps and the power amplifier efficiency is 20%, i.e., $\mu = 0.2$. The pathloss exponent is set equal to 2, i.e., $\alpha = 2$. It is also assumed that the required received SNR for successful decoding at each base station is at least 10dB. For the wireless ad hoc network, the network nodes are randomly distributed within an area of 1500m by 1500m and all the simulation results are averaged over 100000 iterations. Since this study is making a comparative analysis and since the results in the next subsection show that both the proposed and the baseline algorithms have similar number of hops, the impact of transmitter and receiver equipment power consumption would be same for both the algorithms, therefore, this power consumption is ignored in the simulations.

3.5.2 Simulation Results

This section compares the performance of our proposed algorithm with PSR. Note that in the following, when APAR uses the first metric to calculate the next hop destination, i.e., when it simply compares the channel gains, we call it as APAR-M1. On the other hand, when APAR compares the channel gain to remaining distance ratios to calculate the next hop destination, we call it as APAR-M2. Furthermore, in this section, we show the results in terms of power saving gains, which is given as

$$G = \frac{P_{PSR} - P_{APAR}}{P_{PSR}}, \tag{3.18}$$

where P_{PSR} represents the power consumed by PSR while P_{APAR} represents the power consumed by APAR.

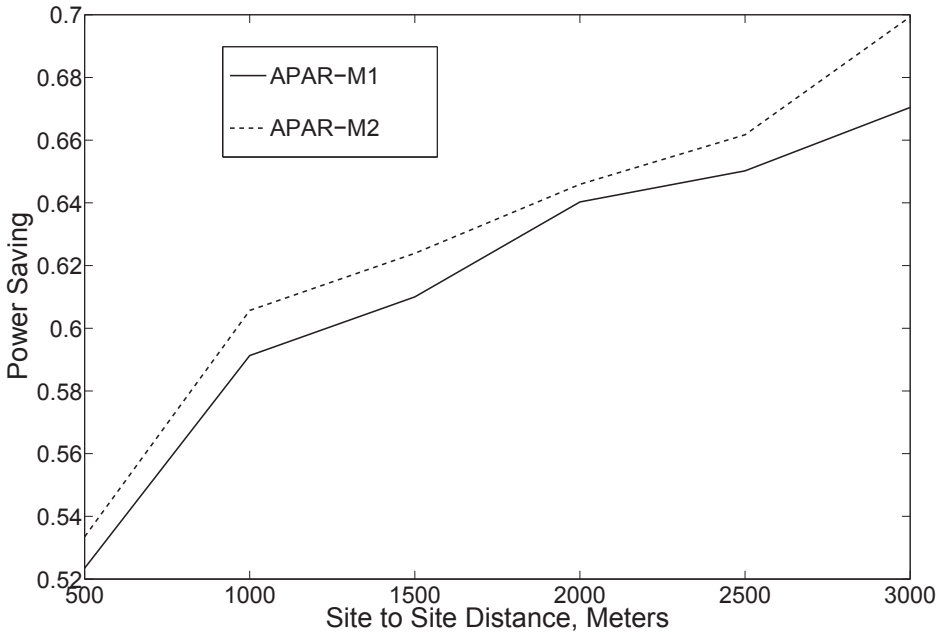

Figure 3.3: Power saving relative to the baseline routing algorithm as a function of site to site distance.

Figure 3.3 shows the power saving gains achieved by APAR-M1 and APAR-M2 as compared to PSR, for the mesh network of Figure 3.1. For the site to site distance varying from 500m to 3km, Figure 3.3 shows that both APAR-M1 and APAR-M2 outperform PSR, i.e., APAR-M1 and APAR-M2 achieve 52% to 67% and 53.5% to 70% power saving gains, respectively, over PSR. Notice that for Figure 3.3, the K factor of the Rician distribution is set equal to 3, i.e., the LOS component is 3 times stronger than the non-LOS component. Note that although APAR-M2 performs better than

APAR-M1, this performance improvement comes at the cost of increased computational time. This result is illustrated later in this section.

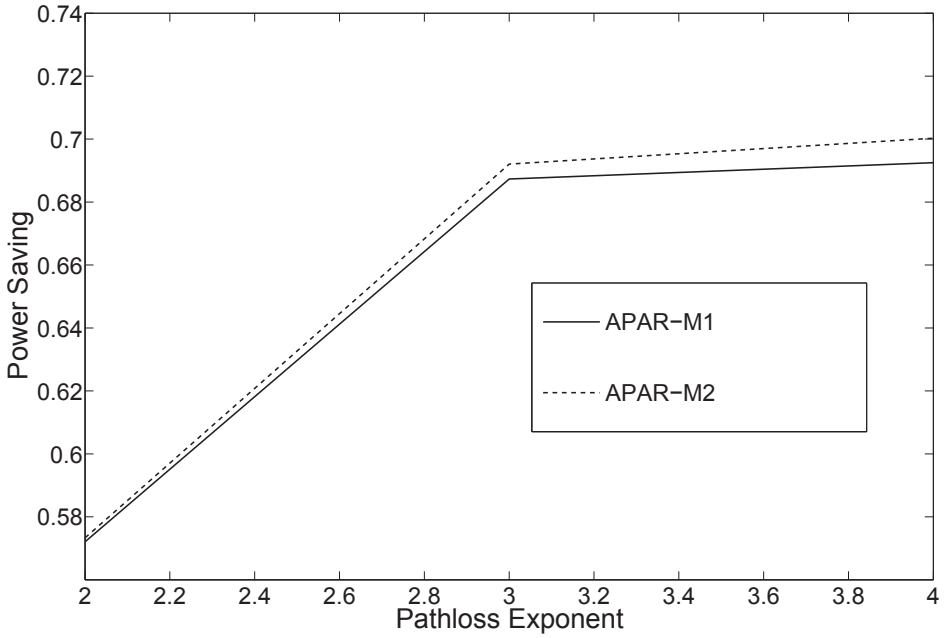

Figure 3.4: Power saving relative to the baseline routing algorithm as a function of the pathloss exponent with site to site distance equal to 500m.

Figure 3.4 demonstrates the achievable power saving gains as a function of pathloss exponents. In this experiment, the Rician distribution was used with K factor equal 3 and the site to site distance was set to 500m. As shown in Figure 3.4, the proposed APAR-M1 and APAR-M2 algorithms outperform PSR for all values of the pathloss exponent by 57% to 59% and 57% to 70%, respectively. Figure 3.3 shows that the power saving increases with an increasing site to site distance. Since the minimum site to site distance is used for the experiment in Figure 3.4, it can be concluded that for each value of the pathloss exponent, Figure 3.4 shows the minimum achievable power saving gains.

Figure 3.5 shows that in channels with Rician distribution, the power saving gain decreases as the K factor increases. This is due to the fact that with an increase in the K factor, the line of sight component dominates the fading effect of the channel and, hence, the performance of the proposed algorithm approaches that of the baseline routing scheme.

Figure 3.6 depicts the power saving gains that can be achieved by the proposed APAR algorithm in a wireless ad hoc network when the number of nodes varies from 100 to 700. It is shown that the proposed APAR-M1 and APAR-M2 algorithms, respectively, achieve gains between $45\% - 60\%$ and $47\% - 62.5\%$. Notice that the

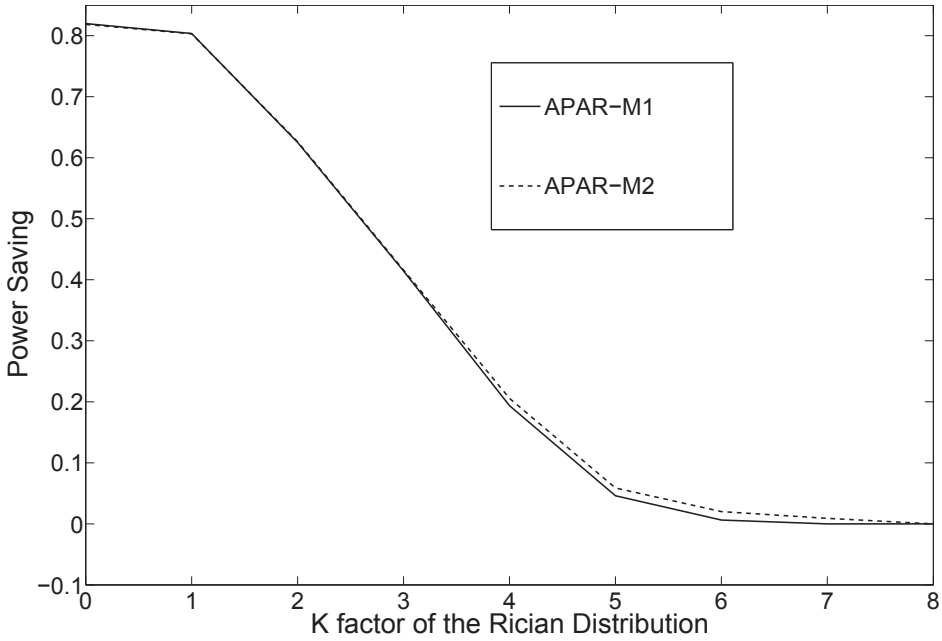

Figure 3.5: Power saving relative to the baseline routing algorithm as a function of the K factor of the Rician Distribution with site to site distance equal to 500m.

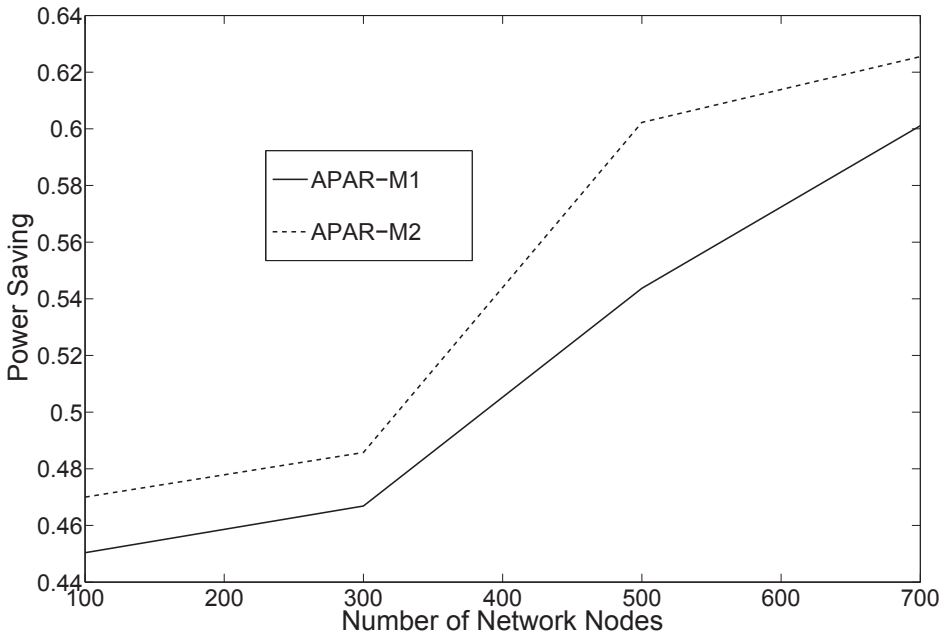

Figure 3.6: Power saving relative to the baseline routing algorithm as a function of the number of nodes in the network.

power saving gain increases with an increasing number of network nodes. This is due to the fact that with an increased node density, there is a higher probability that the two IFN candidates selected by APAR are at a similar distance from the virtual node.

Hence, which ever node the algorithm chooses as the next hop destination, the over all calculated path remains almost the same, yet the node with better channel condition is selected.

Although both APAR-M1 and APAR-M2 produce significant power savings, however, this power saving comes at the cost of increased computational complexity. Figure 3.7, illustrates the time consumed by the three routing algorithms, in calculating the optimal route for an ad hoc network. Notice that time calculation is made by using the tic-toc function in MATLAB, where the timer starts when the first packet is generated at the source and it stops when this packet reaches the destination. As shown in the figure, APAR-M1 and APAR-M2 take longer to calculate the optimal route, as compared to PSR. However, this increase in delay is very small when compared with the power savings that are achieved, e.g., with 700 nodes, APAR-M2 decreases the power consumption by 66.5% at a cost of only 3.24% increase in time consumption.

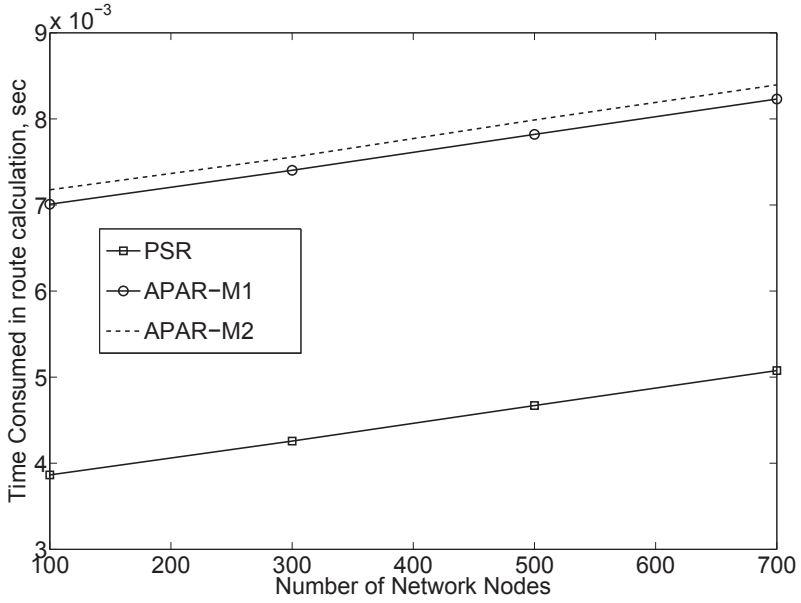

Figure 3.7: Time consumed in calculating route as a function of the number of nodes in the network.

Finally, Table 3.1 shows the mean number of hops consumed by the baseline and the proposed routing schemes, in an adhoc network. Since APAR-M1 and APAR-M2 have PSR as the underlying routing algorithm, we see that all the algorithms use very similar number of hops for each case. Furthermore, notice that as the number of network nodes increases, the average hop counts of APAR-M1 and APAR-M2 approach that of PSR, until they all become the same when the number of network nodes is 700. This further proves our point in the last paragraph, i.e., with a larger number of network nodes, the

Table 3.1: Mean Number of Hops

No. of Nodes	100	300	500	700
PSR	5	5	5	5
APAR-M1	4.83	4.91	4.91	5
APAR-M2	4.77	4.90	4.90	5

calculated paths remain almost the same.

3.6 Concluding Remarks

The chapter focused on power-aware routing in two different types of networks, i.e., a wireless mesh network of cellular base stations and an ad hoc network of randomly placed nodes. The impact of fading on the baseline routing algorithm, i.e., PSR, was investigated. By using the fading coefficients in a localized manner, two decision metrics were introduced that could be used to select the optimal intermediate forwarding node. Then, a characteristic distance was derived which allowed the current node to intelligently decide whether it should transmit directly towards the destination or forward the message to an intermediate forwarding node. Using these metrics and the derived characteristic distance, a new power saving routing algorithm, i.e., APAR, was introduced. APAR was proposed in two categories, APAR-M1 and APAR-M2, where the former utilized the first metric while the latter used the second metric to select the next hop destination. Simulation results showed that, for a wireless mesh network, APAR-M1 achieved a power saving gain ranging from 52% to 67% while APAR-M2 reduced the power consumption by 53.5% to 70%, both with respect to the baseline routing algorithm. For an ad hoc wireless network with randomly placed nodes, simulation results confirmed that APAR-M1 and APAR-M2, respectively, achieved a power saving gain of 45% to 60% and 47% to 62.5% with respect to the baseline algorithm. Furthermore, it was also shown that the proposed algorithms outperformed PSR under different network conditions while consuming a very similar number of hops.

The simulation results and the analysis, carried out in the chapter, clearly highlight the impact of the characteristics of the PHY layer on the routing decisions at the network layer. To design power-aware routing algorithms, cross layer design issues should be considered, i.e., the decisions at the routing layer should be made in conjunction

with the PHY layer characteristics. This implies that better transmission techniques should be used at the PHY layer. This chapter focused on a single-antenna systems where point to point transmission was used to route the data between the source and the destination. However, in the past, it has been shown that multi-antenna systems achieve considerable transmission energy savings compared to single-antenna systems by harvesting spatial diversity inherent in wireless networks. The next chapter focuses on such systems and addresses power-aware routing using multi-antenna systems.

Chapter 4

Power-Aware Cooperative Routing

Having investigated the impact of wireless channel on the performance of the power-aware routing algorithms in the previous chapter, the rest of this thesis focuses on the cross-layer designs for power-aware routing algorithms. Energy efficient transmission techniques are investigated and proposed and the power-aware routing algorithms are tailored to perform optimally using such techniques. Among the many techniques for reducing energy consumption, cooperative transmission has been recently studied intensively. In cooperative transmission, spatially distributed single-antenna nodes cooperate to achieve the so called distributed beamforming (DB). It is shown that DB can achieve highly directional transmissions, resulting in significant power gains compared to independent signal transmissions [65, 76]. This chapter investigates transmission side diversity and energy-efficient routing in a wireless mesh network of cellular base stations. The aim is to design a cooperative routing algorithm which takes the active radio electronic power consumption into consideration when constructing the minimum power route from source to destination. Initially, the properties of single hop cooperative transmission are analyzed. By taking the radio electronics power consumption into consideration, analytic expressions are derived that define the limitations of cooperative transmission in terms of transmission distance. Based on these analysis, the shortcomings of the existing power saving cooperative routing algorithms are highlighted. By introducing the concept of supernode with improved power efficiency, a new power-aware cooperative routing algorithm is proposed. Simulation results show a significant performance improvement over well known power saving routing schemes.

4.1 Introduction

Multi-antenna systems have been recently studied intensively as an optimal transmission strategy in future wireless networks. By harvesting the spatial diversity inherent in wireless networks, multi-antenna systems can achieve significant power savings as compared to single antenna systems. However, it is not always possible to use multiple antennas at the transmitter and/or receiver, e.g., due to small size of sensor nodes or due to costly analog circuitry. Nevertheless, through cooperation between spatially distributed single-antenna nodes, DB can achieve highly directional transmissions, resulting in significant power gains compared to independent signal transmissions, [65, 67, 76, 77].

Recently, power saving cooperative routing algorithms have been studied in several research articles, e.g., [57, 59, 62–64, 66, 68, 78]. In [66] and [68], energy-efficient cooperative routing protocols have been proposed which maximize the network lifetime by balancing the distribution of data traffic over the entire nodes in the network. Authors in [57] introduce two power saving cooperative routing algorithms of CAN-L and PC-L that stand for cooperation along the minimum energy non-cooperative path and progressive cooperation, respectively. Both of these algorithms work in a centralized manner and apply cooperative transmission over a non-cooperatively determined shortest-path between the source and the destination nodes. In [63], Ibrahim *et al.* proposed two cooperative routing algorithms, i.e., minimum power cooperative routing (MPCR) and cooperation along the shortest non-cooperative path (CASNCP). The former, calculates a cooperative link cost for each one of the outgoing links first and, then, distributively implements the Bellman Ford shortest path algorithm [79] to find the minimum power path between the source and the destination . While, the latter, is mainly similar to CAN-L [57] with a variation in cooperative transmission strategy. In [59], Li *et al.* proposed the cooperative shortest path (CSP) algorithm that uses Dijkstra's algorithm as the basic building block and utilizes cooperative transmission in the relaxation procedure [80]. Furthermore, [62] introduces two power-saving cooperative routing algorithms, namely, cooperative routing along truncated non-cooperative route (CTNCR) and source node expansion routing (SNER). The former is again similar to CAN-L with a variation in cooperative transmission strategy. While, the latter is essentially a greedy algorithm similar to the Prim-Dijkstra spanning-tree algorithm except that it stops whenever the destination is included in the tree. Generally, one can broadly classify the existing energy-efficient cooperative routing algorithms in two main categories of the network lifetime maximizing routing algorithms, i.e., [66, 68], and the power-saving routing algorithms, i.e., [57, 59, 62–64, 78].

The power-saving cooperative routing algorithms, reported in [57, 59, 62–64, 78], show high energy saving gains ranging from 30% to 65% under different network conditions. However, none of these algorithms takes into account the power consumption of active radio electronics which can increase significantly as a result of cooperative transmission by multiple nodes. Thus, these algorithms suffer from severe performance degradation, in terms of energy efficiency, if the circuit power consumption is taken into consideration.

In this chapter, a new power-aware cooperative routing (PACR) algorithm is proposed which finds an optimal route from source to destination by taking into consideration the circuit power consumption of the cooperative communication. Unlike the older works, in PACR, the transmitting nodes cooperatively select the next hop destination and the algorithm is distributed, i.e., it does not require a predetermined route from source to destination. The chapter also introduces the concept of supernode with improved power efficiency to model a group of cooperating base stations as a single node and this enables us to find the optimal transmission distance for cooperative transmission. Simulation results confirm PACR's improved energy saving potential over the baseline cooperative routing algorithm, i.e., CAN-L [57] and the baseline non-cooperative routing algorithm, i.e., power saving routing (PSR) [21]. Such improved power saving is produced by incorporating fewer number of hops as compared to the baseline algorithms. Reducing the hop count minimizes the overall circuit power consumption of the route.

The rest of the chapter is organized as follows. Section 4.2 describes the system model. An analysis of cooperative transmission is performed in Section 4.3. The proposed cooperative routing algorithm is presented in Section 4.4. Simulation results are shown in Section 4.5 while the conclusions are drawn in Section 4.6.

4.2 System Model

This section provides a detailed description of the network architecture, the channel model, the link cost model and the overall system power consumption model.

4.2.1 Network Architecture

Consider a wireless mesh network consisting of a large number of cellular base stations, where each BS has a single omni-directional antenna. Figure 4.1 shows this scenario where a source BS sends data to a destination BS and the goal is to find a cooperative route between source and the destination with minimum power consumption.

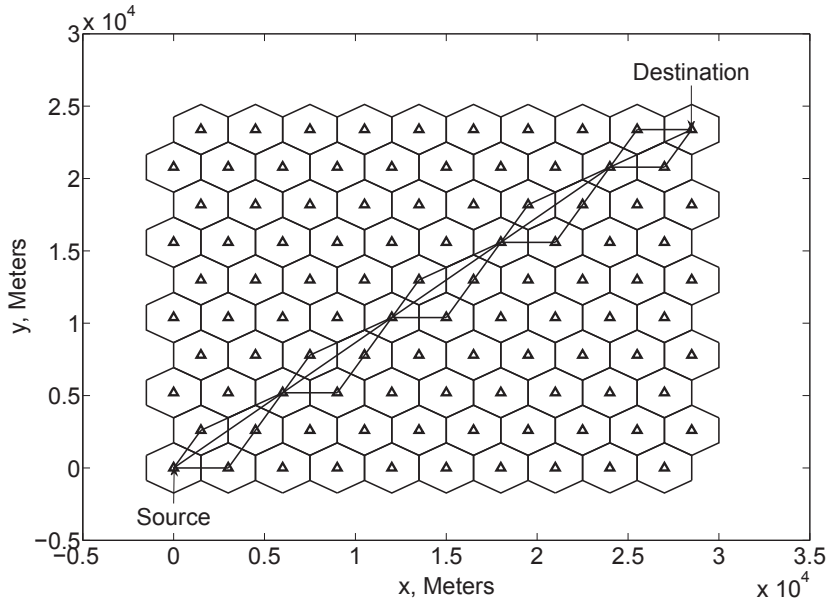

Figure 4.1: Wireless mesh network of base stations.

4.2.2 Channel Model

In the following, the set of source base stations is denoted by $A = \{a_1, a_2, ..., a_i\}$ and the set of receiving base stations is denoted by $Z = \{z_1, z_2, ..., z_r\}$. The channel between base stations a_i and z_r is modeled by two parameters, its magnitude attenuation factor h_{ir} and its phase delay θ_{ir}. The magnitude attenuation factor of the channel, i.e., h_{ir}, can be written as

$$h_{ir} = \sqrt{1/L_{ir}}, \tag{4.1}$$

where L_{ir} is the free space path loss given by

$$L_{ir} = (\frac{4\pi}{\lambda})^2 d_o^{2-\alpha} d_{ir}^{\alpha}, \tag{4.2}$$

where λ is the wavelength, α is the path loss exponent, d_o is the reference distance for the antenna far field and d_{ir} represents the distance between the two base stations.

4.2.3 Link Cost Model

This section formulates the link costs associated with the transmission of information over a single hop. Three modes of transmission are distinguished, i.e., non-cooperative, multicast and cooperative transmissions.

Non-cooperative Link Cost

For non-cooperative transmission, there is a single transmitter and a single receiver. The signal received by base station z_r, is given by

$$y_r = h_{ir} e^{j\theta_{ir}} \sqrt{P_{ti}} s_r + n_r, \tag{4.3}$$

where P_{ti} is the power transmitted by BS a_i, s_r is the data symbol and n_r is the receiver noise with power P_η. For successful decoding, it is assumed that the receiving BS z_r requires a minimum SNR of γ_r. With these assumptions, the non-cooperative transmission link cost is given as

$$LC(a_i, z_r) \equiv P_t = \frac{\gamma_r P_\eta}{|h_{ir}|^2}. \tag{4.4}$$

Multicast Link Cost

For multicast transmission, there is a single source base station a_i and multiple destination base stations $z_1, z_2, ..., z_r$, where r is the total number of base stations that will receive the multicast transmission. Assuming all the base stations have an omni-directional antenna, the multicast transmission link cost can be defined as

$$LC(a_i, Z) \equiv \max\left[LC(a_i, z_1), LC(a_i, z_2), ..., LC(a_i, z_r)\right], \tag{4.5}$$

where $LC(a_i, z_j)$ is given by (4.4). In the work presented in this chapter, the current base station multicasts the message to $l-1$ neighboring base stations, where l is the number of cooperating base stations.

Cooperative Link Cost

In cooperative transmission, there are multiple transmitters and a single receiver. The transmitter set consists of l base stations that cooperatively transmit the same information to a single destination base station z_r. For the simplicity of analysis, it is assumed that all the transmitters are perfectly synchronized for coherent reception at the receiver end and that there is no energy overhead associated with achieving this. This assumption has been made for a fair comparison, since our baseline cooperative routing algorithm does not take this factor into consideration. This type of synchronization can be achieved by using the techniques provided in [81]. With these assumptions, the

received signal is given as

$$y_r = \sum_{j=1}^{l} h_{jr}|\omega_j|s_r + n_r, \tag{4.6}$$

where h_{jr} is the magnitude of the channel gain between the base stations a_j and z_r and is given by (4.1) and ω_j is the scaling factor proportional to the transmitted signal power from the j^{th} transmitter. The problem of optimal power allocation for the cooperative transmission can be stated as

$$\begin{aligned} \underset{\omega_j}{\text{minimize}} \quad & \sum_{j=1}^{l} |\omega_j|^2 \\ \text{subject to} \quad & \frac{|\sum_{j=1}^{l} \omega_j h_{jr}|^2}{P_\eta} \geq \gamma_r. \end{aligned} \tag{4.7}$$

The optimal allocation that satisfy (4.7) for a transmitting BS a_j is calculated as

$$|\hat{\omega}_j| = \frac{h_{jr}}{\sum_{k=1}^{l} h_{kr}^2} \sqrt{\gamma_r P_\eta}. \tag{4.8}$$

The last equation is found by using the Lagrangian method [57, 59] (See Appendix C for detailed derivation). Thus, the link cost for the cooperative transmission can be calculated as

$$LC(A, z_r) \equiv P_t = \sum_{j=1}^{l} |\hat{\omega}_j|^2 = \sum_{j=1}^{l} \frac{h_{jr}^2}{(\sum_{k=1}^{l} h_{kr}^2)^2} \gamma_r P_\eta, \tag{4.9}$$

where A is the set of transmitting base stations $a_1, a_2, ..., a_l$.

4.2.4 System Power Consumption Model

The power consumed per hop is given by

$$P_{consumed} = \frac{P_t}{\mu_{pa}} + C, \tag{4.10}$$

where P_t is the transmission power, μ_{pa} is the transmitter power amplifier efficiency and C is the increase in the circuit power consumed by the transmitter and the receiver as a result of inter-BS message transfer. It is assumed that the increase in the radio electronics power consumption at each base station is equal to E and this accounts for factors such as processing, encoding, and decoding at each base station.

For non-cooperative transmission, C in (4.10) is equal to $2E$, since there is one transmitter and one receiver, each consuming E to operate radio electronics. Using

(4.1), (4.2) and (4.4) in (4.10), one calculates the power consumption of a single hop non-cooperative link as follows

$$P_N = \frac{B}{\mu_{pa}} d_{ir}^{\alpha} + 2E, \tag{4.11}$$

where

$$B = \gamma_r P_\eta (4\pi/\lambda)^2 d_o^{2-\alpha}. \tag{4.12}$$

For multicast transmission, there is a single transmitter and $l-1$ receivers. Hence, using $C = lE$ and substituting from (4.1), (4.2) and (4.5) in (4.10), the power consumption for multicast transmission can be given as

$$P_M = \frac{B}{\mu_{pa}} d_{iR}^{\alpha} + lE, \tag{4.13}$$

where d_{iR} is the distance between the transmitting base station and its farthest located destination base station.

For cooperative transmission, there are l transmitters and a single receiver, therefore, $C = (l+1)E$ and using (4.1), (4.2) and (4.9) in (4.10), the power consumption is given by

$$P_C = \frac{B}{\mu_{pa}(\sum_{k=1}^{l} \frac{1}{d_{kr}^{\alpha}})} + (l+1)E. \tag{4.14}$$

Appendix C outlines a detailed derivation of (4.14).

4.3 Analysis of Cooperative Transmission

In this section, the performance of single-hop cooperative transmission is analyzed. Analytical expressions are derived that define the limitations of cooperative transmission. The analysis in this section serves as the basis for the proposed routing algorithm, to be introduced later in the next section.

Consider a scenario where a set of l BSs coordinate to deliver a message to a receiving BS r. Let d_{ir}, $i = 1, ..., l$, denote the distance between the ith coordinating BS and the receiving BS r and without loss of generality, assume $d_{1r} < d_{2r} < ... < d_{lr}$. For fairness of comparison between cooperative and non-cooperative transmissions, it is assumed that the distance between the transmitter and the receiver in non-cooperative transmission is d_{1r}, i.e., the smallest distance between l transmitters and the receiver in the cooperative case.

Definition 4.1. *The power saving gain of the cooperative transmission over a non-*

cooperative transmission, denoted by G_p, is defined as

$$G_p = \frac{P_N - P_C}{P_N}. \tag{4.15}$$

Lemma 4.1. *In cooperative transmission of l adjacent nodes to a distant destination, the power saving gain G_p can be upper-bounded as*

$$G_p \leq \rho \left(\frac{l-1}{l} \right),$$

where

$$\rho = \left(\frac{\frac{B}{\mu_{pa}} d_{1r}^{\alpha} - lE}{\frac{B}{\mu_{pa}} d_{1r}^{\alpha} + 2E} \right).$$

Proof. Substituting from (4.11) and (4.14) in (4.15), one can write

$$G_p = \frac{\frac{B}{\mu_{pa}} d_{1r}^{\alpha} + 2E - \frac{B}{\mu_{pa} \sum_{k=1}^{l} \frac{1}{d_{kr}^{\alpha}}} - (l+1)E}{\frac{B}{\mu_{pa}} d_{1r}^{\alpha} + 2E}. \tag{4.16}$$

Let $\triangle d_i = d_{ir} - d_{1r}$, for $i = 1, ..., l$, and assume $\frac{\triangle}{d_{1r}} << 1$, where $\triangle = \max_i(\triangle d_i)$. This reflects a scenario where the destination is far enough from the cooperating base stations such that all the cooperating base stations appear to be at an equal distance from the destination. Using $d_{ir} = d_{1r} + \triangle d_i$ for $i = 1, \cdots, l$, (4.16) can be rewritten as follows

$$\begin{aligned} G_p &= \frac{\frac{B}{\mu_{pa}} d_{1r}^{\alpha} - \frac{B}{\mu_{pa} \left(\frac{1}{(d_{1r}+\triangle d_1)^{\alpha}} + ... + \frac{1}{(d_{1r}+\triangle d_l)^{\alpha}} \right)} - (l-1)E}{\frac{B}{\mu_{pa}} d_{1r}^{\alpha} + 2E} \\ &= \frac{\frac{B}{\mu_{pa}} d_{1r}^{\alpha} - \frac{B d_{1r}^{\alpha}}{\mu_{pa} \left(\frac{1}{(1+\frac{\triangle d_1}{d_{1r}})^{\alpha}} + ... + \frac{1}{(1+\frac{\triangle d_l}{d_{1r}})^{\alpha}} \right)} - (l-1)E}{\frac{B}{\mu_{pa}} d_{1r}^{\alpha} + 2E}, \end{aligned}$$

or

$$G_p = \frac{\frac{B}{\mu_{pa}} d_{1r}^{\alpha} - \frac{B d_{1r}^{\alpha}}{\mu_{pa} \sum_{k=1}^{l} \frac{1}{\left(1+\frac{\triangle d_k}{d_{1r}}\right)^{\alpha}}} - (l-1)E}{\frac{B}{\mu_{pa}} d_{1r}^{\alpha} + 2E}. \tag{4.17}$$

Since $\frac{\triangle}{d_{1r}} << 1$, then $\frac{\triangle d_i}{d1r} << 1 \; \forall i$. Thus, G_p can be upper-bounded as

$$G_P \leq \frac{\frac{B}{\mu_{pa}} d_{1r}^{\alpha} - \frac{B}{l\mu_{pa}} d_{1r}^{\alpha} - (l-1)E}{\frac{B}{\mu_{pa}} d_{1r}^{\alpha} + 2E}, \tag{4.18}$$

or equivalently

$$G_P \leq \left(\frac{l-1}{l}\right)\left(\frac{\frac{B}{\mu_{pa}} d_{1r}^{\alpha} - lE}{\frac{B}{\mu_{pa}} d_{1r}^{\alpha} + 2E}\right) \tag{4.19}$$

□

An important observation from the above discussion is that the cooperative transmission consumes the minimum power when all the cooperating base stations appear to be at the same distance from the destination. Results in Lemma 4.1 confirm that the largest upper bound on G_p can be achieved in the absence of circuit power consumption, i.e., $E = 0$. In the presence of circuit power consumption, i.e., $E \neq 0$, the upper-bound on G_p decreases with an increase in the number of cooperating nodes, i.e., l.

Corollary 4.1. *For cooperative transmission to outperform the non-cooperative transmission, d_{1r} should satisfy the following condition:*

$$d_{1r} > \sqrt[\alpha]{\frac{lE\mu_{pa}}{B}}. \tag{4.20}$$

Proof. If the condition is not satisfied, then the ρ factor takes negative values. □

Corollary 4.1 outlines the limitations of cooperative transmission. It gives a lower bound for the distance below which the cooperative transmission is outperformed by the non-cooperative transmission. Since the current cooperative routing algorithms do not take this bound into consideration, they suffer from severe performance degradation when the circuit power consumption is taken into account. A discussion on the impact of circuit power consumption on the performance of cooperative routing algorithms is provided in the next section. Further, a demonstration of Lemma 4.1 and Corollary 4.1 is provided later in Section 4.5.2.

4.4 Power-aware Cooperative Routing

4.4.1 The Baseline Algorithms

As mentioned earlier, the study in this chapter uses CAN-L [57] as the baseline cooperative routing algorithm and PSR [21] as the baseline non-cooperative routing algorithm. PSR has already been explained in detail in Chapter 3, Section 3.3. Therefore, this subsection focuses mainly on CAN-L. In CAN-L, the last L nodes along the optimal non-cooperative route transmit cooperatively towards the next hop destination. Since CAN-L does not take the distance threshold of (4.20) into consideration while selecting the optimal next hop, it suffers from severe performance degradation, in terms of power consumption, when the circuit power consumption is taken into account. Figure 4.2 highlights the impact of circuit power consumption on CAN-L. The figure demonstrates the power consumption of CAN-L and PSR when they route the data between the source-destination pair of Figure 4.1. It can be seen that as far as transmission power is concerned, CAN-L outperforms PSR. However, when the overall system power consumption (transmission power + circuit power) is taken into consideration, the non-cooperative routing algorithm outperforms the cooperative one for a large range of BS to BS distances. In fact, CAN-L outperforms PSR only when the inter-BS distance is larger than 3900m. Thus, it is imperative that the cooperative routing algorithm takes the circuit power consumption into consideration while calculating the optimal route between the source and the destination.

4.4.2 The Proposed Algorithm

The proposed PACR algorithm is introduced in this section. The main assumption is that each base station has knowledge about its own location, the location of its neighbors, i.e., nodes within its transmission range, and the location of the destination. The key idea behind the algorithm is that by translating the transmission power advantage, offered by cooperative transmission, into distance, i.e., by increasing the transmission distance, one can reduce the number of hops required to reach the destination. The advantage of reducing the number of hops is that the circuit power consumption is reduced.

PACR Algorithm

A source BS selects its $l-1$ adjacent BSs, however, it does not transfer any data to these BSs. Instead, it uses their location information to calculate an optimal distance

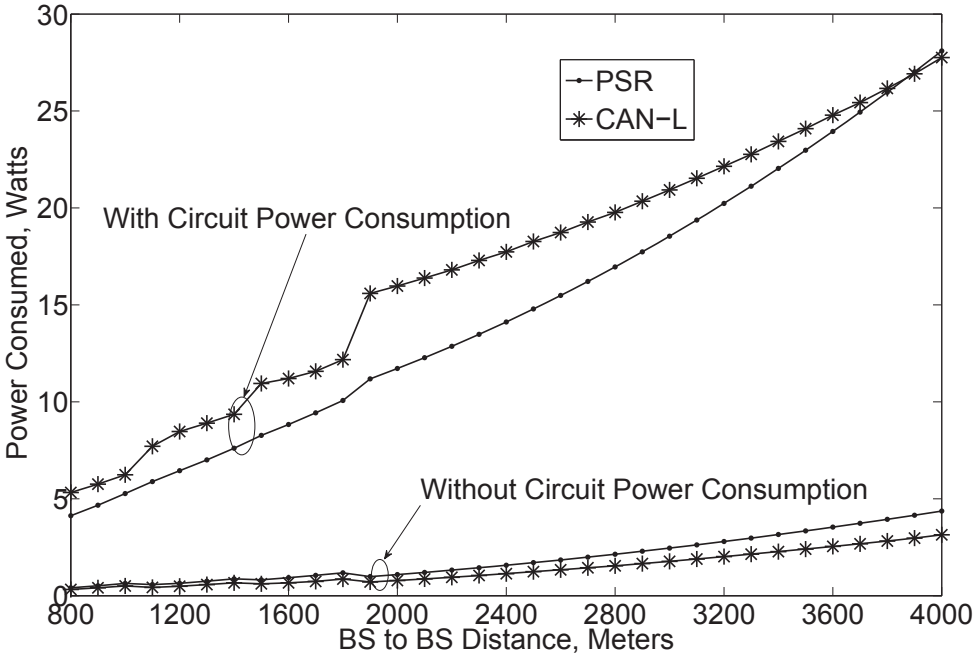

Figure 4.2: Power consumption versus the BS to BS distance. Figure highlights the impact of circuit power consumption on CAN-L when $\alpha = 2, l = 3$.

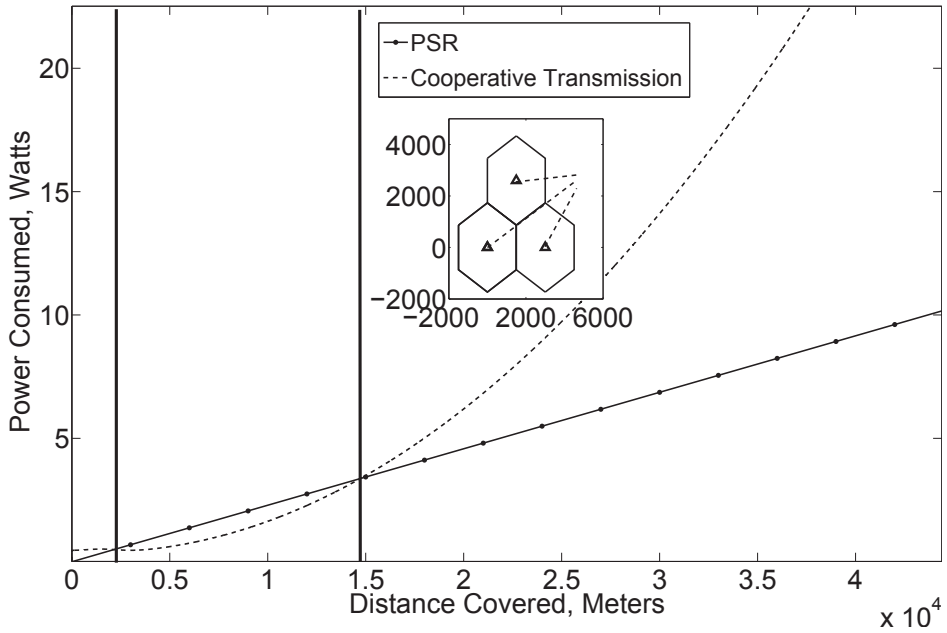

Figure 4.3: Power consumption as a function of the distance traveled by the packet. $\alpha = 2, l = 3$.

for the next hop destination. This optimal distance depends on the distance between the source and the destination, the active radio electronics power consumption and the transmission power consumption of cooperative communication and it strikes a balance

between the circuit power consumption and the transmission power consumption. The distance is explained further with the aid of Figure 4.3 [1]. For the source-destination pair of Figure 4.1, Figure 4.3 compares the power consumed by single hop cooperative transmission with the progressive-power-consumption[2] of PSR. It can be seen that within a certain distance range, i.e., the area between the bold vertical lines, the system power consumption of a single hop cooperative transmission is less than the system power consumption of multi-hop non-cooperative routing. Thus, the optimal next hop should be located within this distance range. In a nutshell, the optimal cooperative routing algorithm should forward the data to a base station which is located within this optimal distance range. For the experiment that produced Figure 4.3, the BS to BS distance was assumed to be 3km. The optimal distance d_{opt} is calculated as follows:

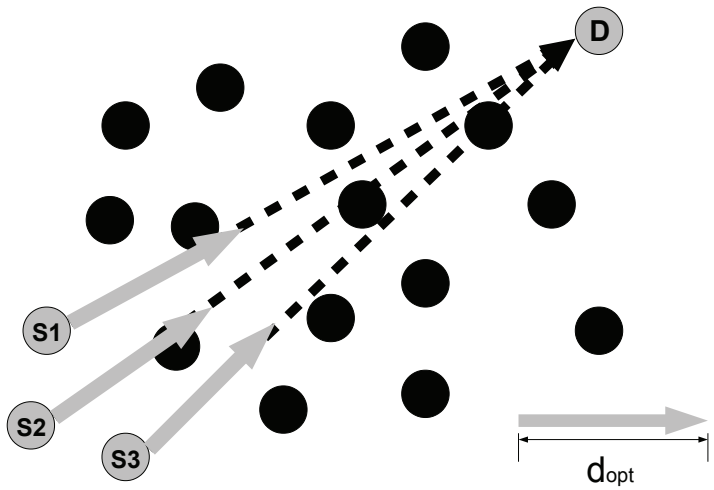

Figure 4.4: Possible choices for the optimal transmission distance for cooperative transmission.

Consider the scenario shown in Figure 4.4 where three cooperating nodes need to route the data towards the destination. As shown in the figure, there are three choices for the optimal distance towards the next hop. It is obvious from the figure that the optimal next hop should be calculated with respect to the location of the cooperating

[1]Note that Figure 4.3 is not a demonstration of Corollary 4.1 since this figure compares single-hop cooperative transmission with multi-hop non-cooperative transmissions. On the other hand, Corollary 4.1 holds for single hop cooperative and non-cooperative transmissions.

[2]Progressive-power-consumption is the total power consumed after each hop along the route towards the destination.

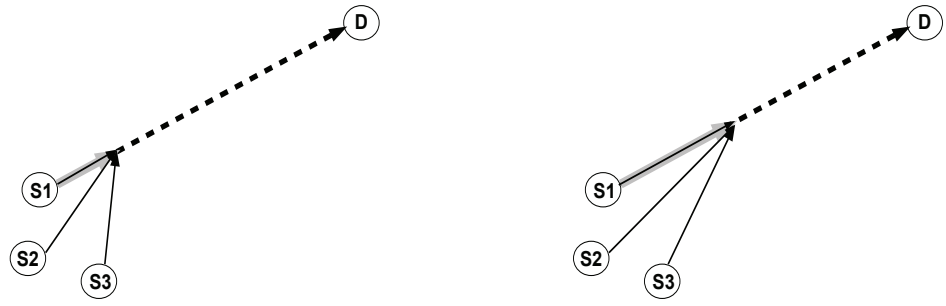

(a) (b)

Figure 4.5: Calculating optimal distance for the next hop destination.

node which is located closest to the destination since this will ensure that the next hop is selected along the shortest path, in terms of euclidean distance, towards the destination. While it is simple to calculate the optimal distance for non-cooperative transmission, as done in Section 3.3, i.e., (3.12), it is not straightforward to derive this distance for cooperative transmission. To illustrate this point further, consider Figure 4.5. As shown in the figure, d_{opt} is calculated along the dashed line and to calculate it for cooperative transmission, the cooperating nodes will be required to share their distance information (black lines) for every point along the dashed line. This will significantly increase the involved overhead. The solution is to model the group of cooperating nodes as a single supernode and then use (3.12) so that it gives the optimal distance for cooperative transmission.

To model a group of cooperating base stations as a single supernode, it is assumed that each of the transmitting nodes adjusts its phase with respect to the supernode, such that all the nodes appear to be at the same distance from the destination. The supernode is modeled as follows:

Assuming equal power amplifier efficiency of μ for each transmitting BS and a target SNR of γ_r at the destination, one can show, using (4.14), that the overall transmit power by l base stations is given by

$$P_t = \frac{B}{\sum_{k=1}^{l} \frac{1}{d_{kr}^{\alpha}}}, \tag{4.21}$$

where $d_{kr},\ k = 1, \cdots, l$, is the distance from the kth transmitting BS to the destination z_r. Hence, the overall power consumption of the power amplifiers of l transmitting BSs can be written as

$$P_c = \frac{B}{\mu \sum_{k=1}^{l} \frac{1}{d_{kr}^{\alpha}}}. \tag{4.22}$$

Let us define a supernode located at the position of the closest transmitting BS to the destination. Let this supernode be equivalent to the l cooperating BSs in terms of maintaining the same target SNR, i.e, γ_r, at a given destination while consuming the same power, i.e., P_c, with a power amplifier efficiency of μ_s. It is assumed without loss of generality that d_{1r} is the closest distance to the destination, i.e., $d_{1r}^{\alpha} \leq d_{2r}^{\alpha} \leq \cdots \leq d_{lr}^{\alpha}$. Equating the total power consumption of l cooperative BSs from (4.22) with the equivalent power consumption of the supernode, one can write

$$\frac{B}{\mu \sum_{k=1}^{l} \frac{1}{d_{kr}^{\alpha}}} = \frac{B}{\mu_s} d_{1r}^{\alpha}. \tag{4.23}$$

Solving (4.23) for μ_s gives

$$\mu_s = \mu \left(1 + \sum_{k=2}^{l} \frac{d_{1r}^{\alpha}}{d_{kr}^{\alpha}} \right). \tag{4.24}$$

It can be seen from (4.24) that the highest power amplifier efficiency of the supernode is obtained when all of the l transmitting BSs are distant enough from the destination BS so that they can be seen at the same distance as the closest node from the destination, i.e., at d_{1r}. Hence, the power amplifier efficiency of the supernode is upper bound as $\mu_s \leq l\mu$. Furthermore, as the distance between the destination BS and the closest transmitting BS diminishes, i.e., $d_{1r} \to 0$, then $\mu_s \to \mu$, which means that the performance of the cooperative transmission reduces to that of the non-cooperative one.

Now, equation (3.12) can be rewritten as

$$d_{opt} = \sqrt[\alpha]{\frac{C\mu_{pa}}{B(\alpha - 1)}}, \tag{4.25}$$

where β in (3.12) has been replaced by B/μ_{pa}, i.e., $\beta = B/\mu_{pa}$. Using $\mu_{pa} = \mu_s = l\mu$, i.e., the condition where cooperation is most efficient, and $C = (l+1)E$ in (4.25), one can calculate d_{opt} for cooperative transmission as

$$d_{opt} = \sqrt[\alpha]{\frac{(l+1)El\mu}{B(\alpha - 1)}}. \tag{4.26}$$

Thus, a virtual node V is placed between the supernode and the destination, at a distance d_{opt} from the supernode. The next hop (BS) destination is chosen as the nearest hop to this virtual node. Let this next hop destination be denoted as BS(n), i.e, the nth hop destination found during the routing process. Since the source BS

knows the location of all its neighbors, and BS(n) will always be one of its neighbors, so it can calculate the optimal non-cooperative route towards BS(n). If the multi-hop non-cooperative transmission towards BS(n) consumes less power than the cooperative transmission, the algorithm switches to non-cooperative transmission, otherwise, the source BS broadcasts its data to its selected adjacent BSs and these BSs then transmit cooperatively.

The aforementioned procedure is summarized in Algorithm 4.1.

Algorithm 4.1 power-aware Cooperative Routing Algorithm

Require: Wireless network, with source S, destination D and location of BSs.

Initialize $n = 0$.
$BS(n) \leftarrow S$.
while $BS(n) \neq D$ **do**
  if D is a first tier neighbor of $BS(n)$ **then**
    $BS(n+1) \leftarrow D$
  else
    Select $(l-1)$ closest neighbors.
    Find the virtual node position and select $BS(n+1)$.
    Select between cooperative and non-cooperative transmission modes and transmit accordingly.
  end if
  Update route table.
  $n = n + 1$.
end while

4.5 Performance Evaluation

In this section, PACR is implemented in a wireless mesh network of cellular base stations and its performance is compared with CAN-L [57] and PSR [21].

4.5.1 Simulation Setup

Table 4.1: System Parameters

$l = 3, 4$	$\alpha = 2, 4$	$\gamma_r = 10$ dB
$\mu_{pa} = 20\%$	$f = 2.4$ GHz	$E = 115.9$ mW
$P_\eta = -101$ dBm		

For performance evaluation, a network of 400 base stations is considered with the source and the destination base stations located on the opposite corners of the network, as shown in Figure 4.1. For fairness of comparison, the experiments are also performed for randomly selected source-destination pairs. For detailed analysis, the algorithms are tested under a variety of conditions, i.e., $\alpha = 2, 4$ and $l = 3, 4$. For $\alpha = 2$, the BS to BS distance varies from $800m$ to $4000m$, while for $\alpha = 4$, the inter-BS distances range from $100m$ to $1000m$, reflecting the urban environment. The rest of the parameters used in the simulations are outlined in Table 4.1. For the randomly selected source-destination pairs, the results are averaged over 10000 iterations.

4.5.2 Simulation Results

This section presents the simulation results. Unless stated otherwise, all the results shown in this section include transmission power consumption and the circuit power consumption.

Figure 4.6 demonstrates the transmission power saving that is produced by single hop cooperative transmission with respect to non-cooperative transmission when $E = 0$. As shown in the figure, the power saving increases with increasing transmission distance, until it becomes saturated after a certain distance. This maximum power saving is roughly equal to the previously derived upper bound on the power saving, i.e., (4.19).

Figure 4.7 verifies the claim in Corollary 4.1 and the discussion made in Lemma 4.1. As discussed in Lemma 4.1, single-hop cooperative transmission consumes the minimum power when all the cooperating base stations are equidistant from the destination. Realistically, it is difficult to have a practical scenario where all the cooperating nodes are at the same distance from the destination. However, this result indicates that the cooperating base stations should be as close to each other as possible, so that they appear to be at a similar distance from the destination. For this reason, a transmitting base station in PACR broadcasts its information to its nearest adjacent BSs, so that the cooperating BSs are as close to each other as possible. Figure 4.7 also shows that the cooperative transmission outperforms the non-cooperative transmission, in terms of power consumption, when the transmission distance is greater than the distance threshold derived in Corollary 4.1. The figure also shows the locations of the transmitting base stations when they are not equidistant from the destination.

Figure 4.8 and Figure 4.9, respectively, illustrate the effect of varying BS to BS distances on the different routing algorithms for the scenario shown in Figure 4.1 and for randomly selected source-destination pairs. The power consumption values for

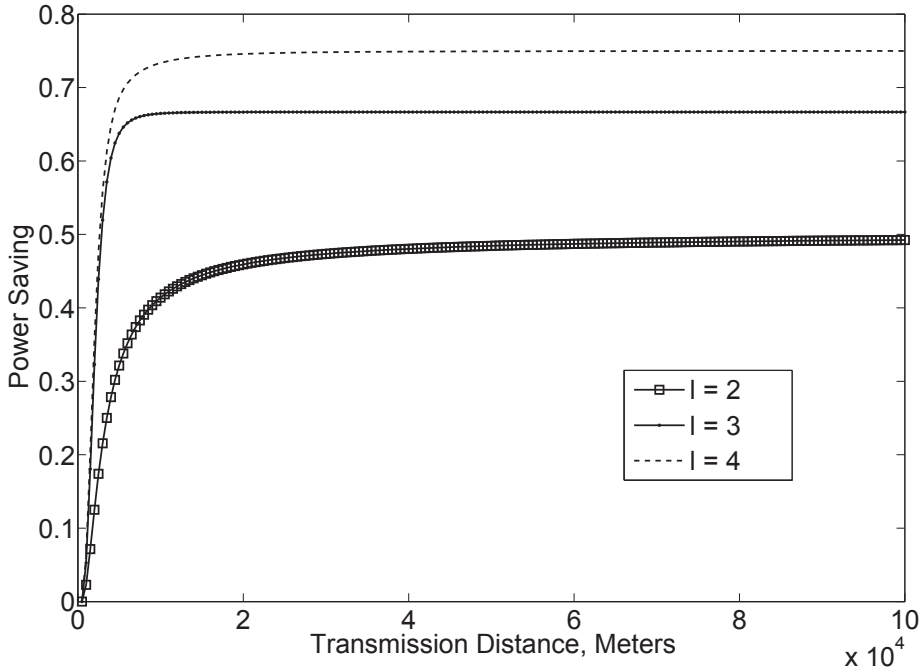

Figure 4.6: Power saving achieved by single-hop cooperative transmission as a function of the transmission distance for $\alpha = 2, l = 3$.

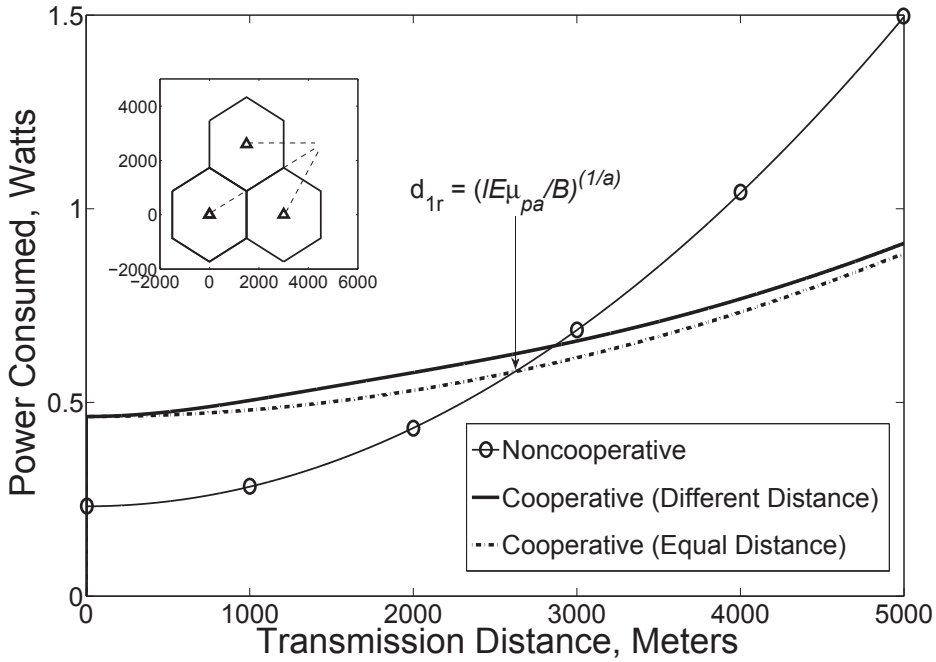

Figure 4.7: Power consumption versus the transmission distance for $\alpha = 2$, $l = 3$.

PACR are calculated by adding the sums of the powers consumed by the cooperative and the broadcast transmissions. It is shown that PACR outperforms both CAN-L and PSR for the whole range of site to site distances. The power consumption values in Figure 4.8 and Figure 4.9 correspond roughly to an energy saving of upto 12% over PSR and between 15% - 50% over CAN-L.

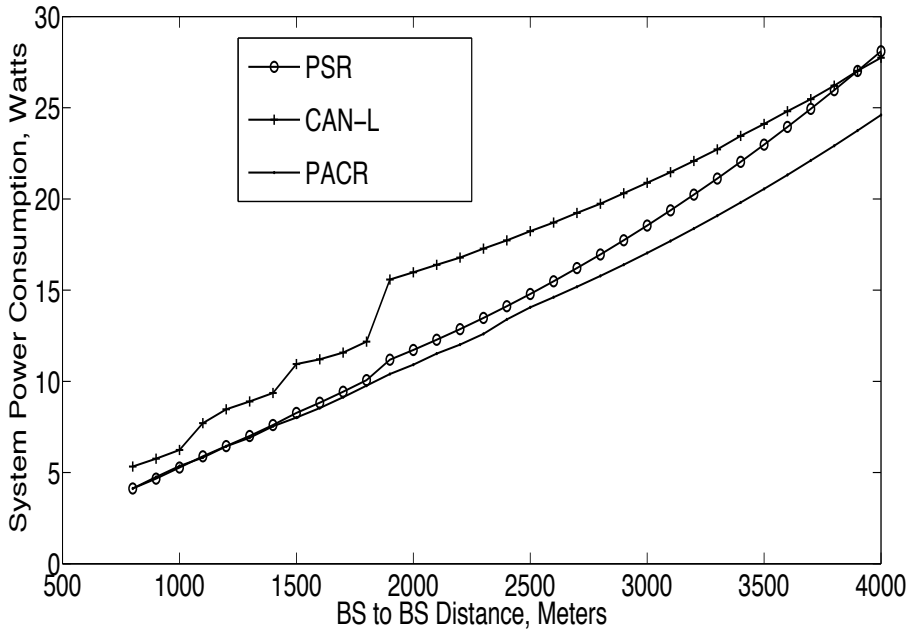

Figure 4.8: Power consumption of the routing algorithms versus the BS to BS distance for $\alpha = 2, l = 3$.

The results in Figure 4.8 are for rural environments with large cells and low pathloss exponents. For urban environments, the inter-BS distances are smaller and the pathloss exponents are relatively higher. Figure 4.10 demonstrates the energy consumption gain (ECG) of PACR with respect to PSR and CAN-L for $\alpha = 4$ and $l = 4$. It can be seen that PACR produces a minimum power saving of around 30% over PSR and about 19% over CAN-L. The figure also shows that the algorithm transmits non-cooperatively until the BS to BS distance is 300m, after which, it switches to cooperative transmission. This shows that the proposed algorithm intelligently switches between cooperative and non-cooperative transmissions, depending on the specific scenario. More discussion and results on this switching mechanism are included later in this section.

Figure 4.11 illustrates the effect of l on the cooperative routing algorithms. It is shown that an increase in the number of cooperating base stations does not necessarily improve the performance of cooperative transmission. This is due to the increased circuit power consumption. As shown in the figure, both CAN-L and PACR consume

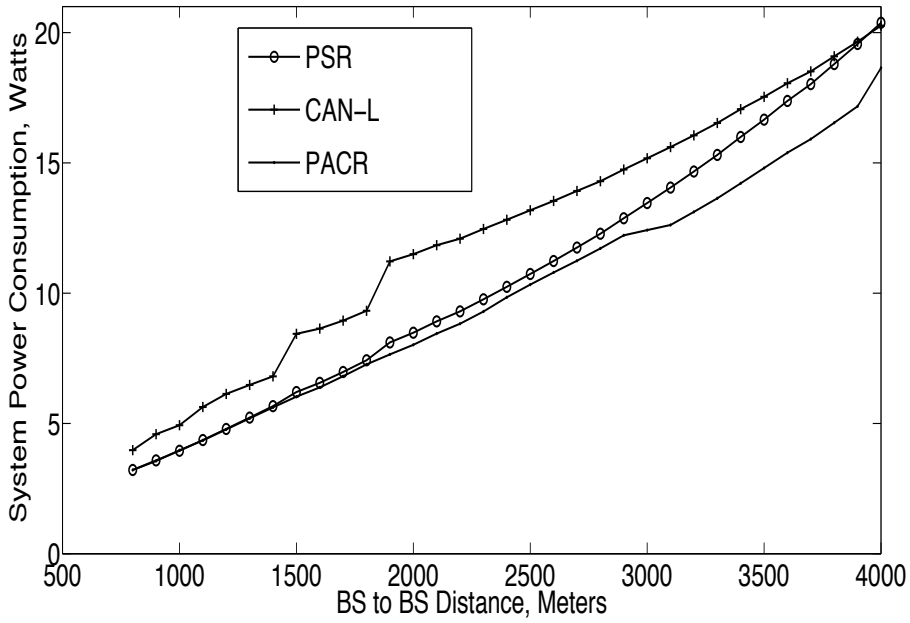

Figure 4.9: Power consumption of the routing algorithms versus the BS to BS distance for $\alpha = 2, l = 3$.

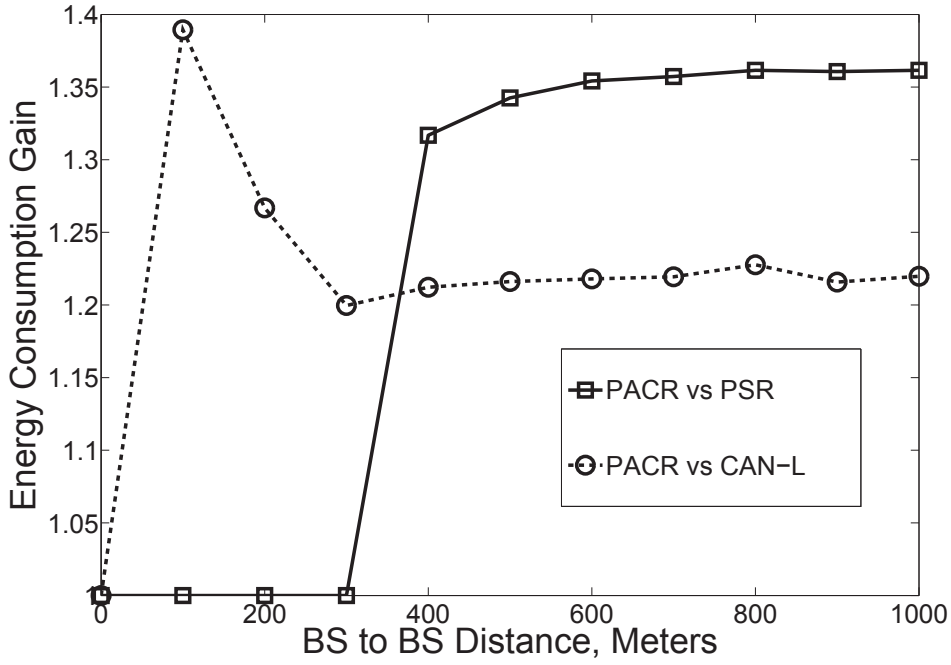

Figure 4.10: Power saving achieved by PACR as a function of the BS to BS distance for $\alpha = 4, l = 4$.

more power with larger l. This is contrary to the findings in [57] and [59], which conclude that increasing the number of cooperating nodes increases the power saving.

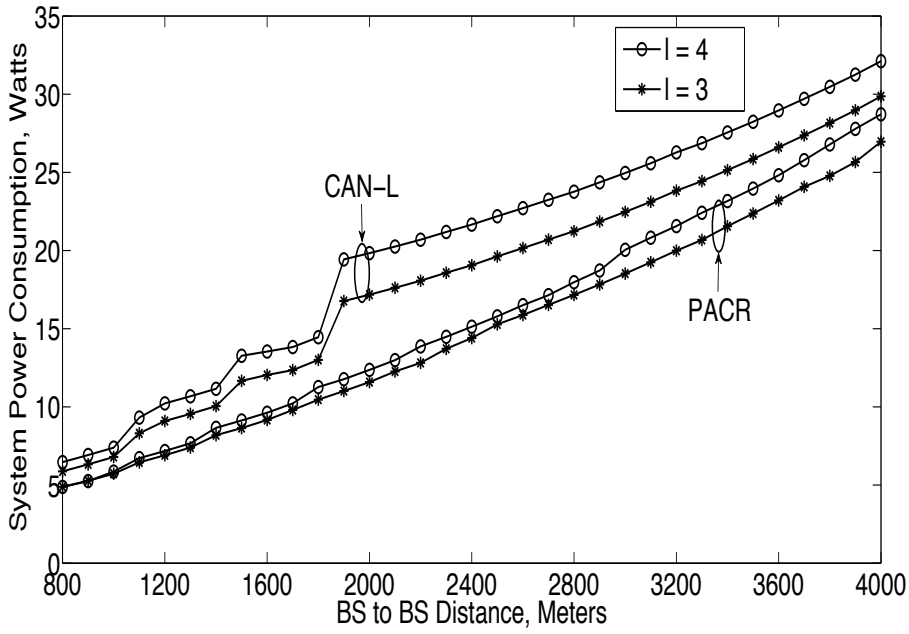

Figure 4.11: Power consumption of the routing algorithms versus the BS to BS distance for $\alpha = 2$.

Fig. 4.12 demonstrates the switching mechanism that was incorporated into the proposed algorithm. The figure shows the power consumption of PSR, PACR without switching (PACRWO) and PACR with switching. PACRWO skips Step 9 in Algorithm 4.1, i.e., it always transmits cooperatively irrespective of the channel conditions. Notice how PACR with dynamic switching uses PSR as long as it performs better than PACRWO and vice versa.

Finally, Table 4.2 shows the average number of hops required by PSR and PACR to reach the destination for $\alpha = 2; l = 3$. The averages are taken over 10000 randomly generated source destination pairs. The hop count for PACR is calculated by adding the total number of cooperative and broadcast transmissions. Notice that CAN-L consumes the same number of hops as PSR, since it just transmits cooperatively over the optimal non-cooperative route.

4.6 Concluding Remarks

In this chapter, a new power saving cooperative routing algorithm was proposed for a wireless mesh network of cellular base stations. The main assumption was that all

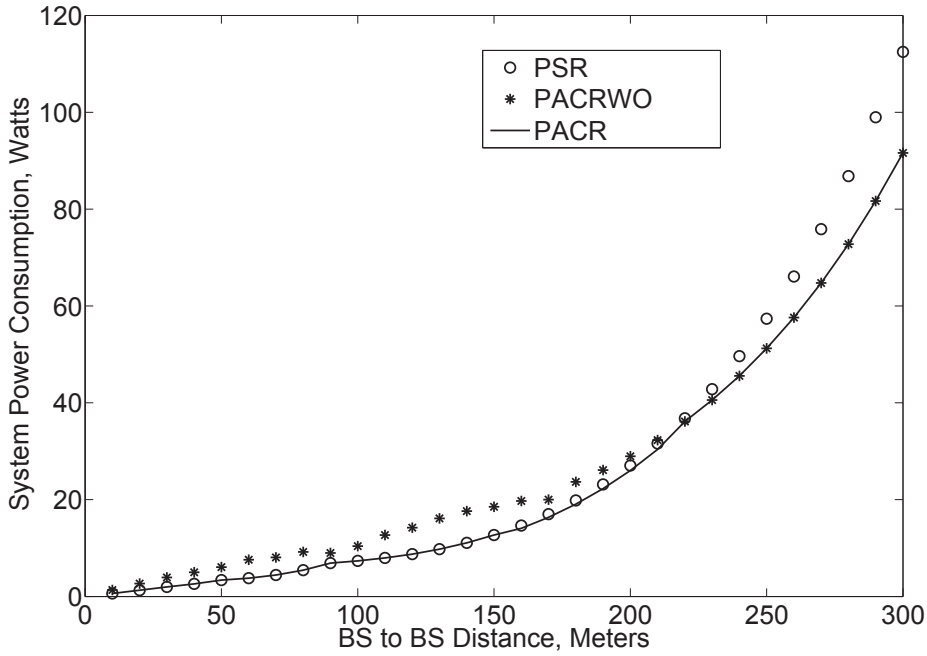

Figure 4.12: Power consumption versus the BS to BS distance for $\alpha = 4, l = 4$.

Table 4.2: Mean Number of Hops

Inter-BS Distance	**800**	**1300**	**1800**	**2300**	**2800**	**3000**
PSR	6.38	9.67	12.90	17.86	17.87	18.00
PACR	5.16	7.45	9.70	10.70	12.42	12.53

the transmitters are perfectly synchronized for coherent reception at the receiver. By taking the radio electronics power consumption into consideration, the performance of single hop cooperative transmission was analyzed. As a result of this analysis, a distance threshold was derived which could be used to decide whether to use cooperative or non-cooperative transmission, for a specific scenario. On the basis of this distance threshold, the chapter emphasized on the inadequacies of the existing power saving cooperative routing algorithms. Then, the novel concept of equivalent power amplifier efficiency was introduced to model the group of cooperating base stations as a single supernode and this enabled us to find an optimal location for the next hop destination and to design a new power-aware cooperative routing algorithm. The proposed PACR algorithm intelligently switches between cooperative and non-cooperative transmissions, depending on the network parameters and conditions. Simulation results

showed that increasing the number of cooperating base stations does not necessarily guarantee reduced system power consumption. The results also confirmed that, depending on the network conditions, PACR could achieve a power saving of between 15% to 50% over a baseline cooperative-routing scheme and upto 30% over a baseline non-cooperative routing algorithm. Furthermore, this power saving was achieved while consuming lesser number of hops as compared to the baseline routing algorithms.

Chapter 5

Power-Aware Routing in Multihop Cognitive Radio Networks

In all the work presented so far in this thesis, only the end to end power consumption and the hop count of the optimal route were taken into consideration. This chapter, in addition to the total power consumption of the route, focuses on the interference generated within the network and its impact on the network throughput. To this end, a multi-hop cognitive radio network scenario is considered. The study addresses the problem of coexistence between a multi-hop secondary underlay network and a set of primary receivers operating in the same region. Taking into account the positions of the primary and the secondary nodes, a transmit beamforming strategy is introduced and investigated. Using local information, the beamforming strategy is then used to define a novel path optimization scheme that modifies a power saving path pre-selected from the routing module. The path is modified based on a relay selection metric designed so to improve both, the coexistence with primary receivers and the performance of the secondary network. The proposed strategy is compared with a baseline solution that does not adopt beamforming and with a strategy that applies beamforming on each hop without modifying the original path. Computer simulations are performed by combining a signal processing tool and a network simulator. Results show that the proposed strategy is capable of improving coexistence with primary nodes, while guaranteeing lower interference towards other secondary receivers. Furthermore, the proposed strategy also outperforms the baseline algorithms in terms of power consumption. Finally, packet level simulations highlight that potential trade-offs exist between meeting coexistence constraints and maximizing secondary network performance.

5.1 Introduction

Recently, the huge successes of wireless applications have lead to an exponential increase in the demand to regulatory authorities for spectrum allocation. Consequently, the spectrum has become an expensive entity, leading to a struggle between the private, public and military sectors for the right to access the spectrum resource. Among the various solutions that have been proposed to tackle this problem, cognitive radio networks (CRN) have achieved the highest popularity. The more general concept of the cognitive radios (CR) enables the primary and the secondary users to co-exist within the same spectrum band, provided that the quality of service (QoS) requirements of the primary users are not affected. The primary spectrum users allow spectrum access to the secondary users as long as the interference generated within the secondary network is less than a tolerable interference level for the primary users.

So far, most of the research on cognitive radios has been focused on single-hop scenarios, tackling physical (PHY) layer and/or medium access control (MAC) layer issues [82]. However, recent research finding have highlighted the potentials of multi-hop cognitive radio networks [83]. The cognitive paradigm can be applied to different scenarios of multi-hop wireless networks, one such scenario being the cognitive radio ad hoc network which consists of CR nodes which communicate with each other in a peer to peer fashion through ad hoc connections [84]. To fully realize the potential of such networks, cross-layer design issues must be addressed, for example, the routing decisions at the network layer should be made in conjunction with the PHY layer characteristics.

In the above framework, the present work focuses on power and interference aware routing in an underlay multi-hop secondary network. Transmit beamforming is utilized in order guarantee coexistence with the primary nodes. Although beamforming has been proposed in the past as a way to improve the capability of secondary network nodes [85], [86], this work goes beyond previous attempts by taking into account beamforming in the selection of relays in multi-hop connections. The proposed approach defines a metric that, relying on position information available at local level, modifies the path originally selected by Dijkstra's shortest path routing algorithm so to improve network performance while guaranteeing coexistence requirements. The proposed strategy is compared with previous work that adopted beamforming in the secondary network without changing the path. The computer simulations are performed by combining a signal processing tool, i.e., MATLAB, and a network simulator, i.e., OMNet++.

The chapter is organized as follows. Section 5.2 introduces the transmit beamforming strategy and investigates its performance for single hop scenarios. The path opti-

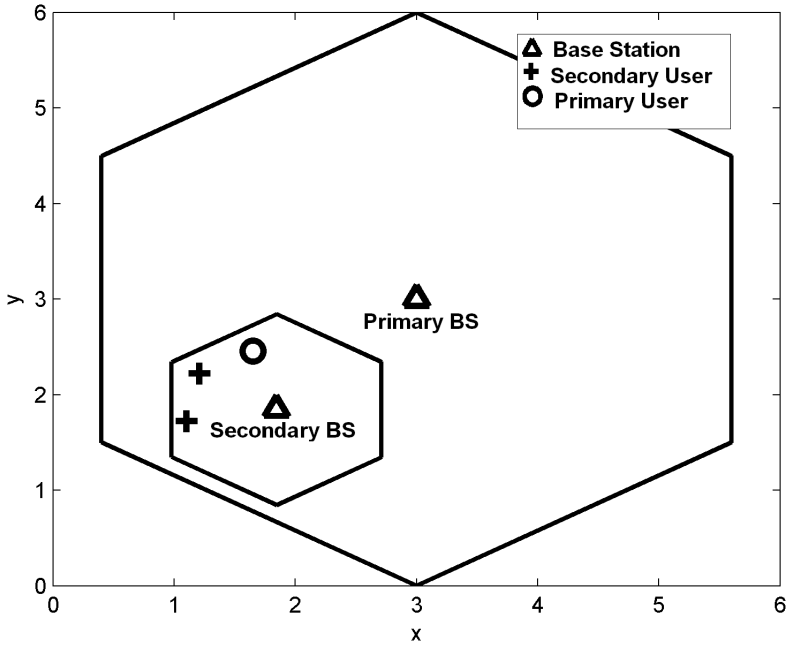

Figure 5.1: Cognitive cellular network with one secondary cell within a primary cell.

mization strategy is described in Section 5.3. Finally, the performance of the proposed routing strategy is evaluated in Section 5.4, while Section 5.5 draws the conclusions.

5.2 Transmit Beamforming

The transmit beamforming strategy is introduced and evaluated in this section. The goal is to keep the interference imposed on the primary users by the secondary transmissions within the allowed interference shaping margins (ISM) required by each primary user while satisfying the QoS requirements of the secondary receivers.

5.2.1 System Model

Consider a system of K secondary users, a secondary BS, M primary users and a primary BS. Figure 5.1 illustrates this scenario. In the figure, the BS at the center of the larger cell is the primary BS, whereas the one at center of the smaller cell is the secondary BS. The secondary user BS consists of a uniform linear array (ULA) with N transmit antennas, while each receiver (primary or secondary) has a single receive antenna. The ULA has a spacing of half a wavelength between adjacent antenna elements.

Let the beamforming weight vectors be denoted by $\mathbf{w}_i \in \mathcal{C}^{N\times 1}$, where i represents the i^{th} secondary user. The transmitted signal is given as

$$\mathbf{x} = \sum_{i=1}^{K} \mathbf{w}_i s_i, \tag{5.1}$$

where the data symbol intended for the secondary user i is s_i. For the k^{th} secondary user, the received signal can be expressed as

$$y_k = \sum_{i=1}^{K} \mathbf{h}_k \mathbf{w}_i s_i + n_k, \qquad 1 \leq k \leq K, \tag{5.2}$$

where $\mathbf{h}_k \in \mathcal{C}^{1\times N}$ represents the spatial channel response vector between the secondary base station and the k^{th} secondary user, $n_k \in \mathcal{C}$ represents complex AWGN with zero mean and variance σ_k^2. The spatial channel response vector $\mathbf{h}_k$ can be written as

$$\mathbf{h}_k = [h_{k,1}\ h_{k,2} \ldots h_{k,N}], \tag{5.3}$$

where $h_{k,q}$, $q \in [1 \ldots N]$, models the channel between the q^{th} element of the transmitting secondary BS and the k^{th} secondary receiver. $h_{k,q}$ can be written as

$$h_{k,q} = e^{j\frac{2\pi\Delta}{\zeta}(q-1)\sin(\theta_k+\phi)} A\sqrt{1/L_k}, \tag{5.4}$$

where Δ is the antenna element spacing, ζ is the carrier wavelength while θ_k is the angle-of-departure (AoD) relative to the array antenna broadside; ϕ represents a small deviation from θ_k with normal distribution, i.e., $\phi \sim \mathcal{N}(0, \sigma^2)$, where σ represents the angular spread of local scatterers surrounding the receiver. Finally, A represents the fading coefficient between the transmitter and the receiver while L_k is the distance dependent pathloss. The channel response vector between the secondary BS and m^{th} primary user is denoted by $\mathbf{h}_{pm} \in \mathcal{C}^{1\times N}$.

5.2.2 Orthogonal Transmit Beamforming Strategy

The main concept behind OTBF is that the transmitted signals should be made orthogonal to each other to overcome co-channel interference among the users without a need for further processing at the receiver ends. OTBF is applied in cognitive radio network environment based on specific constraints. These constraints would be in terms of the interference margin for the primary users and the signal to interference

plus noise ratio (SINR) requirements by the secondary users.

Instead of instantaneous channel state information, the second order statistics of the channel state information (CSI) are used at the secondary BS, i.e., $\mathbf{R}_k = \mathbf{E}[\mathbf{h}_k^{\mathbf{H}}\mathbf{h}_k]$, $1 \leq k \leq K$ and $\mathbf{R}_{pm} = \mathbf{E}[\mathbf{h}_{pm}^{\mathbf{H}}\mathbf{h}_{pm}]$, $1 \leq m \leq M$, where $\mathbf{R}_k$ and $\mathbf{R}_{pm}$ are the channel autocorrelation matrices for the k^{th} secondary m^{th} primary user, respectively. Channel ergodicity is assumed and the statistical average is obtained by averaging over sufficient number of time samples as follows,

$$\mathbf{R} \stackrel{\triangle}{=} \lim_{M\to\infty} \frac{1}{M} \sum_{i=1}^{M} \mathbf{h}^{\mathbf{H}}(t_i)\mathbf{h}(t_i), \tag{5.5}$$

where $\mathbf{h}(t_i)$ is a multiple-input single-output (MISO) channel vector at time t_i.

Next, the OTBF strategy is formulated for a cognitive scenario with K secondary users and M primary users. It is assumed that the secondary BS can pre-subtract the interference caused by the primary BS in the secondary users by Dirty Paper Coding (DPC), [87]. Applying DPC becomes a more realistic assumption, in particular, when the secondary and primary BS, are located in a close vicinity such that the primary BS information can be correctly revealed to the secondary BS via a reliable backhaul link. The details of well researched area of DPC can be found in literature, e.g. [88, 89] and its treatment is beyond the scope of this work. In the absence of a reliable backhaul link, the interference caused by the primary BS is simply treated as additional noise on the secondary users and it does not impact our formulations. Hence, in the following formulations, the interference caused by the primary BS on the secondary users is ignored.

The impinging directions of the secondary users can be estimated by the secondary BS using the algorithm described in [90]. As shown in [90], the resolution of this estimation depends on the number of antenna elements. In the Monte-Carlo simulation carried out in this paper, we have modeled the inaccuracy in estimating the impinging directions by allowing the angular direction of the users to be a uniformly distributed random variable, that is, over $\pm\delta$ of their nominal values.

Minimum Transmit Power Beamforming Strategy

The strategy aims to minimize the sum transmit power at the secondary BS as follows,

$$\begin{aligned} \underset{p_k^t}{\text{minimize}} \quad & \sum_{k=1}^{K} p_k^t \\ \text{subject to} \quad & SINR_k \geq \gamma_k,\ 1 \leq k \leq K, \\ & \sum_{k=1}^{K} I_{km} \leq \varphi_m,\ 1 \leq m \leq M, \end{aligned} \tag{5.6}$$

where p_k^t is the transmitted power from the secondary BS to the k^{th} secondary user, $SINR_k$ denotes the SINR at the k^{th} secondary user with γ_k as its minimum desired level, I_{km} is the interference inflicted on the m^{th} primary user as a result of the transmission by the secondary BS to the k^{th} secondary user. The second constraint in (5.6) models the interference shaping, wherein, φ_m is the upper limit on the allowed interference margin imposed by the m^{th} primary user due to secondary transmission. The SINR at the k^{th} secondary user is given as

$$SINR_k = \frac{p_k^r}{I_k + \sigma_k^2}, \tag{5.7}$$

where p_k^r, I_k and σ_k^2 are, respectively, the received signal power, multiuser interference and noise variance at the secondary user k.

The average received signal power at the k^{th} secondary user can be written as

$$p_k^r = \underset{s_k, \mathbf{h}_k}{E}[\mathbf{w}_k^{\mathbf{H}} \mathbf{h}_k^{\mathbf{H}} s_k^* s_k \mathbf{h}_k \mathbf{w}_k],$$

where the expectation is taken over the channel and the transmitted symbols statistics. Since these random quantities are independent from one another and the average energy of symbol constellation is normalized to unity, i.e., $\underset{s_k}{E}[|s_k|^2] = 1$, one can write

$$p_k^r = \mathbf{w}_k^{\mathbf{H}} \mathbf{R}_k \mathbf{w}_k, \tag{5.8}$$

where $\mathbf{R}_k = \underset{\mathbf{h}_k}{E}[\mathbf{h}_k^{\mathbf{H}} \mathbf{h}_k]$.

Similarly, the average transmit power allocated to the k^{th} user at the secondary BS

can be written as

$$\begin{aligned} p_k^t &= \underset{s_k}{E}[\mathbf{w}_k^{\mathbf{H}} s_k^* s_k \mathbf{w}_k] \\ &= \mathbf{w}_k^{\mathbf{H}} \mathbf{w}_k \end{aligned} \tag{5.9}$$

Hence, the optimization problem in (5.6) is equivalent to the following problem

$$\begin{aligned} \underset{\mathbf{w_k}}{\text{minimize}} \quad & \sum_{k=1}^{K} \mathbf{w}_k^{\mathbf{H}} \mathbf{w}_k \\ \text{subject to} \quad & \frac{\mathbf{w}_k^{\mathbf{H}} \mathbf{R}_k \mathbf{w}_k}{\sum_{j=1, j\neq k}^{K} \mathbf{w}_j^{\mathbf{H}} \mathbf{R}_k \mathbf{w}_j + \sigma_k^2} \geq \gamma_k, \ 1 \leq k \leq K, \\ & \sum_{k=1}^{K} \mathbf{w}_k^{\mathbf{H}} \mathbf{R}_{pm} \mathbf{w}_k \leq \varphi_m, \ 1 \leq m \leq M, \end{aligned} \tag{5.10}$$

where $I_k = \sum_{j=1, j\neq k}^{K} \mathbf{w}_j^{\mathbf{H}} \mathbf{R}_k \mathbf{w}_j$ is the overall multiuser interference in the secondary system imposed on the k^{th} secondary user. Similar to (5.8), one can easily show that $I_{km} = \mathbf{w}_k^{\mathbf{H}} \mathbf{R}_{pm} \mathbf{w}_k$.

Note also that the thresholds γ_k and φ_m in (5.10) can be different for different users, and, hence, each secondary user can have its own SINR requirement and the interference margin on a primary user.

Next, the non-convex optimization problem (5.10) is converted into a convex semidefinite programming (SDP) problem solvable by the SeDuMi [91] solver. Defining $\mathbf{F}_k = \mathbf{w}_k \mathbf{w}_k^{\mathbf{H}}$, one can write the problem (5.10) as follows

$$\begin{aligned} \underset{\mathbf{F}_k}{\text{minimize}} \quad & \sum_{\mathrm{k}=1}^{K} \mathrm{tr}[\mathbf{F}_k] \\ \text{subject to} \quad & \mathrm{tr}[\mathbf{R}_k \mathbf{F}_k] - \gamma_k \sum_{j\neq k} \mathrm{tr}[\mathbf{R}_k \mathbf{F}_j] \geq \gamma_k \sigma_k^2 \\ & \sum_{k=1}^{K} \mathrm{tr}[\mathbf{R}_{pm} \mathbf{F}_k] \leq \varphi_m, \ 1 \leq m \leq M, \\ & \mathbf{F}_k = \mathbf{F}_k^{\mathbf{H}} \succeq 0, \ 1 \leq k \leq K. \end{aligned} \tag{5.11}$$

Notice that the rotation property of the trace operator, i.e., $\mathrm{tr}[\mathbf{AB}]=\mathrm{tr}[\mathbf{BA}]$, has been used to arrive at $\mathbf{w}_k^{\mathbf{H}} \mathbf{R}_k \mathbf{w}_k = \mathrm{tr}[\mathbf{R}_k \mathbf{w}_k \mathbf{w}_k^{\mathbf{H}}] = \mathrm{tr}[\mathbf{R}_k \mathbf{F}_k]$. As implied from the definition, $\mathbf{F}_k$ is a Rank 1 and Hermitian positive semidefinite matrix. The latter condition on $\mathbf{F}_k$ appears as an additional constraint in (5.11), but the former one, i.e., Rank 1 condition,

which is a non-convex constraint [92–94], has been relaxed and excluded from (5.11) to maintain the convexity of the problem. In a convex problem, the objective function and the constraints must be convex and in such problem, a local minimum is also a global minimum [95].

Next, to ensure that multiuser interference at each of the secondary users is directly removed from the signal without any further processing, orthogonality of the transmitted signals is enforced at the BS by setting $\sum_{j\neq k} \mathrm{tr}[\mathbf{R}_{sk}\mathbf{F}_{sj}] = 0$ in (5.11). Finally, an equivalent form of the original problem (5.6) is presented in the standard SDP form as follows,

$$\begin{aligned} \underset{\mathbf{F}_k}{\text{minimize}} \quad & \sum_{k=1}^{K} \mathrm{tr}[\mathbf{F}_k] \\ \text{subject to} \quad & \mathrm{tr}[\mathbf{R}_k\mathbf{F}_k] \geq \gamma_k\sigma_k^2 \\ & \mathrm{tr}[\mathbf{R}_k\mathbf{F}_j] = 0 \;\; j \neq k \\ & \sum_{k=1}^{K} \mathrm{tr}[\mathbf{R}_{pm}\mathbf{F}_k] \leq \varphi_m, \; 1 \leq m \leq M, \\ & \mathbf{F}_k = \mathbf{F}_k^{\mathbf{H}} \succeq 0, \; 1 \leq k \leq K. \end{aligned} \tag{5.12}$$

The problem (5.12) can be solved by the SeDuMi solver [91] to find $\mathbf{F}_k$. However, to obtain the optimal beamforming vectors $\mathbf{w}_k, k = 1...K$, one is mainly interested in $\mathbf{F}_k$ solutions of (5.12) that are of Rank 1.

An OTBF beamforming vector $\mathbf{w}_k$ is obtained by, first, finding a rank 1 feasible $\mathbf{F}_k$, as a solution to (5.12), and then, extracting the eigenvector associated to the only nonzero eigenvalue, through the eigen decomposition of resulting $\mathbf{F}_k$. Denoting this single nonzero eigenvalue as $\lambda_{n,k}$ and its corresponding eigenvector as $\mathbf{e_{n,k}}$, one can find the square root of $\mathbf{F}_{sk}$ as follows

$$\begin{aligned} \mathbf{F}_k &= \lambda_{N,k}\mathbf{e_{N,k}}\mathbf{e_{N,k}^H} \\ &= (\sqrt{\lambda_{N,k}}\mathbf{e_{N,k}})(\sqrt{\lambda_{N,k}}\mathbf{e_{N,k}})^{\mathbf{H}} \\ &= \mathbf{w}_k\mathbf{w}_k^{\mathbf{H}}, \end{aligned} \tag{5.13}$$

where $\mathbf{w}_k = \sqrt{\lambda_{N,k}}\mathbf{e_{N,k}}$.

5.2.3 Performance Evaluation of OTBF

This section evaluates the performance of OTBF for the scenario shown in Figure 5.1. The SDP problem of (5.12) is implemented by using the SeDuMi solver under CVX [95].

Simulation Setup

For experimental set up, the secondary BS is assumed to be equipped with a uniform linear antenna array with 8 antenna elements and a spacing of a half of a wavelength between the adjacent elements. The number of secondary users is 2 and there is one active primary user within the primary network. It is assumed that the primary user is located in 10 degree angular position relative to the secondary BS antenna broadside. While the first secondary user is considered to be at an angular position of 20 degrees, the second secondary user is allowed to move between 25 and 50 degrees of angular positions, all relative to the secondary BS antenna broadside. An angle spread of 2 degrees around the main angular position is assumed for all users. Furthermore, a fixed noise variance of 0.01 is assumed at all users while different interference shaping margins of ISM= 3dB, -3dB, -13dB and -16dB are used at the primary user. A minimum SINR level of $\gamma_k = 10$dB is used for all the secondary users in the simulation setup.

Simulation Results

Figure 5.2 shows the performance of minimum transmit power strategy, i.e., (5.12), in minimising the total transmit power at the secondary BS as a function of the angular separation between the secondary users and the interference margin allowed by the primary user. The results are shown for a uniform linear antenna array with 8 and 4 antenna elements. The curve without an ISM constraint is our benchmark curve. The results for 4 antenna elements show that with angular separations of less than 6 and 8 degrees for ISM thresholds of -3dB, -13dB and -16dB, respectively, the users cannot be resolved with finite transmission power. Whereas, with 8 antenna elements all user can be resolved under the ISM thresholds. These results are also confirmed in Figure 5.3 in terms of satisfying the ISM thresholds at the primary users for 4, 6 and 8 antenna elements. For instance, ISM = -16dB is always satisfied with 8 antenna elements, whereas with 6 and 4 antenna elements this ISM threshold cannot be supported for angular separations below 6 and 8 degrees, respectively.

Figure 5.4 shows that due to a reduced ISM on the primary user, i.e. from ISM = 3dB to ISM = -16dB, the solution to the optimization problem 5.12 shifts the beam pattern of the secondary BS slightly to the right and increases the minimized objective function value, i.e., the overall transmit power at the secondary BS. This increase in the secondary BS transmit power can also be verified from Figure 5.2. The radiation

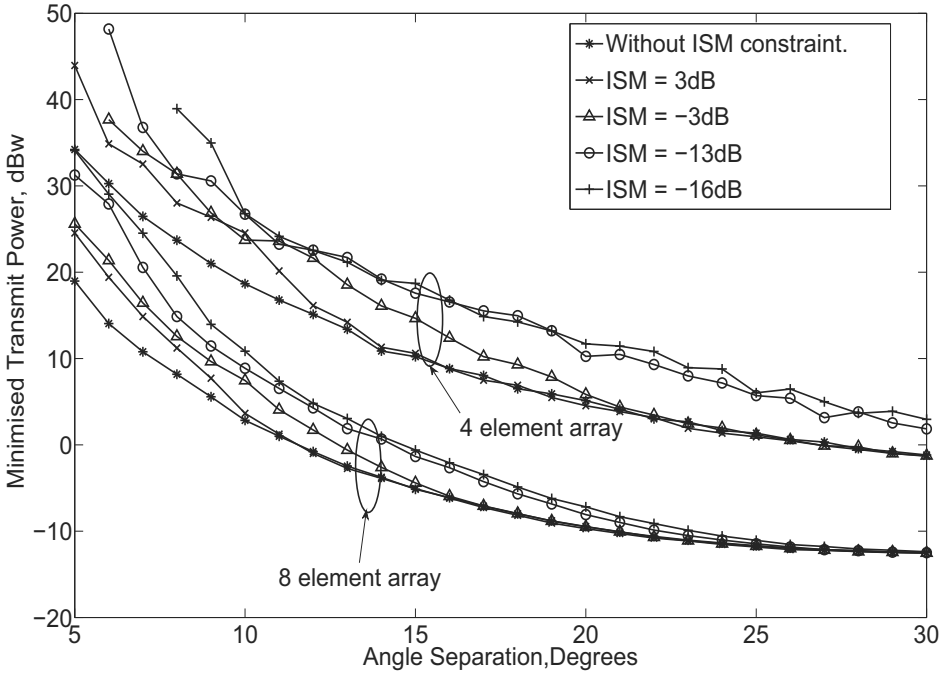

Figure 5.2: Minimized transmit power at the secondary BS versus angular separation between the secondary users as a function of allowed interference shaping margin by the primary user.

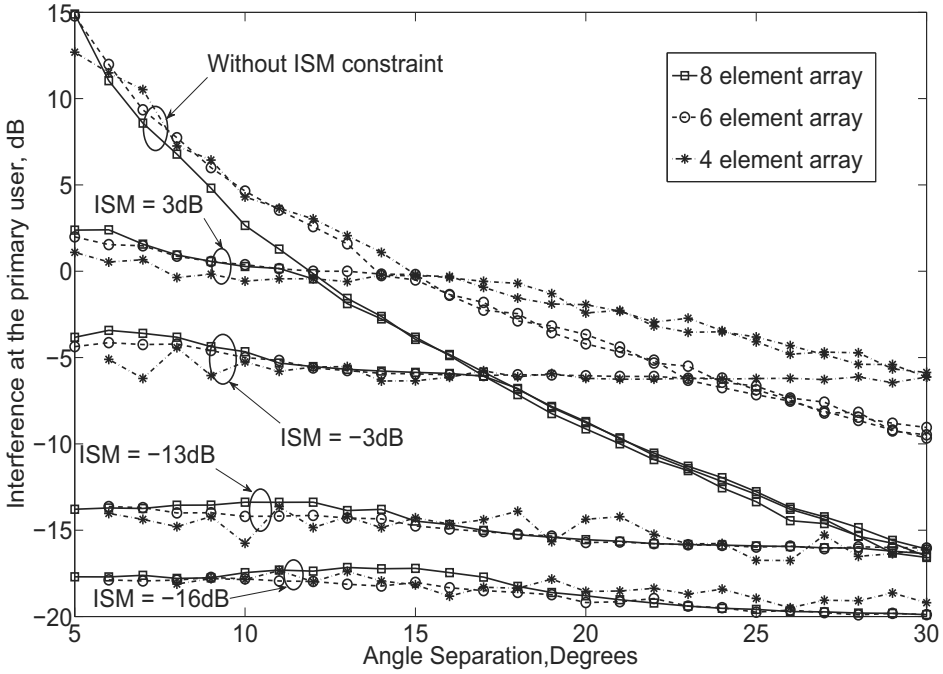

Figure 5.3: Interference imposed on the primary user versus angular separation between the secondary users as a function of allowed interference shaping margin by the primary user.

power patterns in Figure 5.4 have been plotted using

$$P(\theta) = \mathrm{tr}[\mathbf{h}^{\mathrm{H}}(\theta)\mathbf{h}(\theta)(\sum_{i=1}^{K}\mathbf{w}_i\mathbf{w}_i^{\mathrm{H}})], \tag{5.14}$$

where $P(\theta)$ represents the power radiated in the angular direction θ and $\mathbf{h}(\theta) = [1\ e^{j\pi sin(\theta)} \dots e^{j(N-1)\pi sin(\theta)}]$. A derivation of (5.14) is given in Appendix G. For our plots, θ is varied from -90 to 90 Degrees. It is apparent from Figure 5.4 that, overall, more transmit power is required by the secondary BS as we decrease the allowed interference margin at the primary user from 3dB to -16dB. However, although the overall transmitted power increases for the smaller ISM, yet, it decreases in the location area of the primary users, shown between the bold vertical lines in Figure 5.4.

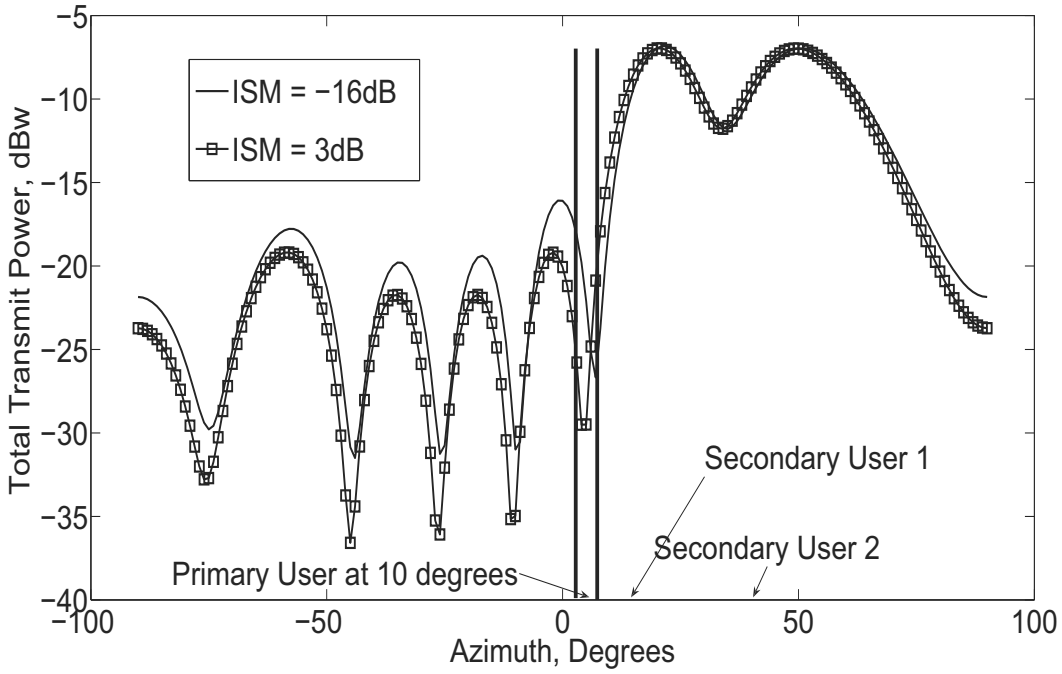

Figure 5.4: Overall secondary BS radiation pattern in azimuthal plane as a function of allowed interference shaping margin by the primary user.

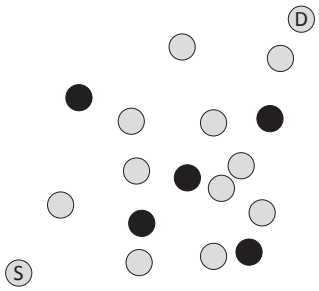

Figure 5.5: An ad hoc network consisting of randomly distributed primary and secondary nodes.

5.3 Multi-hop Cognitive Radio Routing Schemes with Hop-by-Hop Beamforming

5.3.1 The Network Architecture & System Model

Consider a multi-hop cognitive radio network where the primary and the secondary nodes are randomly distributed within a specified region. The goal is to route the data between the secondary source and destination nodes in an energy efficient manner while minimizing the co-channel interference among the secondary nodes and keeping the interference imposed on the primary users by the secondary transmissions within the allowed ISMs required by each primary user. Figure 5.5 shows an example scenario where the black circles represent the primary nodes while the gray circles represent the secondary nodes. The secondary source and the destination nodes are also labeled in the figure. In the following, the set of secondary transmitters is denoted by $X = \{x_1, x_2, ..., x_i\}$ and the set of secondary receivers is denoted by $Z = \{z_1, z_2, ..., z_k\}$.

It is assumed that each secondary node consists of a ULA with N transmit antennas with an element spacing of half a wavelength. For reception, both the primary and the secondary nodes utilize a single receive antenna. Thus, the considered scenario forms a MISO communication link. Such scenario makes sense in a multi-hop network, as the adoption of receive beamforming would make the implementation of broadcast and flooding procedures overly complicated. In the considered scenario, the secondary transmitter transmits to a single secondary receiver at a given time instance. Thus, the orthogonality constraint in (5.12) is not required and the optimization problem is modified such that it only satisfies the SNR requirement of secondary receiver. The

modified problem can be written as

$$\begin{aligned} \underset{\mathbf{F}_k}{\text{minimize}} \quad & \text{tr}[\mathbf{F}_k] \\ \text{subject to} \quad & \text{tr}[\mathbf{R}_k\mathbf{F}_k] \geq \gamma_k\sigma_k^2 \\ & \text{tr}[\mathbf{R}_{pm}\mathbf{F}_k] \leq \varphi_m,\ 1 \leq m \leq M, \\ & \mathbf{F}_k = \mathbf{F}_k^{\mathbf{H}} \succeq 0,\ 1 \leq k \leq K. \end{aligned} \tag{5.15}$$

In the above problem, γ_k represents the minimum required SNR of the secondary receiver z_k while σ_k^2 represents the receiver noise variance.

5.3.2 Multi-hop Position-Based Underlay Cognitive Radio Routing Concept

The availability at network nodes of position information on both neighboring nodes in the secondary network and primary receivers allows for the introduction of position-based optimization in the routing protocol, with the goal of guaranteeing the best possible performance to the secondary network, while meeting the constraints imposed by coexistence with primary receivers. In general, position information can be introduced in two different ways in the operation of a routing protocol: either in the routing algorithm (e.g. determining which nodes participate in the routing discovery process based on their position, as in [28]), or in the routing metric, as proposed in [96], [97]. A detailed discussion of how position information can be used in the routing algorithm for underlay cognitive radio networks is presented in [98], where a preliminary analysis of the potential advantages of introducing a beamforming technique in a multi-hop cognitive radio network is carried out. Note that in the analysis presented in [98] beamforming was not taken into account at all in the selection of the end-to-end path, but rather introduced when forwarding data packets along the selected path. In the present work the idea of introducing beamforming in a multi-hop cognitive network is taken a step farther by allowing limited modifications to the path selected at the routing layer based on the expected impact on neighboring secondary nodes and primary receivers. Details on the proposed solution are provided in the following subsection.

5.3.3 The Proposed Algorithm

In this section, transmit beamforming is utilized to design a routing algorithm for a multi-hop cognitive radio network. The objective of the algorithm is three-fold:

1. To minimize the end to end transmission power consumption.

2. To minimize the co-channel interference imposed within the secondary network.

3. To minimize the number of primary interference constraint violations.

To achieve the goals set above, a centralized approach is adopted whereby the optimal power saving route is initially calculated through Dijkstra's algorithm [99] by using the point to point link costs without beamforming, which can be written as

$$LC(x_i, z_k) = \frac{\gamma_k \sigma_k^2}{|h_{ik}|^2}, \tag{5.16}$$

where h_{ik} is the channel coefficient between the transmitter and the receiver while $LC(x_i, z_k)$ represents the link cost between the transmitter x_i and the receiver z_k.

After this initial step, the algorithm modifies the selected route by using a new cost metric which is introduced later in this section. To ensure that the modified route does not deviate too much from the optimal power saving route, the cost metric is used only on alternate hops, for example, for every odd numbered hop of the optimal route, the hop destination is selected based on the proposed cost metric, while the destinations of the even numbered hops remain unchanged.

Next, the cost metric is proposed which is used to select the node which is most suitable to act as a relay. The proposed metric takes into account the potential impact of the selection of a relay on the primary receivers and other secondary nodes, within the transmission range of the source and the candidate relay node. In the following, the source, relay and the destination nodes are referred to as S, R and D, respectively. A terminal R will only be eligible as a relay if it meets all the following conditions:

1. S does not violate the interference constraint of any of the primary users when it transmits data to R using beamforming;

2. R does not violate the interference constraint of any of the primary users when it transmits data to D using beamforming;

3. The position of R is such that the distance between R and D, indicated as $dist_{RD}$, is not larger than the distance from S to D, $dist_{SD}$. This condition ensures physical connectivity between the selected relay and D and it ensures that the algorithm remains loop free.

The above description translates into the cost $Cost(S, D, R)$ associated to the generic terminal R as a potential relay between S and D defined by eq.(5.17) where:

$$Cost\left(S,D,R\right)=\begin{cases}\sum_{i=1,i\neq R}^{N_S^{\mathcal{S}}} I\left(S,R,i\right)+\sum_{k=1,k\neq D}^{N_R^{\mathcal{S}}} I\left(R,D,k\right) & if \begin{cases}\sum_{l=1}^{N_S^{\mathcal{P}}}\lfloor\frac{I(S,R,l)}{I_{MAX}(l)}\rfloor+\\ \sum_{l=1}^{N_R^{\mathcal{P}}}\lfloor\frac{I(R,D,m)}{I_{MAX}(m)}\rfloor=0\end{cases}\\ & dist_{RD}\leq dist_{SD}\\ +\infty & otherwise\end{cases} \tag{5.17}$$

1. $N_k^{\mathcal{S}}$ is the number of secondary terminals within the transmission range of terminal k;

2. $N_k^{\mathcal{P}}$ is the number of primary receivers within the transmission range of terminal k;

3. $I(x,y,z)$ is the interference generated by x towards the generic receiver y (either primary or secondary) when transmitting to z.

The candidate relay node which gives the minimum value for the above cost function is selected as the next hop destination. Figure 5.6 shows an example scenario where the nodes labeled as S and D are, respectively, the secondary source and destination nodes, the black nodes labeled as P1,...,P3 are the primary nodes while the nodes labeled as R1,...,R6 are the secondary *candidate relay* nodes. Among the candidate relay nodes, R4 and R6 are not eligible to act as relays. R4 is rejected because S cannot transmit to R4 without violating the interference constraint of P2 while the distance between S and R6 is larger than the distance between S and D. The Dijkstra's algorithm selects R1 as the best option to act as a relay. However, it can be seen that if the data is transmitted to R1, a lot of interference is exerted upon R3. On the other hand, if R3 is selected as the relay, then interference will be exerted upon R1 when R3 forwards the data to D. Using the proposed cost metric, the best option in this case is to select R2 as the relay.

As a final comment, it is worth noting that the relay selection metric is defined so to operate at local level, without any interaction with the routing algorithm; this allows, in theory, to combine the proposed path optimization approach with any routing algorithm.

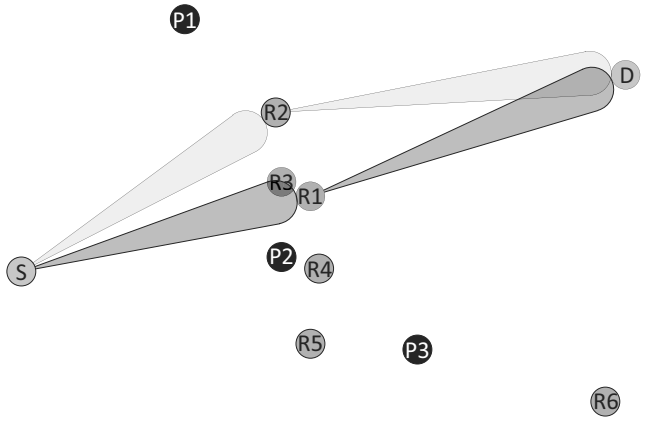

Figure 5.6: Demonstration of the proposed cost metric.

5.4 Performance Evaluation

The performance of the proposed solution was evaluated by means of computer simulations executed by combining a signal processing tool (MATLAB) and a network simulator (OMNeT++) as follows:

1. MATLAB was used to implement the transmit beamforming strategy and to analyze the performance of the route optimization approach defined in Section 5.3.3 by measuring the interference generated towards each secondary node as well as the average number of constraints set by primary receivers that are met.

2. OMNeT++ was used to test the proposed strategy in presence of actual packet transmissions, moving from results generated in MATLAB.

Details on the implementation, the scenario considered during simulations, as well as simulation results are presented in the following subsections.

5.4.1 Simulation scenario and setup

The MATLAB code was used to simulate a network of secondary nodes equipped with a ULA with $N = 8$ antenna elements and a spacing between adjacent elements $d = 0.0625\ m$, corresponding to half a wavelength for a carrier frequency $f_c = 2.4\ GHz$, and capable thus to perform DOA estimation and beamforming. An angular spread $\phi = 2^o$ was introduced around the exact angle for each measurement and taken into account in the optimization procedure. A noise power $P_n = -101dBm$ was assumed at each receiver, while the pathloss exponent for propagation was set equal to $\alpha = 2$.

MATLAB was used to solve the optimization problem of (5.15) by taking advantage of the SeDuMi solver provided by the cvx package [100], imposing an upper bound φ_m on the allowed interference towards the primary nodes and a minimum SNR level of $\gamma_k = 10\ dB$ for all the secondary nodes. The following steps were executed in MATLAB for each run:

1. Generation of a topology composed of N_S secondary nodes and N_P primary nodes randomly deployed in an area of $X_{max} = 50\ m$ by $Y_{max} = 50\ m$ square meters;

2. Generation of N_{conn} connection requests in the secondary network with random source and destination nodes, random duration uniformly distributed between $minDuration$ and $maxDuration$ and random delay from the previous connection request from same source node uniformly distributed between $minDelay$ and $maxDelay$; then, for each connection request:

   (a) Selection of the best path according to the minimum power routing strategy defined in Section 5.3.3;

   (b) Optimization of the path according to the proposed metric, defined again in Section 5.3.3;

   (c) Measurement of interference generated towards secondary nodes not involved in the connection with and without optimization;

   (d) Measurement of number of primaries for which the constraint on the maximum interference value is met with and without optimization;

3. Export to file of the data required by OMNeT++, consisting in:

   (a) primary and secondary network topology;

   (b) the list of the N_{conn} generated connection requests, including source, destination and duration;

   (c) original and optimized paths for each connection;

   (d) the reduction in the interference $I(x, y, z)$ perceived in y guaranteed by the introduction of beamforming in the link from x to z, for all x-z pairs involved in any connection, for both original and optimized paths.

The inputs generated in MATLAB were used in a simulated secondary network built in OMNeT++, with each secondary node characterized by the architecture shown in Figure 5.7. With reference to such architecture, it should be noted that:

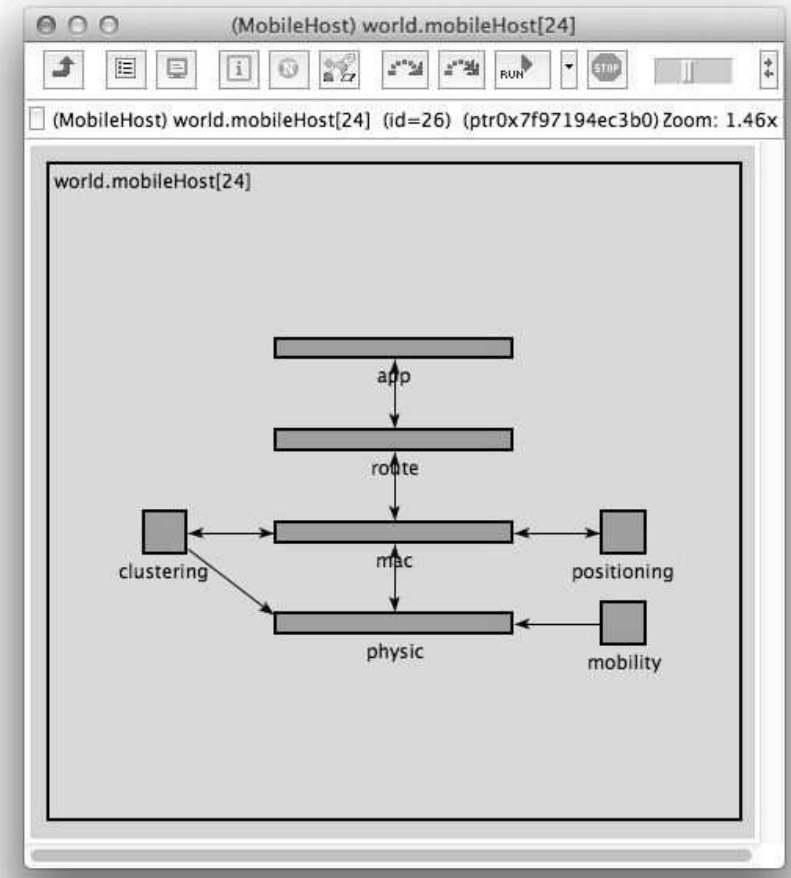

Figure 5.7: Secondary node architecture implemented in OMNeT++.

- the mobility and clustering modules were not activated, as a static network with flat organization was assumed in this work.
- the positioning module was configured so to provide perfect position information about all network nodes.
- the application module for a generic node x was in charge of reading from file connection requests having x as source, and generate for each connection packets of size $appPacketSize$ bits spaced in time by a constant delay set to $applicationRate/appPacketSize$ (modeling thus a Constant Bit Rate (CBR) packet stream) for a time equal to the connection duration read from file;
- the routing module for a source node x, upon receiving from the application module the first packet of a connection, was in charge of a) loading from file the

corresponding end-to-end path determined in MATLAB, b) record such path in each packet; the routing module of intermediate nodes took care of forwarding the packet towards the destination by reading the next hop from the packet itself, while the routing module of a destination node simply forwarded the packet to the application module.

- the MAC module implemented a simple Aloha protocol without retransmission, taking care of immediately forwarding packets received from the routing module to the physical layer module and vice versa.

- the physical layer module had the responsibility of transmitting and receiving packets taking into account path loss, propagation delays and interference generated by packet collisions.

The impact of interference, in particular, was modeled with an accuracy significantly higher than that currently found in existing OMNeT++ frameworks, such as INET [101] and MixiM [102], in order to ensure a correct analysis of the impact of the proposed optimization on network performance. The simulator is in fact able to keep track of all transmitted packets and, for each packet reception, determines the interference level on a symbol by symbol basis (note that, as binary modulation was considered in all simulations, in the following bits will be considered in place of symbols). Consecutive bits subject to the same interference are grouped into so called bit regions: Figure 5.8 shows an example of packet reception where four different regions are identified due to varying interference conditions.

Next, for each bit region the average Bit Error Probability (BEP) is evaluated by adopting the Standard Gaussian Approximation for the interference power, and the number of bit errors is randomly determined according to the BEP. Finally the total number of bit errors generated is evaluated by summing up errors introduced in each bit region, and compared with the maximum number of errors admitted for the packet as determined by the adoption of a Reed-Solomon code with a coding rate $RS_{rate} = 0.835$ (corresponding to a correction capability roughly equal to 10% of the packet bits) in order to decide if the packet is correctly received or discarded.

The following steps were executed in OMNeT++ for each run:

1. Loading of primary and secondary network topologies from file;

2. Loading of connection requests from file and for each request:

   (a) Generation of packets

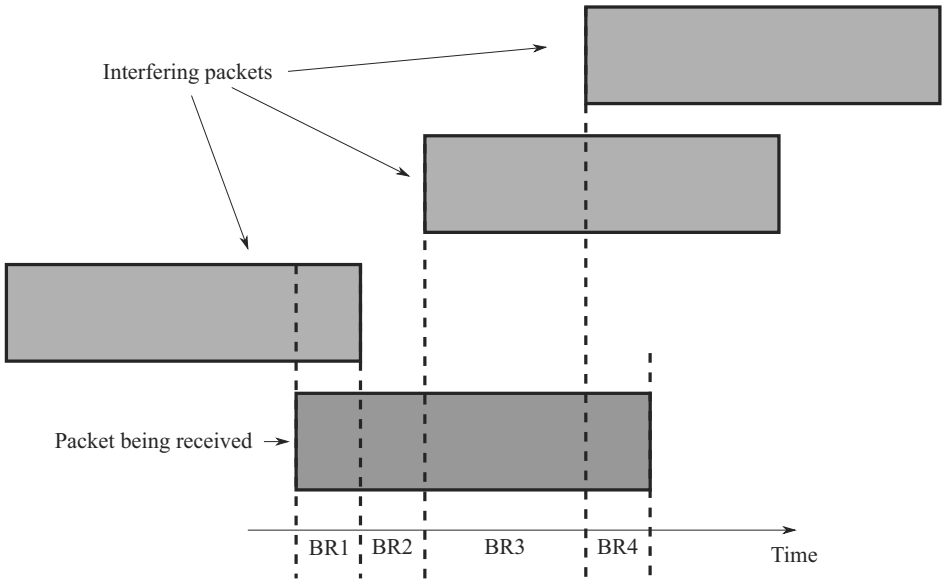

Figure 5.8: Example of bit region identification during a packet reception in OMNeT++; 4 Bit Regions (BR1 to BR4) are identified based on the variations in the set of interfering packets.

(b) Forwarding of packets along the end-to-end path read from file;

(c) Measurement of end-to-end throughput and other relevant metrics.

3. Averaging of measured metrics.

Table 5.1 presents values assumed by the simulation parameters defined above.

5.4.2 Simulation Results

Matlab results

Figure 5.9 shows the average interference imposed on the secondary nodes when the data is routed between the secondary source and destination nodes. To ensure continuity of the simulations, the constraint on primary interference is relaxed if the cost of (5.17) is $+\infty$ for all the secondary nodes within the transmission range of the transmitter for a specific hop. As can be seen from the figure, the optimized routing with beamforming, i.e., routing with the proposed cost metric, gives the best performance in terms of interference imposed within the secondary network. As expected, routing without beamforming gives the worst performance. Furthermore, it must be mentioned here that to compare the performance of routing with beamforming and optimized routing with beamforming, one must also consider the number of primary constraint

Table 5.1: Simulation settings

Parameter	Value(s)
Number of secondary nodes N_S	50
Number of secondary nodes N_P	from 10 to 50
Number of connection requests per run N_connn	1000
Minimum connection duration $minDuration$	25 s
Maximum connection duration $maxDuration$	75 s
Min delay between connection requests $minDelay$	50 s (High Traffic) / 500 s (Low Traffic)
Max delay between connection requests $maxDelay$	100 s (High Traffic) / 750 s (Low Traffic)
Transmission rate at physical layer	1 Mb/s
Maximum transmission power for secondary nodes	1 μW
Application packet length $appPacketSize$	512 bits
Application source rate $applicationRate$	320 kbit/s

violations, since the primary interference constraint is relaxed when none of the secondaries is able to satisfy this constraint. To make this comparison, Figure 5.10 shows the number of primary constraint violations for different number of primary nodes.

From Figure 5.9 and Figure 5.10, it can be seen that the difference in performance between the optimized and non-optimized routing with beamforming in Figure 5.9 is large when the corresponding difference in primary violations in Figure 5.10 is relatively small, e.g., the performance when the number of primary nodes is 30. Otherwise, when the difference in performance in Figure 5.9 is small, the difference in the number of primary constraint violations is relatively large. In order to have a fair comparison between the two, the number of primary constraint violations for routing with beamforming and optimized routing with beamforming should forced to be the same.

Figure 5.11 shows the power consumption of the routing with beamforming and optimized routing with beamforming algorithms. The first important observation from the figure is that the power consumption increases as the number of primary users increases. This result is related to the results presented in Section 5.2.3 where it was shown that the minimized transmit power increases as the primary ISM constraint gets tighter. As the number of primary nodes increases, the transmitting node is required

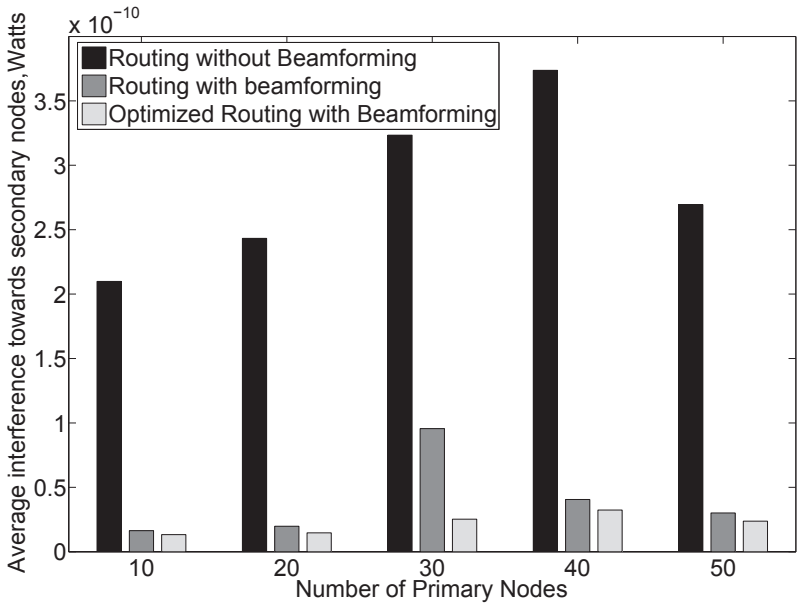

Figure 5.9: Average total interference exerted upon the secondary nodes between source and destination versus the total number of primary nodes within the network.

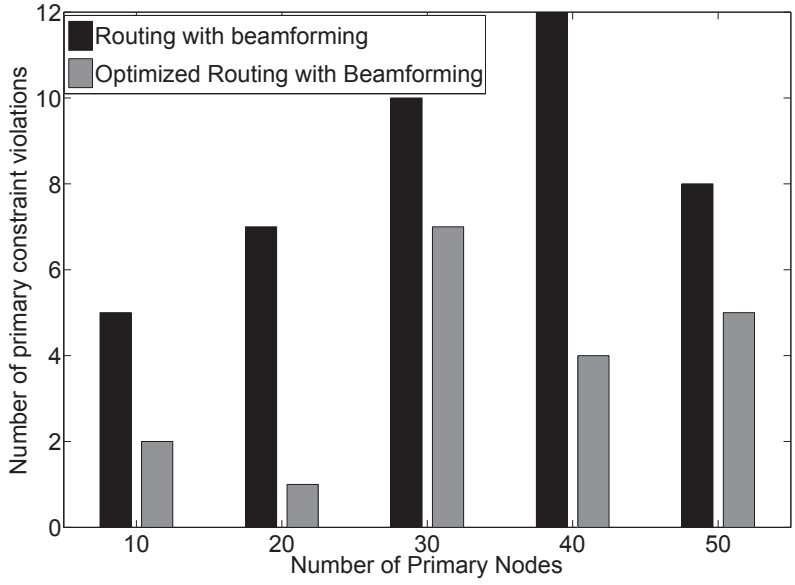

Figure 5.10: Number of primary constraint violations versus the total number of primary nodes within the network.

to satisfy the ISM constraints of a larger number of primary users, resultantly, the constraints get tighter and the minimized transmit power per hop increases. Furthermore, it can be seen that when the number of primaries is small, routing with beamforming

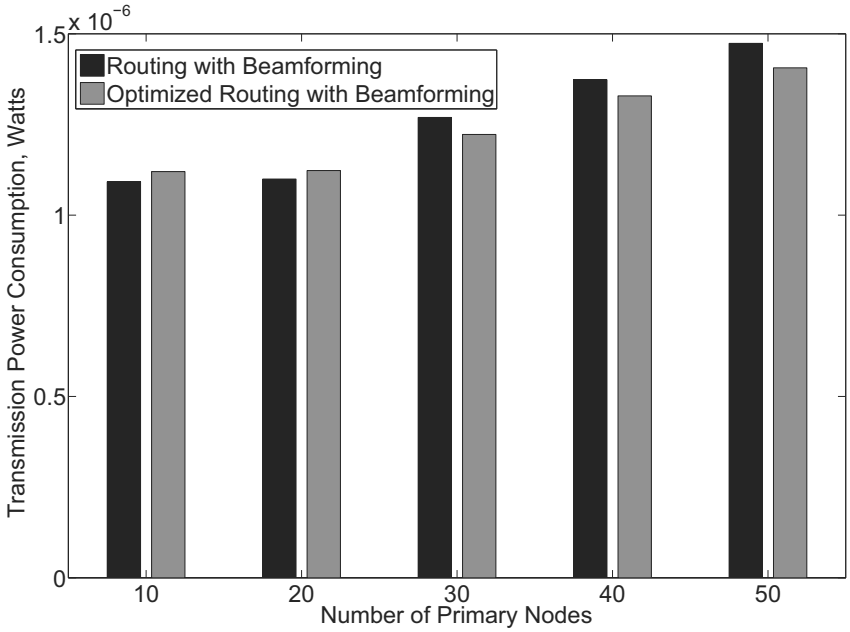

Figure 5.11: Total power consumption of the routing algorithms versus the total number of primary nodes within the network.

consumes less power than optimized routing with beamforming, while optimized routing with beamforming consumes lesser power as the number of primaries becomes large. An explanation for this behavior of the routing algorithms is as follows: As discussed above, the transmit power increases when number of primary nodes increases. Consequently, when the number of primaries is large, the cost metric of (5.17) is dependent on the transmit power of the current node and the candidate relay node and the density of the secondary nodes around them; on the other hand, when the number of primaries is small, the density of the secondary nodes around the current node and candidate relay node becomes the dominant factor in (5.17) since the transmit power remains small for all the involved nodes. Since optimized routing with beamforming selects the next hop which minimizes (5.17), it indirectly selects the nodes with less transmit power when the number of primaries is large. Consequently, the power consumption decreases when compared with the routing with beamforming algorithm, which just transmits towards a pre-selected next hop.

OMNET++ results

OMNeT++ simulations considered the following four different scenarios, obtained by varying the traffic load in the secondary network and the number of primary nodes:

- *Low traffic, free network* - Low traffic (obtained by setting the *minDelay* and

maxDelay variables to the corresponding values in Table 5.1) and no primary nodes;

- *Low traffic, constrained network* - Low traffic and $N_P = 10$ primary nodes;
- *High traffic, free network* - High traffic (obtained by setting the *minDelay* and *maxDelay* variables to the corresponding values in Table 5.1) and no primary nodes;
- *High traffic, constrained network* - High traffic and $N_P = 10$ primary nodes.

The throughput, defined as the ratio between end-to-end received packets and generated packets was measured in the four scenarios above for the three strategies previously introduced in the paper:

- Routing without beamforming, where omni-directional antennas are considered;
- Routing with Beamforming, where beamforming is adopted for each hop, but the path is not modified;
- Optimized Routing with Beamforming, where beamforming is adopted for each hop, on a path optimized as proposed in Section 5.3.3.

Figure 5.12 present the throughput in the case of the *Low traffic, free network* scenario. The Figure shows that in this scenario the optimization in the routing path leads to an increase in throughput, as on each other hop the strategy is able to select the node that provides the lowest amount of interference to neighboring nodes, thus increasing the probability of correct packet reception throughout the network.

Moving to the *Low traffic, constrained network* scenario, Figure 5.13 shows that the introduction of constraints determined by the presence of a significant number of primaries has the impact of reversing the gap between the two BF-based strategies, due to the fact that in several cases potential relays that would lead to lower interference in the secondary network are discarded as they do not satisfy the hard constraint on the level of interference towards one or more primary receivers. Figure 5.14 shows how the throughput is affected in the *High traffic, free network*; results show how for all strategies performance is significantly reduced due to the higher number of collisions, and the corresponding higher average value of the interference power during packet reception.

Finally, Figure 5.15 shows results in the *High traffic, constrained network*, that introduces again the presence of the primary nodes; interestingly, results highlight that

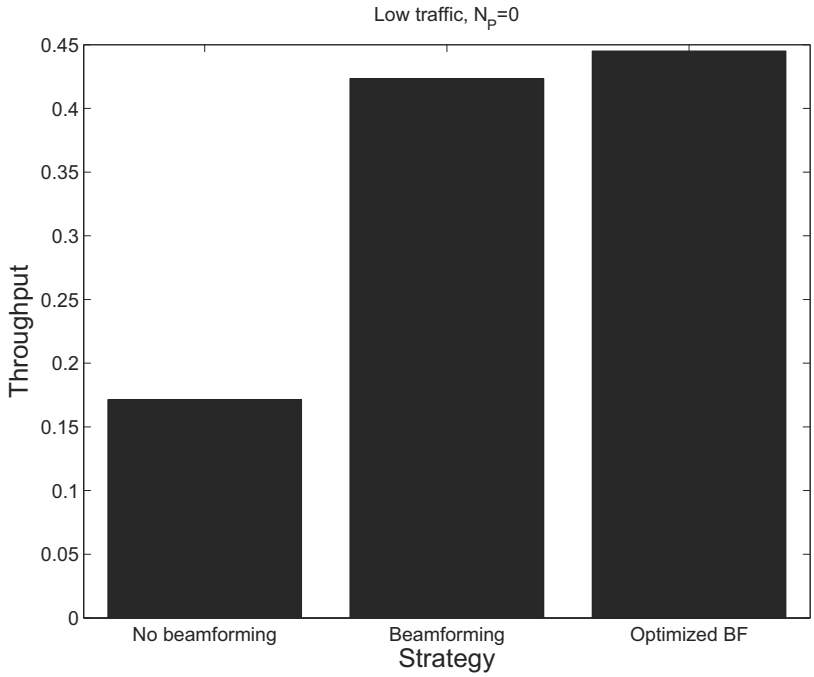

Figure 5.12: Throughput in the *Low traffic, free network* scenario for the three considered routing strategies.

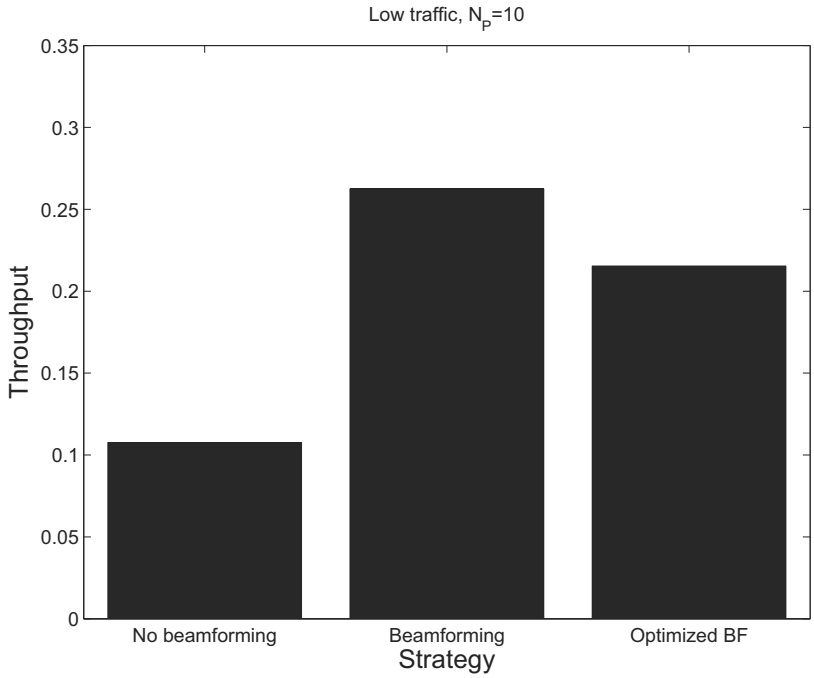

Figure 5.13: Throughput in the *Low traffic, constrained network* scenario for the three considered routing strategies.

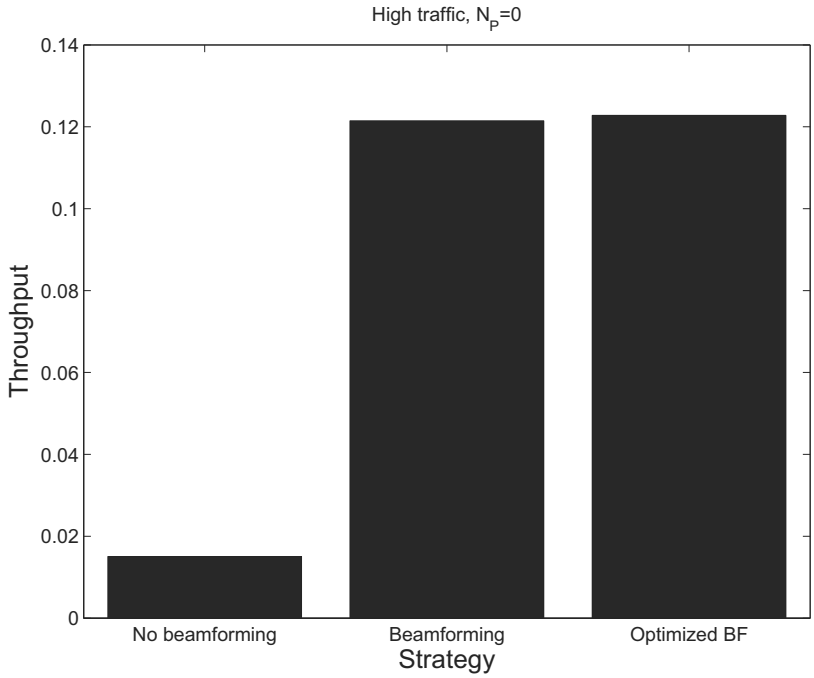

Figure 5.14: Throughput in the *High traffic, free network* scenario for the three considered routing strategies.

in this case the Optimized Routing with Beamforming leads to slightly worse results compared to simple Routing with Beamforming. It should be note however that, as shown by Figure 5.10, this comes together with a better coexistence capability with primary receivers, highlighting the presence of a trade-off between coexistence and secondary network performance. A fair comparison of the different routing strategies would require to force all of them to meet to the same extent the requirements set by the primary nodes.

5.5 Concluding Remarks

The chapter focused on transmit beamforming and routing in a multi-hop, ad hoc cognitive radio network. After introducing and investigating a transmit beamforming strategy, a new cost metric was proposed which was used to design an optimized, beamforming based routing algorithm with three-fold objective: to minimize the end to end path power consumption; to minimize the co-channel interference imposed within the secondary network and to minimize the number of primary interference constraint violations. To evaluate the performance of the proposed algorithms, two different simulation platforms were combined, i.e., MATLAB and OMNet++. While MATLAB was

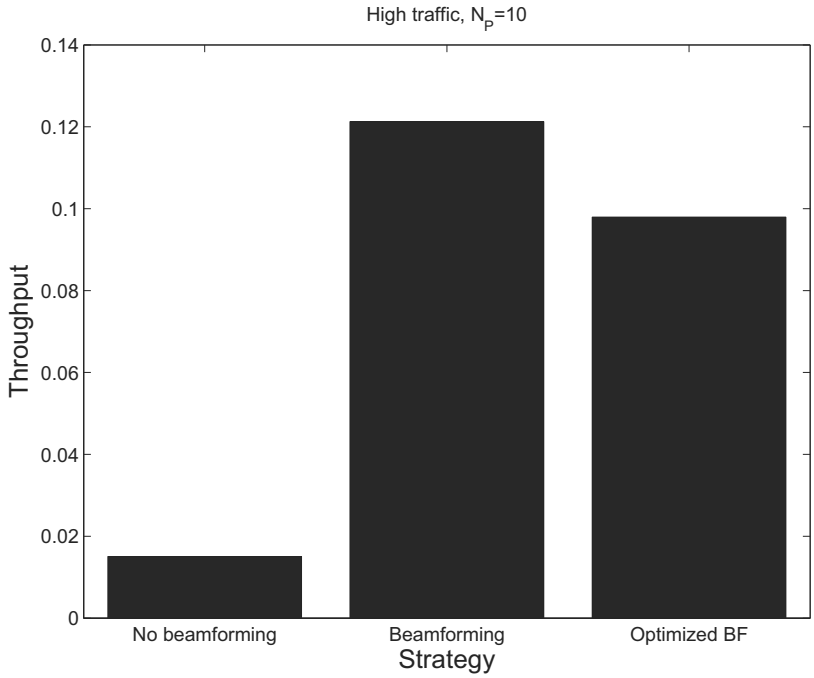

Figure 5.15: Throughput in the *High traffic, constrained network* scenario for the three considered routing strategies.

used to implement the transmit beamforming strategy and to analyze the performance of the route optimization approach, OMNeT++ was utilized to test the proposed strategy in presence of actual packet transmissions, moving from results generated in MATLAB. Simulation results from MATLAB confirmed that the optimized routing algorithm outperformed the original routing algorithm in terms of both, the interference generated within the secondary network and the number of primary interference constraint violations. Furthermore, it was shown that for networks with a large number of primary nodes, the optimized algorithm outperformed the baseline algorithm in terms of power consumption. Finally, the simulations carried out in OMNet++ confirmed the improved throughput of the secondary network when no constraints from primary nodes are imposed, while they highlight a trade-of between coexistence capability and secondary network performance when the presence of primary nodes has to be taken into account.

Chapter 6

Conclusions and Future Research

The thesis focused on energy-efficient routing in static wireless ad hoc networks. The primary objective of this research was to design progressive energy saving routing algorithms for WAHNs and WMNs. To this end, initially, various energy efficient transmission strategies were proposed and investigated. These strategies included single antenna point-to-point transmissions, distributed beamforming, physical layer network coding and centralized beamforming. Several power saving routing algorithms were proposed, each tailored for a specific transmission strategy. The algorithms were designed based on the transmission power consumption and the fixed circuit power consumption. The power consumption was minimized under the constraint that the SNR requirements of each hop destination must be satisfied. Through extensive simulations, the performances of the proposed schemes were evaluated for different network scenarios. Various figures of merit such as the end-to-end power consumption, hop count, end-to-end delay and throughput were used to demonstrate the potential energy saving gains that can be achieved by using the proposed algorithms.

The current chapter summarizes the contributions of this thesis and explores some avenues for future research.

6.1 Thesis Summary

The introductory chapter discussed the scope of the work presented in this thesis and highlighted the importance of the proposed research topic in context of green ICT. Further, the contributions of this thesis were also outlined.

6.1.1 Summary of Chapter 2

Chapter 2 provided a detailed background study on energy-efficient routing in wireless ad hoc networks. Based on the transmission strategy used at the physical layer, the study divided the power-aware routing algorithms into two main categories, i.e., non-cooperative and cooperative routing algorithms. Non-cooperative routing algorithms were further divided into unicast, multicast/broadcast and network structure and connectivity based algorithms. Cooperative routing algorithms were classified into progressive energy saving and maximizing the network lifetime routing algorithms. Each of the above categories and sub-categories were discussed in detail.

6.1.2 Summary of Chapter 3

Non-cooperative energy-efficient routing was the focal point of Chapter 3. Initially, the chapter highlighted the impact of fading on existing power saving routing algorithms. Through analysis, it was shown that the fading coefficients, due to their randomness, cannot be incorporated directly into the baseline routing algorithm, i.e., PSR [21]. Following this analysis, two power and fading-aware decision metrics were presented which helped the source and the intermediate forwarding nodes in selecting the optimal next hop destination. Based on the two decision metrics, a new distributed power-aware non-cooperative routing algorithm, APAR, was proposed. APAR selects the optimal next hop destination by using the location information and the localized channel conditions of its neighboring nodes. Monte-Carlo simulations revealed that, depending on the network conditions, the proposed algorithm can achieve a power saving of up to 70% as compared to PSR.

6.1.3 Summary of Chapter 4

Chapter 4 presented a power-aware cooperative routing algorithm based on distributed beamforming. Initially, the impact of circuit power consumption on cooperative transmission was investigated. The chapter derived an upper bound on the power saving gains that can be achieved by using cooperative transmission, as compared to non-cooperative point to point transmission. It was shown that the cooperative transmission outperforms the non-cooperative transmission, in terms of power consumption, only when the smallest distance between the cooperating nodes and the destination is larger than a minimum threshold. This threshold distance was derived analytically and the analysis was verified through simulations conducted in MATLAB. Using the

derived threshold distance, a new distributed power-aware cooperative routing algorithm, PACR, was proposed. PACR was shown to outperform the baseline cooperative [57] and the baseline non-cooperative [21] routing algorithms in terms of power consumption. Further, this improved power saving was achieved while consuming lesser number of hops as compared to the baseline routing algorithms.

6.1.4 Summary of Chapter 5

Chapter 6 focused on transmit beamforming and routing in a multi-hop, ad hoc cognitive radio network. Initially, the chapter introduced and discussed the orthogonal transmit beamforming strategy in context of cognitive radio networks. The performance of OTBF was investigated for single-hop scenarios. Following this, a new, beamforming based, optimized routing algorithm was proposed with three-fold objective: to minimize the end to end path power consumption; to minimize the co-channel interference imposed within the secondary network and to minimize the number of primary interference constraint violations. While MATLAB was used to implement the transmit beamforming strategy and to analyze the performance of the route optimization approach, OMNeT++ was utilized to test the proposed strategy in presence of actual packet transmissions. Extensive simulations were used to demonstrate the performance improvements achieved by using the proposed routing algorithm.

6.2 Avenues of Future Research

Continuing from the work presented in this thesis, the current section suggests directions for future research.

6.2.1 Robust Distributed Beamforming

The distributed beamforming strategy used in Chapter 4 works on the assumption that the cooperative transmitters have very accurate channel state information about each others' channel towards the receiver. In reality, however, the obtained CSI is not always accurate, e.g., due to location estimation errors. In such a case, distributed beamforming fails since the signals that arrive at the receiver are not synchronized or because the beamforming weights are not properly distributed among the cooperating nodes. Therefore, distributed beamforming should be made robust to such errors. Particularly, making DB robust to location estimation errors is a challenging

task since synchronizing the transmissions for coherent reception at multiple receivers, from multiple transmitters, is not feasible [57]. Although the authors in [65] propose a beamforming strategy in which multiple transmitters beamform towards multiple destinations simultaneously, the work is valid only for scenarios where the destinations have distinct locations. To make DB robust to location estimation errors, the beamforming weights need to designed under the assumption that the destination could be located anywhere within a certain small area, depending the extent of the error in location estimation. Thus, the design of robust distributed beamforming remains an open and challenging issue.

6.2.2 Turning off node radios

Nearly all the routing algorithms proposed in this thesis minimize the total hop count of the energy-efficient routing path between the source and the destination. While this research focused on minimizing the active energy consumption, the proposed algorithms inherently create an opportunity to turn-off extra nodes that are not participating in the routing process. Thus, there is room to explore the potential energy saving gains that can be achieved through this turning-off of node radios.

Appendix A

Impact of Fading on Power Saving Routing Algorithm: derivation of equation 3.13

The power-saving routing algorithm calculates an optimal desirable position for the next hop destination, then forwards the packet to the node which is closest to this position. From Fig. 3.2, let $e = |SI|$, $f = |ID|$ and $d = |SD|$. To minimize the power consumption from source to destination via intermediate node I, one needs to minimize the function [21]

$$u(e, f) = \beta e^{\alpha} + C + f(C(\beta(\alpha - 1)/c)^{1/\alpha} + \beta(\beta(\alpha - 1)/C)^{(1-\alpha)/\alpha}) \tag{1}$$

over the constraint function $e + f \geq d$. If fading is incorporated in the above equation, then $u(e, f)$ can be written as

$$u(e, f) = \frac{\beta}{|F_{SI}|^2} e^{\alpha} + C + f(C(\frac{\beta}{|F_{ID}|^2}(\alpha - 1)/c)^{1/\alpha} + \frac{\beta}{|F_{ID}|^2}(\frac{\beta}{|F_{ID}|^2}(\alpha - 1)/C)^{(1-\alpha)/\alpha}) \tag{2}$$

The problem can be stated as

$$\begin{aligned} &\text{minimize} && u(e, f) \\ &\text{subject to} && v(e, f) \leq d \end{aligned} \tag{3}$$

where $v(e, f) = e + f$. The method of Lagrange multipliers can be used to solve this optimization problem. Taking the partial derivatives of $u(e, f)$ and $v(e, f)$, w.r.t e and f, one gets

$$\nabla u = (\frac{\alpha\beta e^{\alpha-1}}{|F_{SI}|^2}, C(\frac{\beta}{|F_{ID}|^2}(\alpha-1)/C)^{1/\alpha} + \frac{\beta}{|F_{ID}|^2}(\frac{\beta}{|F_{ID}|^2}(\alpha-1)/C)^{(1-\alpha)/\alpha})$$
$$\nabla v = (1, 1)$$

The minimum occurs when

$$\frac{\alpha\beta e^{\alpha-1}}{|F_{SI}|^2} - \lambda_L = 0$$
$$C(\frac{\beta}{|F_{ID}|^2}(\alpha-1)/C)^{1/\alpha} + \frac{\beta}{|F_{ID}|^2}(\frac{\beta}{|F_{ID}|^2}(\alpha-1)/C)^{(1-\alpha)/\alpha} - \lambda_L = 0$$

where λ_L is the Lagrange multiplier. Solving the above two equations, we get the optimal value for the distance between the source base station and desirable position of the next hop destination, which is given as

$$d_{opt} = e = \sqrt[\alpha]{\frac{C|F_{ID}|^2}{\beta(\alpha-1)}} \sqrt[\alpha-1]{\frac{|F_{SI}|^2((\alpha-1)/|F_{ID}|^2+1)}{\alpha}} \tag{4}$$

Appendix B

Adaptive Power-Aware Routing Algorithm: derivation of equation 3.14

Let us assume that S, D and I in Fig. 3.2 are collinear, i.e., if the distance between S and D is d, then $|SI| = x$ and $|ID| = d - x$. Furthermore, it is assumed that if S transmits directly to D, then the transmitted signal experiences multipath fading given by $|F_{SD}|$, otherwise, it experiences fading given by $|F_{SI}|$ for the first hop, and $|F_{ID}|$ for the second hop. The power consumed through multi-hop transmission is given by

$$(\frac{\beta}{|F_{SI}|^2}x^\alpha + C) + (\frac{\beta}{|F_{ID}|^2}(d-x)^\alpha + C) = 2C + \frac{\beta}{|F_{SI}|^2}x^\alpha + \frac{\beta}{|F_{ID}|^2}(d-x)^\alpha.$$

The power consumed by intermediate node forwarding is less than the power consumed by direct transmission from S to D, i.e.

$$2C + \frac{\beta}{|F_{SI}|^2}x^\alpha + \frac{\beta}{|F_{ID}|^2}(d-x)^\alpha < \frac{\beta}{|F_{SD}|^2}d^\alpha + C$$

if

$$g(x) = \beta(\frac{x^\alpha}{|F_{SI}|^2} + \frac{(d-x)^\alpha}{|F_{ID}|^2} - \frac{d^\alpha}{|F_{SD}|^2}) + C < 0. \quad (5)$$

The minimum for $g(x)$ is obtained by putting $g'(x)$ equal to 0, i.e.

$$g'(x) = \beta(\frac{\alpha x^{\alpha-1}}{|F_{SI}|^2} - \frac{\alpha(d-x)^{\alpha-1}}{|F_{ID}|^2}) = 0,$$

which gives us

$$x^{\alpha-1} = \frac{|F_{SI}|^2}{|F_{ID}|^2}(d-x)^{\alpha-1}$$

or

$$x = \frac{\sqrt[\alpha-1]{\frac{|F_{SI}|^2}{|F_{ID}|^2}}}{1+\sqrt[\alpha-1]{\frac{|F_{SI}|^2}{|F_{ID}|^2}}}d. \tag{6}$$

Using (6) in (5) and solving for d, we get the final form, which is given as

$$d > \sqrt[\alpha]{\frac{C}{\beta\left(\frac{1}{|F_{SD}|^2} - \frac{\left(\frac{1}{1+\sqrt[\alpha-1]{\frac{|F_{SI}|^2}{|F_{ID}|^2}}}\right)^{\alpha}}{|F_{ID}|^2} - \frac{\left(\frac{\sqrt[\alpha-1]{\frac{|F_{SI}|^2}{|F_{ID}|^2}}}{1+\sqrt[\alpha-1]{\frac{|F_{SI}|^2}{|F_{ID}|^2}}}\right)^{\alpha}}{|F_{SI}|^2}\right)}} \tag{7}$$

If the denominator term in (7) is less than or equal to zero, then we have a special case where multipath fading has a positive impact at the receiver SNR and it compensates for the path loss. In such cases, it is always better to transmit directly, instead of intermediate node forwarding. Furthermore, if $F_{SD} = F_{SI} = F_{ID} = 1$, then (7) reduces to the condition in (3.9), which shows that the impact of fading can only be ignored if $F_{SD} = F_{SI} = F_{ID} = 1$.

Appendix C

Link Cost and System Power Consumption Model for Cooperative Transmission: derivation of equations 4.8 and 4.14

The optimal power allocation problem can be stated as

$$\begin{aligned} \underset{\omega_j}{\text{minimize}} \quad & \sum_{j=1}^{l} |\omega_j|^2 \\ \text{subject to} \quad & \frac{|\sum_{j=1}^{l} \omega_j h_{jr}|^2}{P_\eta} \geq \gamma_r. \end{aligned} \tag{8}$$

Taking the square root of the constraint function, (8) can be written as

$$\begin{aligned} \underset{\omega_j}{\text{minimize}} \quad & \sum_{j=1}^{l} |\omega_j|^2 \\ \text{subject to} \quad & \sum_{j=1}^{l} \omega_j h_{jr} = \sqrt{\gamma_r P_\eta}. \end{aligned} \tag{9}$$

The reason for the equality constraint in (9) is that SNR is an increasing function of the transmission power. Thus, when the equality is satisfied, the minimum transmission power is achieved. Let us denote the objective and the constraint function by $f(\omega)$

and $g(\omega)$, respectively. The minimum is found by solving the function

$$\nabla f = \lambda_L \nabla g, \tag{10}$$

where λ_L represents the lagrange multiplier. The lagrangian function can be written as

$$\begin{aligned} L &= f - \lambda_L g \\ &= \omega_1^2 + ... + \omega_l^2 - \lambda_L(\omega_1 h_{1r} + ... + \omega_l h_{lr}). \end{aligned} \tag{11}$$

Taking the partial derivative of the above equation w.r.t w_j, $j = 1, ..., l$, and equating it to 0, one gets

$$\omega_j = \frac{\lambda_L h_{jr}}{2},\ j = 1, ..., l. \tag{12}$$

By replacing the values for ω_j, $j = 1, ..., l$, from (12) into the constraint equation in (9), λ_L can be found as

$$\lambda_L = \frac{2\sqrt{\gamma_r P_\eta}}{h_{1r}^2 + ... + h_{lr}^2}. \tag{13}$$

Using (13) in (12), ω_j can be written as

$$|\hat{\omega}_j| = \frac{h_{jr}}{\sum_{k=1}^{l} h_{kr}^2}\sqrt{\gamma_r P_\eta},\ j = 1, ..., l. \tag{14}$$

From (4.9), for l cooperating base stations, the optimal power allocation for the j^{th} transmitting base station is given by

$$|\widehat{\omega_j}|^2 = \frac{h_{jr}^2}{(\sum_{k=1}^{l} h_{kr}^2)^2}\gamma_r P_\eta.$$

For l cooperating base stations, total transmission power required for cooperative transmission is given by

$$\begin{aligned} P_t &= |\widehat{\omega_1}|^2 + |\widehat{\omega_2}|^2 + ... + |\widehat{\omega_l}|^2, \\ &= \frac{h_{1r}^2 + h_{2r}^2 + ... + h_{lr}^2}{(h_{1r}^2 + h_{2r}^2 + ... + h_{lr}^2)^2}\gamma_r P_\eta, \\ &= \frac{\gamma_r P_\eta}{h_{1r}^2 + h_{2r}^2 + ... + h_{lr}^2}. \end{aligned} \tag{15}$$

Using (4.1) and (4.2) in (15), we get

$$\begin{aligned} P_t &= \frac{\gamma_r P_\eta}{\frac{\lambda^2}{(4\pi)^2 d_{1r}^\alpha} + \frac{\lambda^2}{(4\pi)^2 d_{2r}^\alpha} + ... + \frac{\lambda^2}{(4\pi)^2 d_{lr}^\alpha}}, \\ &= \frac{(\gamma_r P_\eta (4\pi/\lambda)^2)}{\frac{1}{d_{1r}^\alpha} + \frac{1}{d_{2r}^\alpha} + ... + \frac{1}{d_{lr}^\alpha}}, \qquad (16) \\ &= \frac{B}{\sum_{k=1}^{l} \frac{1}{d_{kr}^\alpha}}. \qquad (17) \end{aligned}$$

where B is given by (4.12). Now, for cooperative transmission, we have one receiver base station and l transmitter base stations, giving us a total circuit power consumption of $(l+1)$ times E, i.e., $C = (l+1)E$. Using this value of C and (17) in (4.10), we get

$$P_{mtp} = \frac{B}{\mu_{PA}(\sum_{k=1}^{l} \frac{1}{d_{kr}^\alpha})} + (l+1)E,$$

which gives the total power consumption for cooperative transmission over a single hop.

Appendix D

Radiation Power Pattern $P(\theta)$

The average radiated power P at the secondary BS in direction θ relative to the secondary BS antenna array broadside can be written as

$$\begin{aligned} P(\theta) &= \underset{s}{E}[\mathbf{h}(\theta)(\sum_{i=1}^{K}\mathbf{w}_i s_i)(\sum_{j=1}^{K}s_j^*\mathbf{w}_j)^H\mathbf{h}^{\mathrm{H}}(\theta)] \\ &= \mathbf{h}(\theta)\underset{s}{E}[(\sum_{i=1}^{K}\mathbf{w}_i s_i)(\sum_{j=1}^{K}s_j^*\mathbf{w}_j)^H]\mathbf{h}^{\mathrm{H}}(\theta) \end{aligned} \tag{18}$$

where $\mathbf{h}(\theta) = [1\ e^{j\pi sin(\theta)} \dots e^{j(N-1)\pi sin(\theta)}]$, and the expectation is taken over the transmitted symbol distribution. Since the K transmitted streams are independent from one another and the average energy of transmitted symbols is normalized to unity, i.e., $\underset{s}{E}[s_i s_i^*] = 1$, $\forall\ i$, therefore,

$$\begin{aligned} P(\theta) &= \mathbf{h}(\theta)(\sum_{i=1}^{K}\mathbf{w}_i\mathbf{w}_i^{\mathrm{H}})\mathbf{h}^{\mathrm{H}}(\theta) \\ &= \mathrm{tr}[(\sum_{i=1}^{K}\mathbf{w}_i\mathbf{w}_i^{\mathrm{H}})\mathbf{h}^{\mathrm{H}}(\theta)\mathbf{h}(\theta)] \end{aligned} \tag{19}$$

Using the rotational property of trace operator, (19) can be written as

$$P(\theta) = \mathrm{tr}[\mathbf{h}^{\mathrm{H}}(\theta)\mathbf{h}(\theta)(\sum_{i=1}^{K}\mathbf{w}_i\mathbf{w}_i^{\mathrm{H}})] \tag{20}$$

References

[1] L. Junhai, Y. Danxia, X. Liu, and F. Mingyu, "A survey of multicast routing protocols for mobile Ad-Hoc networks," *IEEE Communications Surveys & Tutorials*, vol. 11, no. 1, pp. 78–91, 2009.

[2] G. V. Kumar, Y. V. Reddyr, and M. Nagendra, "Current Research Work on Routing Protocols for MANET: A Literature Survey," *International Journal on Computer Science and Engineering (IJCSE)*, vol. 02, no. 03, pp. 706–713, 2010.

[3] C. Sreedhar, S. M. Verma, and N. Kasiviswanath, "A survey on security issues in wireless ad hoc network routing protocols," *International Journal on Computer Science and Engineering (IJCSE)*, vol. 02, no. 02, pp. 224–232, 2010.

[4] M. Mauve, J. Widmer, and H. Hartenstein, "A survey on position-based routing in mobile ad hoc networks," *Network, IEEE*, vol. 15, no. 6, pp. 30–39, 2001.

[5] J. Li, D. Cordes, and J. Zhang, "Power-aware routing protocols in ad hoc wireless networks," *Wireless Communications, IEEE*, vol. 12, no. 6, pp. 69–81, 2005.

[6] G. Fettweis and E. Zimmermann, "ICT Energy Consumption -Trends and Challenges," in *Proc. 11th International Symposium on Wireless Personal Multimedia Communications (WPMC2008)*, Lapland, Finland, 2008.

[7] W. Vereecken, "Overall ICT footprint and green communication technologies," in *Proc. of 4th International Symposium On Commun., Control and SP (ISCCP)*, 2010.

[8] L. Correia, D. Zeller, and O. Blume, "Challenges and enabling technologies for energy aware mobile radio networks," *IEEE Communications Magazine*, vol. 48, no. 11, pp. 66–72, 2010.

[9] C. Han, T. Harrold, S. Armour, I. Krikidis, S. Videv, P. Grant, H. Haas, J. Thompson, I. Ku, C.-X. Wang, T. Le, M. Nakhai, J. Zhang, and L. Hanzo,

"Green radio: radio techniques to enable energy-efficient wireless networks," *IEEE Communications Magazine*, vol. 49, no. 6, pp. 46–54, Jun. 2011.

[10] "Green IT." [Online]. Available: http://www.greenit-pc.jp/e/about/

[11] P. Ross and J. Ricciardone, "GreenTouch Overview," *Green Touch*. [Online]. Available: www.greentouch.org/uploads/documents/GreenTouchOverview.pdf

[12] S. S. N. Rao, Y. K. S. Krishna, and K. N. Rao, "A Survey : Routing Protocols for Wireless Mesh Networks," *Interl. Journal of Resrch. and Reviews in Wirels. Sensor Networks (IJRRWSN)*, vol. 1, no. 3, pp. 43–47, 2011.

[13] F. H. Koch, "Hydropower-Internalised Costs and Externalised Benefits," in *International Energy Agency (IEA)-Implementing Agreement for Hydropower Technologies and Programmes*, Ottawa, Canada, 2000.

[14] S. Singh, M. Woo, and C. Raghavendra, "Power-aware routing in mobile ad hoc networks," in *Proceedings of the 4th annual ACM/IEEE international conference on Mobile computing and networking*, 1998, pp. 181–190.

[15] C. E. Jones, K. M. Sivalingam, P. Agrawal, and J. C. Chen., "A Survey of Energy Efficient Network Protocols for Wireless Networks," *Wireless Networks*, vol. 7, no. 4, pp. 343–358, 2001.

[16] A. Goldsmith and S. B. Wicker, "Design Challenges for Energy-Constrained Ad Hoc Wireless Networks," *Wireless Communications, IEEE*, vol. 9, no. 4, pp. 8–27, 2002.

[17] Al-Karaki and A. Kamal, "Routing Techniques in Wireless Sensor networks: A Survey," *Security and Networks*, vol. 11, no. 6, pp. 6–28, 2004.

[18] S. Guo and O. W. Yang, "Energy-aware multicasting in wireless ad hoc networks: A survey and discussion," *Computer Communications*, vol. 30, no. 9, pp. 2129–2148, Jun. 2007.

[19] S. Ehsan and B. Hamdaoui, "A Survey on Energy-Efficient Routing Techniques with QoS Assurances for Wireless Multimedia Sensor Networks," *Communications Surveys & Tutorials, IEEE*, vol. 14, no. 2, pp. 265–278, 2012.

[20] N. A. Pantazis, S. A. Nikolidakis, and D. D. Vergados, "Energy-Efcient Routing Protocols in Wireless Sensor Networks: A Survey," *Communications Surveys & Tutorials, IEEE*, vol. PP, no. 99, pp. 1–41, 2012.

[21] I. Stojmenovic and X. Lin, "Power-aware localized routing in wireless networks," *IEEE transactions on parallel and distributed systems*, vol. 12, no. 11, pp. 1122–1133, 2001.

[22] B. Peng and A. Kemp, "Energy-efcient geographic routing in the presence of localization errors.pdf," *Computer Networks, Elsevier*, vol. 55, no. 3, pp. 856–872, 2011.

[23] V. Rodoplu and T. Meng, "Minimum energy mobile wireless networks," *Selected Areas in Communications, IEEE Journal on*, vol. 17, no. 8, pp. 1333–1344, 1999.

[24] M. Mauve, A. Widmer, and H. Hartenstein, "A survey on position-based routing in mobile ad hoc networks," *Network, IEEE*, no. December, pp. 30–39, 2001.

[25] J. Kuruvila, A. Nayak, and I. Stojmenovic, "Progress and Location Based Localized Power Aware Routing for Ad Hoc and Sensor Wireless Networks," *International Journal of Distributed Sensor Networks*, vol. 2, no. 2, pp. 147–159, 2006.

[26] Y. Xue and B. Li, "A location-aided power-aware routing protocol in mobile ad hoc networks," in *Global Telecommunications Conference, 2001. GLOBECOM'01. IEEE*, vol. 5, 2001, pp. 2837–2841.

[27] J. Gomez, A. Campbell, M. Naghshineh, and C. Bisdikian, "Conserving transmission power in wireless ad hoc networks," in *Network Protocols Ninth International Conference on ICNP 2001*, 2001, pp. 24–34.

[28] Y. B. Ko and N. H. Vaidya, "Location aided (LAR) routing in mobile ad hoc networks," in *ACM International Conference on Mobile Computing and Networking (Mobicom)*, 1998, pp. 66–75.

[29] M. W. Subbarao, "Dynamic Power-conscious Routing for MANETs: an Initial Approach," in *IEEE 50th Vehicular Technology Conference, (VTC 1999-Fall),*, 1999, pp. 1–6.

[30] M. Zimmerling, W. Dargie, and J. M. Reason, "Energy-Efficient Routing in Linear Wireless Sensor Networks," in *Mobile Adhoc and Sensor Systems, 2007. MASS 2007. IEEE Internatonal Conference on*, 2007, pp. 1–3.

[31] L. Lin, N. Shroff, and R. Srikant, "Asymptotically optimal energy-aware routing for multihop wireless networks with renewable energy sources," *Networking, IEEE/ACM Transactions on*, vol. 15, no. 5, pp. 1021–1034, 2007.

[32] F. Yu, Y. Li, F. Fang, and Q. Chen, "A New TORA-based Energy Aware Routing Protocol in Mobile Ad Hoc Networks," in *Internet, 2007. ICI 2007. 3rd IEEE/IFIP International Conference in Central Asia on*, 2007, pp. 1–4.

[33] J.-h. Chang and L. Tassiulas, "Energy Conserving Routing in Wireless Ad-hoc Networks," in *INFOCOM 2000. Nineteenth Annual Joint Conference of the IEEE Computer and Communications Societies. Proceedings. IEEE*, Tel-Aviv, Israel, 2000, pp. 22–31.

[34] J. Chang and L. Tassiulas, "Maximum lifetime routing in wireless sensor networks," *IEEE/ACM Transactions on Networking (TON)*, vol. 12, no. 4, pp. 609–619, 2004.

[35] C. Toh, "Maximum battery life routing to support ubiquitous mobile computing in wireless ad hoc networks," *Communications Magazine, IEEE*, vol. 39, no. 6, pp. 138–147, 2001.

[36] Y. Yu, R. Govindan, and D. Estrin, "Geographical and Energy Aware Routing : a recursive data dissemination protocol for wireless sensor networks," *UCLA Computer Science Department Technical Report*, pp. 1 – 11, 2001.

[37] V. Marbukh and M. Subbarao, "Framework for maximum survivability routing for a MANET," in *MILCOM 2000 Proceedings. 21st Century Military Communications. Architectures and Technologies for Information Superiority (Cat. No.00CH37155)*, vol. 1, no. 1. Ieee, 2000, pp. 282–286.

[38] D. Kim, J. J. G. Luna Aceves, K. Obraczka, J. C. Cano, and P. Manzoni, "Power-aware routing based on the energy drain rate for mobile ad hoc networks," in *Proc. 11th Intl. Conf. Comp. Commun. and Net.,*, 2002, pp. 565–569.

[39] A. Michail and A. Ephremides, "Energy Efficient Routing for Connection-Oriented Traffic in Ad-Hoc Wireless Networks," in *Proc. 11th IEEE Intl. Symp. Personal, Indoor and Mobile Radio Commun.*, 2000, pp. 762–766.

[40] Q. Li, J. Aslam, and D. Rus, "Online power-aware routing in wireless ad-hoc networks," in *Proceedings of the 7th annual international conference on Mobile computing and networking*, 2001, pp. 97–107.

[41] C. E. Chiasserini and R. R. Rao, "Routing Protocols to Maximize Battery Efficiency," in *MILCOM 2000. 21st Century Military Communications Conference Proceedings*, vol. 00, no. C, 2000, pp. 496–500.

[42] P. Wan, G. Calinescu, and C. Yi, "Minimum-power multicast routing in static ad hoc wireless networks," *IEEE/ACM Transactions on Networking*, vol. 12, no. 3, pp. 507–514, 2004.

[43] H. Takahashi and A. Matsuyama, "An approximate solution for the Steiner problem in graphs," *Mathematica Japonica*, vol. 24, pp. 73–577, 1986.

[44] J. Wieselthier and G. Nguyen, "Energy-efficient broadcast and multicast trees in wireless networks," *Mobile Networks and Applications*, pp. 481–492, 2002.

[45] I. Kang and R. Poovendran, "On the lifetime extension of energy-efficient multihop broadcast networks," *Proceedings of the 2002 International Joint Conference on Neural Networks. IJCNN'02 (Cat. No.02CH37290)*, pp. 365–370, 2002.

[46] S. Guo and O. Yang, "A dynamic multicast tree reconstruction algorithm for minimum-energy multicasting in wireless ad hoc networks," in *Performance, Computing, and Communications, 2004 IEEE International Conference on*, 2004, pp. 637–642.

[47] V. Leung, V. Leung, and O. Yang, "A Distributed Minimum Energy Multicast Algorithm in MANETs," in *2006 International Symposium on a World of Wireless, Mobile and Multimedia Networks(WoWMoM'06)*. Ieee, 2006, pp. 134–142.

[48] H. Jiang, S. Cheng, Y. He, and B. Sun, "Multicasting along Energy-Efficient Meshes in Mobile Ad Hoc Networks," in *Wireless Communications and Networking Conference, 2002. WCNC2002. 2002 IEEE*, vol. 00, no. c, 2002, pp. 807–811.

[49] Y. T. Hou, Y. Shi, H. U. Sheral, and J. E. Wieselthie, "Online lifetime-centric multicast routing for ad hoc networks with directional antennas," in *INFOCOM 2005. 24th Annual Joint Conference of the IEEE Computer and Communications Societies. Proceedings IEEE*, vol. 00, no. C, 2005, pp. 761 – 772.

[50] B. S. Olagbegi and N. Meghanathan, "A Review of the Energy Efficient and Secure Multicast Routing Protocols for Mobile Ad hoc Networks," *International journal on applications of graph theory in wireless ad hoc networks and sensor networks (GRAPH-HOC)*, vol. 2, no. 2, pp. 1–15, 2010.

[51] W. Heinzelman, A. Chandrakasan, and H. Balakrishnan, "An application-specific protocol architecture for wireless microsensor networks," *Wireless Communications, IEEE Transactions on*, vol. 1, no. 4, pp. 660–670, 2002.

[52] Y. Xu, J. Heidemann, and D. Estrin, "Adaptive Energy-Conserving Routing for Multihop Ad Hoc Networks," USC/Information Sciences Institute, Tech. Rep., 2000.

[53] A. Manjeshwar and D. Agrawal, "APTEEN: A Hybrid Protocol for Effi- cient Routing and Comprehensive Information Retrieval in Wireless Sensor Networks," in *Proc. International Parallel and Distributed Processing Symposium*, Florida, 2002, pp. 195–202.

[54] J. J. Lotf, M. N. Bolab, and S. Khorsandi, "A Novel Cluster-based Routing Protocol with Extending Lifetime for Wireless Sensor Networks," in *Wireless and Optical Communications Networks, 2008. WOCN '08. 5th IFIP International Conference on*, 2008, pp. 1–5.

[55] D. Kandris, P. Tsioumas, A. Tzes, G. Nikolakopoulos, and D. D. Vergados, "Power Conservation through Energy Efficient Routing in Wireless Sensor Networks." *Sensors (Basel, Switzerland)*, vol. 9, no. 9, pp. 7320–42, Jan. 2009.

[56] A. E. Khandani, J. Abounadi, E. Modiano, and L. Zheng, "Cooperative Routing in Wireless Networks," *Proc. Allerton Conf. 2003*, 2003.

[57] A. Khandani, J. Abounadi, E. Modiano, and L. Zheng, "Cooperative routing in static wireless networks," *Communications, IEEE Transactions on*, vol. 55, no. 11, pp. 2185–2192, 2007.

[58] F. Li, A. Lippman, and K. Wu, "Minimum energy cooperative path routing in wireless networks: an integer programming formulation," in *Vehicular Technology Conference, 2006. VTC 2006-Spring. IEEE 63rd*, vol. 1, 2006, pp. 1–6.

[59] F. Li, K. Wu, and A. Lippman, "Minimum Energy Cooperative Path Routing in All-Wireless Networks: NP-Completeness and Heuristic Algorithms," *Journal of Communications and Networks*, vol. 10, no. 2, p. 1, 2008.

[60] a. Lippman, "Energy-Efficient Cooperative Routing in Multi-hop Wireless Ad Hoc Networks," *2006 IEEE International Performance Computing and Communications Conference*, pp. 215–222, 2006.

[61] M. Sikora and J. Laneman, "Bandwidth-and power-efficient routing in linear wireless networks," *Information Theory, IEEE Transactions on*, vol. 52, no. 6, pp. 2624–2633, 2006.

[62] Z. Yang and A. Hø st Madsen, "Routing and Power Allocation in Asynchronous Gaussian Multiple-Relay Channels," *EURASIP Journal on Wireless Communications and Networking*, vol. 2006, no. 1, pp. 1–11, 2006.

[63] A. Ibrahim, Z. Han, and K. Liu, "Distributed energy-efficient cooperative routing in wireless networks," *Wireless Communications, IEEE Transactions on*, vol. 7, no. 10, pp. 3930–3941, 2008.

[64] M. Dehghan, M. Ghaderi, and D. L. Goeckel, "On the performance of cooperative routing in wireless networks," in *INFOCOM IEEE Conference on Computer Communications Workshops , 2010.* Ieee, Mar. 2010, pp. 1–5.

[65] L. Dong and A. Petropulu, "Weighted cross-layer cooperative beamforming for wireless networks," *IEEE TRANSACTIONS ON SIGNAL PROCESSING*, vol. 57, no. 8, pp. 3240–3252, 2009.

[66] P. Zhou, W. Liu, W. Yuan, W. Cheng, and S. Wang, "An energy-efficient cooperative MISO-based routing protocol for wireless sensor networks," in *Wireless Communications and Networking Conference, 2009. WCNC 2009. IEEE*, 2009, pp. 1–6.

[67] X. Li, M. Chen, and W. Liu, "Application of STBC-encoded cooperative transmissions in wireless sensor networks," *Signal Processing Letters, IEEE*, vol. 12, no. 2, pp. 134–137, 2005.

[68] C. Pandana, W. Siriwongpairat, T. Himsoon, and K. J. R. Liu, "Distributed cooperative routing algorithms for maximizing network lifetime," in *Proc. IEEE Wireless Communications and Networking Conference (WCNC).* Ieee, 2006, pp. 451–456.

[69] B. Peng, A. Kemp, and H. Maheshwari, "Power-saving geographic routing in the presence of location errors," in *Communications, 2009. ICC'09. IEEE International Conference on*, 2009, pp. 1–5.

[70] M. Grabner, V. Kvicera, P. Pechac, and M. Mudroch, "Multipath fading measurement and prediction on 10 GHz fixed terrestrial link," in *Microwave Techniques (COMITE), 2010 15th International Conference on*, 2010, pp. 145–148.

[71] M. Touati, G. El Zein, and J. Citerne, "An experimental investigation of line-of-sight multipath propagation at 15 GHz over 500 MHz bandwidth," in *Antennas*

and Propagation Society International Symposium, 1993. AP-S. Digest, 1993, pp. 1061–1064.

[72] M. Grabner, V. Kcicera, P. Pechac, and V. P., "Multipath Signal Variation Characteristics of 10 GHz Fixed Terrestrial Multi-Receiver Path," in *Proceedings of International Symposium on Antennas and Propagation 2008*, Taipei, Taiwan, 2008.

[73] F. R. Farrokhi, A. Lozano, G. J. Foschini, and R. A. Valenzuela, "Spectral efficiency of wireless systems with multiple transmit and receive antennas," in *Personal, Indoor and Mobile Radio Communications, 2000. PIMRC 2000. The 11th IEEE International Symposium on*, 2000, pp. 373–377.

[74] Y. S. Cho, J. Kim, W. Y. Yang, and C. G. Kang, *MIMO-OFDM Wireless Communications with MATLAB*. John Wiley & Sons (Asia) Pte Ltd, 2010.

[75] Z. Sun, R. Yu, and S. Mei, "A robust power-aware routing algorithm for wireless sensor networks," in *Military Communications Conference, 2006. MILCOM 2006. IEEE*, 2006, pp. 1–7.

[76] H. Ochiai, P. Mitran, S. Member, and H. V. Poor, "Collaborative Beamforming for Distributed Wireless Ad Hoc Sensor Networks," *IEEE Trans. Sign. Processing.*, vol. 53, no. 11, pp. 4110–4124, 2005.

[77] R. Mudumbai, D. R. Brown, U. Madhow, and H. V. Poor, "Distributed transmit beamforming: challenges and recent progress," *IEEE Communications Magazine*, vol. 47, no. 2, pp. 102–110, 2009.

[78] B. Maham, R. Narasimhan, and A. Hjorungnes, "Energy-efficient space-time coded cooperative routing in multihop wireless networks," in *Global Telecommunications Conference, 2009. GLOBECOM 2009. IEEE*, 2009, pp. 1–7.

[79] D. Bertsekas and R. Gallager, *Data Networks*, 2nd ed. Prentice Hall, 1991.

[80] M. T. Goodrich and R. Tamassia, *Algorithm design: foundations, analysis, and Internet examples*. Wiley, 2003.

[81] Y. Tu and G. Pottie, "Coherent cooperative transmission from multiple adjacent antennas to a distant stationary antenna through AWGN channels," in *Vehicular Technology Conference, 2002. VTC Spring 2002. IEEE 55th*, vol. 1, 2002, pp. 130–134.

[82] C. Cormio and K. R. Chowdhury, "A survey on MAC protocols for cognitive radio networks," *Ad Hoc Networks*, vol. 7, no. 7, pp. 1315–1329, Sep. 2009.

[83] M. Cesana, F. Cuomo, and E. Ekici, "Routing in cognitive radio networks: Challenges and solutions," *Ad Hoc Networks*, vol. 9, no. 3, pp. 228–248, May 2011.

[84] I. F. Akyildiz, W.-Y. Lee, and K. R. Chowdhury, "CRAHNs: Cognitive radio ad hoc networks," *Ad Hoc Networks*, vol. 7, no. 5, pp. 810–836, Jul. 2009.

[85] G. Zheng, S. Ma, K.-k. Wong, and T.-S. Ng, "Robust beamforming in cognitive radio," *IEEE Transactions on Wireless Communications*, vol. 9, no. 2, pp. 570–576, Feb. 2010.

[86] W. Zong, S. Shao, Q. Meng, and W. Zhu, "Joint user scheduling and beamforming for underlay cognitive radio systems," in *2009 15th Asia-Pacific Conference on Communications*, no. Apcc, Oct. 2009, pp. 99–103.

[87] G. Caire and S. Shamai, "On the achievable throughput of a multiantenna Gaussian broadcast channel," *IEEE Transactions on Information Theory*, vol. 49, no. 7, pp. 1691–1706, 2003.

[88] U. Erez and S. Brink, "A close-to-capacity dirty paper coding scheme," *IEEE Transactions on Information Theory*, vol. 51, no. 10, pp. 3417– 3432, 2005.

[89] M. Costa, "Writing on dirty paper," *IEEE Transactions on Information Theory*, vol. IT-29, pp. 439–441, 1983.

[90] T. Trump and B. Ottersten, "Estimation of nominal direction of arrival and angular spread using an array of sensors," *Signal Processing, KTH*, vol. 50, pp. 57 – 69, 1996.

[91] J. F. Sturm, "Using SeDuMi 1.02, a MATLAB toolbox for optimization over symmetric cones," *Optimization Methods and Software*, vol. 11, no. 1, pp. 625–653, 1999.

[92] S. Vorobyov, A. Gershman, and Z. Luo, "Estimation of nominal direction of arrival and angular spread using an array of sensors," *IEEE Transacations on Signal Processing*, vol. 51, no. 2, pp. 313–324, 2003.

[93] M. Bengtsson and B. Ottersten, "Optimal downlink beamforming using semidenite optimization," in *Proc. 37th Annual Allerton Conf. on Communication, Control, and Computing*, 1999, pp. 987–996.

[94] V. Sharma, I. Wajid, A. Gershman, H. Chen, and S. Lambotharan, "Robust downlink beamforming using positive semidenite covariance constraints," in *Proc. 2008 Int. ITG Workshop on Smart Antenna (WSA 2008)*, 2008, pp. 36– 41.

[95] S. Boyd and L. Vandenberghe, *Convex optimization*. Cambridge University Press, 2004.

[96] M.-G. Di Benedetto and L. De Nardis, "Cognitive routing models in UWB networks," in *2008 3rd International Conference on Cognitive Radio Oriented Wireless Networks and Communications (CrownCom 2008)*, May 2008, pp. 1–6.

[97] K. R. Chowdhury and I. F. Akyildiz, "CRP : A Routing Protocol for Cognitive Radio Ad Hoc Networks," *IEEE Journal on Selected Areas in Communications*, vol. 29, no. 4, pp. 794–804, 2011.

[98] L. D. Nardis, M.-G. De Benedetto, A. M. Akhtar, and O. D. Holland, "Combination of doa and beamforming in position based routing for underlay cognitive wireless networks," in *IEEE Cognitive Radio Oriented Wireless Networks and Communications 2012 (CROWNCOM 2012)*, 2012.

[99] T. H. Cormen, C. E. Leiserson, R. L. Rivest, and C. Stein, "Section 24.3: Dijkstra's algorithm," in *Introduction to Algorithms*, 2nd ed. MIT Press and McGraw-Hill, 2001, pp. 595–601.

[100] S. Boyd and M. Grant, "cvx users guide for cvx version 1.22," Tech. Rep., 2012. [Online]. Available: http://cvxr.com/cvx/cvxusrguide.pdf

[101] "The INET framework." [Online]. Available: http://inet.omnetpp.org/index.php?n=Main.HomePage.

[102] "The MIXIM OMNeT++ modeling framework." [Online]. Available: http://mixim.sourceforge.net/